1
VECSEL Semiconductor Lasers: A Path to High-Power, Quality Beam and UV to IR Wavelength by Design

Mark Kuznetsov

1.1
Introduction

Since its invention and demonstration in 1960, several types of laser have been developed, such as solid-state, semiconductor, gas, excimer, and dye lasers [1]. Today, lasers are used in a wide range of important applications, particularly in optical fiber communication, optical digital recording (CD, DVD, and Blu-ray), laser materials processing, biology and medicine, spectroscopy, imaging, entertainment, and many others. A number of properties enable the application of lasers in these diverse areas, each application requiring a particular combination of these properties. Some of the most important laser properties are laser emission wavelength; output optical power; method of laser excitation, whether by optical pumping or electrical current injection; laser power consumption and efficiency; high-speed modulation or short pulse generation ability; wavelength tunability; output beam quality; device size; and so on. Thus, optical fiber communication [2], a major application that enables modern Internet, commonly requires lasers with emission wavelengths in the 1.55 μm low-loss band of glass fibers and with single-transverse mode output beams for coupling into single-mode optical fibers. Typically, a given laser type excels in some of these properties, while exhibiting shortcomings in others. For example, by using different material compositions and structures, the most widely used semiconductor diode laser [3–12] can cover a wide range of wavelengths from the ultraviolet (UV) to the mid-IR, can be advantageously driven by diode current injection, and is very compact and efficient. However, the good beam quality, that is, single-transverse mode near-circular beam operation, can be typically achieved in semiconductor lasers only for output powers below 1 W. Much higher power levels are achievable from semiconductor lasers only with large aspect ratio highly multimoded poor quality optical beams. On the other hand, the solid-state lasers [13, 14], including fiber lasers [15], can emit hundreds of watts of output power with excellent beam quality, however, their emission wavelengths are restricted to discrete values of electronic transitions in ions, such as the classic 1064 nm wavelength of the Nd:YAG laser, making them

Semiconductor Disk Lasers. Physics and Technology. Edited by Oleg G. Okhotnikov

ISBN: 978-3-527-40933-4

inapplicable for applications requiring specific inaccessible wavelengths. For example, the 488 nm excitation wavelength required for many fluorescent labels in biomedical applications [16], such as the green fluorescent protein (GFP), is not accessible by direct solid-state laser transitions. Therefore, the 488 nm wavelength biomedical applications have required in the past the use of large and inefficient Ar gas lasers, which serendipitously have the required emission wavelength. This explains the large variety of laser types used today, where one or another type fits a given application with its beneficial properties, while carrying the baggage of its undesirable properties.

It is therefore useful and important to develop a laser that exhibits simultaneously the application required and desired laser properties, such as emission wavelength, optical power, beam quality, efficiency, compact size, and so on. Vertical-external-cavity surface-emitting laser (VECSEL) [17–24], also called optically pumped semiconductor laser (OPSL) or semiconductor disk laser (SDL), is a relatively new laser family that uniquely combines many of these desirable laser properties simultaneously, and because of this, it is becoming the laser of choice for a wide range of laser applications. This chapter describes VECSEL lasers and their history; discusses how they are made and characterized; explains how VECSEL structure enables their basic properties; and indicates key applications enabled by this unique combination of properties. Other chapters in this book address in more detail the various aspects and applications of this remarkable new class of lasers.

1.2 What Are VECSEL Semiconductor Lasers

1.2.1 History of VECSELs: Semiconductor Lasers, Optical Pumping, and External Cavity

Vertical-external-cavity surface-emitting lasers were developed in the mid-1990s [17, 18] to overcome a key problem with conventional semiconductor lasers: how to generate watt-level and higher optical powers with fundamental transverse mode circular optical beam quality. The versatile semiconductor diode lasers are very widely used because of their numerous advantageous properties, such as size, efficiency, electrical current laser excitation and modulation, and wide wavelength coverage. Using GaN, GaAs, InP, and GaSb semiconductor material systems, for example, these lasers can access 0.4, 0.8, 1.5, and 2.0 μm emission wavelength regions. However, obtaining lasers with both high optical power and good beam quality simultaneously has always been a difficult task, although it is key for many important scientific and commercial laser applications. Such combination is required, for example, for efficient nonlinear optical second harmonic generation [14, 25].

The conventional semiconductor lasers have two major configurations: edge-emitting [3–6] and surface-emitting lasers [9–11] (see Figure 1.1). The edge-emitting

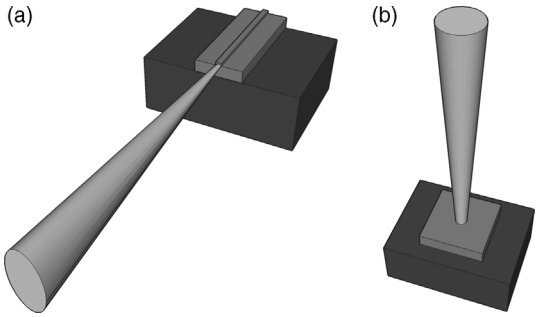

Figure 1.1 (a) Semiconductor edge-emitting laser. (b) Semiconductor vertical-cavity surface-emitting laser (VCSEL).

lasers use a waveguide to confine light to the plane of the semiconductor chip and emit light from the edge of the chip (Figure 1.1a). Output beam cross section is typically about one by several microns, with the wider dimension in the plane of the chip. Such small waveguide dimensions are required for single-transverse mode operation, but result in the asymmetric and strong angular divergence of the laser beam. Laser output power is typically limited by the required excess heat dissipation from the chip active region or catastrophic optical damage at the semiconductor surface [9, 12]. Scaling up laser output power requires wider waveguides with larger area beams: this improves heat dissipation by reducing active stripe thermal impedance and avoids catastrophic optical damage by decreasing beam optical intensity. In this way, up to several hundred milliwatts of output power is achievable in a single-transverse mode waveguide configuration [9, 12]. For still wider waveguides, of the order of a 100 μm, single-stripe edge-emitting lasers can emit tens of watts of output power, but the waveguide is then highly multimoded in the plane of the chip, and output beam is very elongated with a very large, 100: 1, aspect ratio. Multiple stripe semiconductor laser bars can emit hundreds of watts, but again with a highly multimoded output beam [9, 12].

In contrast, vertical-cavity surface-emitting lasers [10, 11] have laser cavity axis and emit light perpendicular to the plane of the laser chip (Figure 1.1b). Such lasers can emit circular fundamental transverse mode beam with powers up to several milliwatts and beam diameter of several microns. With circular cross section and larger beam size, the laser output beam is also symmetrical and has much smaller divergence than for edge-emitting lasers. Again, the required heat dissipation limits the output power and the scaling to higher powers demands larger active areas. But for output beam diameters greater than about 10 μm, laser output beam quickly becomes multimoded, and uniform current injection over such large areas is difficult with edge injection through transparent contact layers. Arrays of semiconductor lasers have been a typical path to high output power [12, 25]. In short, surface-emitting lasers have good fundamental mode circular beams, but at powers of only a few milliwatts, while edge-emitting lasers can emit up to several hundred milliwatts but with elliptical beam profile. For still higher powers, both laser types

emit highly transverse multimoded output beams. In short, high power and good beam quality cannot be achieved simultaneously with conventional edge- or surface-emitting semiconductor lasers.

Two things become clear from the above description of semiconductor lasers. First, scaling up optical power to watt and higher levels with circular output beams requires beam diameters of tens and possibly hundreds of microns, which can be satisfied only by surface-emitting laser geometry. Second, good beam quality with fundamental transverse mode operation requires strong transverse mode control of the laser cavity. Such transverse mode control can be provided by optical cavity elements external to the laser chip, which assure that fundamental transverse mode of the laser cavity, the desired operating laser mode, has diameter approximately equal to the gain region diameter. In this way we arrive to the concept of vertical-external-cavity surface-emitting laser.

When the beam diameter of a surface-emitting laser becomes tens of microns large and the laser cavity is extended by an external optical element, the issue of laser excitation acquires additional importance. Injecting carriers uniformly across a wide area is difficult in the traditional diode current injection [10]; this requires a thick doped semiconductor current spreading layer. Such a doped layer has strong free carrier absorption inside the extended laser cavity, which can degrade laser threshold and efficiency. One possible solution to this problem is the use of optical pumping, which can inject excitation carriers uniformly across a wide area without using intracavity lossy doped regions. Simple and efficient semiconductor diode pump lasers with multimode beams and very high powers have been developed and are available for pumping solid-state and fiber lasers. VECSEL lasers have been made with both types of excitation, optical pumping and diode current injection. To emphasize their distinction from the common semiconductor diode lasers that use electrical pumping, optically pumped VECSELs are frequently referred to as OPSLs or optically pumped semiconductor lasers.

External optical cavity elements had been used previously with semiconductor lasers. For edge-emitting lasers, external reflectors provide a longer laser cavity for pulse repetition rate control in mode locking [27] and for inserting intracavity optical elements, such as spectral-filtering gratings [27]. There had also been attempts to stabilize transverse modes of surface-emitting lasers using external spherical mirrors [28].

Optical pumping of semiconductor lasers has a long history, where optical pumping had been used not only for characterization of novel semiconductor laser structures but also for generation of higher output powers or for short pulse generation. As early as in 1973, pulsed operation was demonstrated with optically pumped edge-emitting GaAs semiconductor lasers [29]. Later, surface-emitting thin-film InGaAsP lasers [30] were used to generate gain-switched picosecond pulses in the 0.83–1.59 μm wavelength range using dye laser pumping. Using an external optical cavity for pulse repetition rate and transverse mode control, optically pumped mode locking was demonstrated with a CdS platelet laser [31]. High peak power was observed in an external-cavity GaAs platelet laser pumped by a Ti:sapphire laser [32].

Using diode laser pumping, low-power 10 mW CW operation was demonstrated with GaAs VCSEL lasers [33]; in external cavity, however, such lasers emitted only 20 μW [34]. A diode-laser-pumped surface-emitting optical amplifier was demonstrated at 1.5 μm using InGaAs–InGaAlAs multiquantum well structures [35]. Using 77 K low temperature operation and a Nd:YAG pump laser, 190 mW continuous output power was obtained from an external-cavity InGaAs–InP surface emitting laser [36]. In a similar configuration, an external-cavity GaAs VCSEL laser at 77 K has demonstrated CW output power of 700 mW using a 1.8 W krypton–ion pump laser [37]. To obtain high power from a diode-laser-pumped semiconductor laser, specially designed edge-emitting InGaAs–GaAs laser structures were used to generate as much as 4 W average power [38, 39], however the beams were strongly elongated with aspect ratios between 10 and 50 to 1. These works had demonstrated the potential capabilities of the optically pumped semiconductor lasers; however, the goal of a high-power compact and efficient diode-pumped room-temperature laser with circular diffraction-limited beam profile had remained elusive prior to OPS-VECSEL demonstration in 1997 [17]. What enabled the appearance of the modern VECSEL lasers is the availability of sophisticated custom-designed multilayered bandgap-engineered semiconductor structures, modern high-power multimode semiconductor pump lasers, and thermal designs for efficient heat dissipation from the active semiconductor chip.

Figure 1.2 shows basic configuration of an optically pumped VECSEL. A thin active semiconductor chip, containing gain region and multilayer high-reflectivity mirror, is placed on a heat sink and is excited by an incident optical pump beam. Laser cavity consists of the on-chip mirror and an external spherical mirror, which defines the laser transverse mode and also serves as the output coupler. Typical laser beam diameters on the gain chip range between 50 and 500 μm; VECSELs have been made

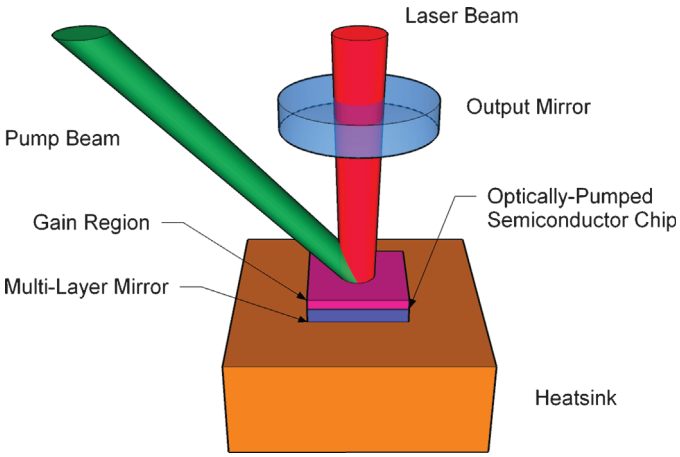

Figure 1.2 Optically pumped semiconductor vertical-external-cavity surface-emitting laser (VECSEL).

with output powers ranging from 20 mW to 20 W and higher. Optically pumped VECSEL can be thought of as a brightness or mode converter, converting a high-power low-quality multimode pump beam with poor spatial and spectral brightness into a high-power high-quality fundamental transverse mode laser output beam with the desired spatial and spectral properties. In this way an optically pumped VECSEL is similar to solid-state and fiber lasers [13–15], which similarly act as brightness or mode converters. Indeed, an optically pumped VECSEL can be thought of as a solid-state laser, where the gain medium, instead of the traditional active ions in a transparent host material, uses bandgap-engineered semiconductor structures to achieve the desired laser absorption and emission properties. Just as evolution of semiconductor lasers to high power and good beam operation has arrived at the VECSEL laser configuration, diode pumped solid-state DPSS lasers have arrived at the very similar solid-state disk laser configuration [40, 41], which has demonstrated kilowatt-level output powers. In such a solid-state disk laser, with a geometry similar to that in Figure 1.2, a thin solid-state gain medium, such as a Yb:YAG crystal, with a thin-film high-reflectivity mirror coating is placed directly on a heat sink with external spherical mirror stabilizing the cavity transverse mode and diode optical pumping providing laser excitation. An important benefit of using semiconductors, in contrast to other solid-state gain media, is that the on-chip multilayer mirror can be made of alternating different composition semiconductor layers and can be grown in the same epitaxial growth step as the gain region itself. Externally deposited mirror on the semiconductor laser chip can also be used. Because of their similarity to the solid-state disk lasers, VECSELs have also been referred to as semiconductor disk lasers or SDLs. Optically pumped VECSELs form a hybrid between traditional semiconductor and solid-state lasers, hence the interest in these lasers has come from both of these laser communities. For high-power good beam quality operation with wavelength versatility, such optically pumped VECSEL lasers have many significant advantages compared to both the traditional semiconductor diode lasers and the traditional solid-state lasers, including disk lasers.

1.2.2
Basic Principles of Operation: VECSEL Structure and Function

Basic operating principles of VECSEL lasers are illustrated in Figure 1.3. The key element of the laser is the semiconductor chip, which contains both a multilayer laser mirror and a gain region; Figure 1.3 shows the conduction and valence band energy levels across the semiconductor layers and explains the functions of the various layers. For optically pumped operation, incident pump photons with higher photon energy are absorbed in separate pump-absorbing layers that also serve as the quantum well barriers. The excited carriers, electrons and holes, then diffuse to the smaller bandgap quantum wells that provide gain to the optical wave, emitting lasing photons with lower photon energy. These separate pump absorption and quantum well laser emission layers allow independent optimization of the pump absorption and laser gain properties. For optically pumped VECSEL operation,

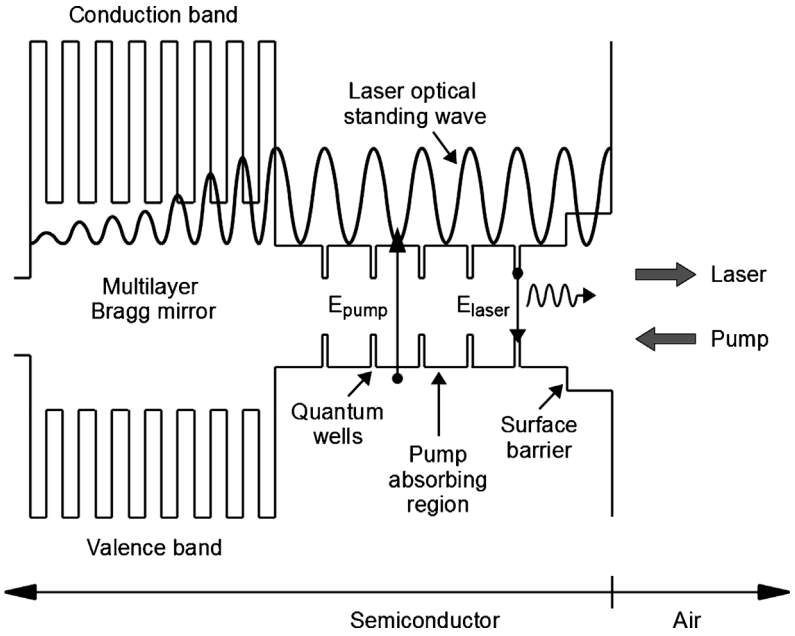

Figure 1.3 Operating principles of optically pumped VECSELs.

semiconductor layers are typically undoped, thus significantly simplifying semiconductor wafer growth and eliminating free carrier absorption of the doped regions. For electrically pumped operation, p- and n-doped regions are used to form a p–n junction for diode current carrier injection, but this also results in optical losses inside the laser cavity. A higher bandgap surface barrier window layer on the chip prevents carriers from diffusing to the semiconductor–air interface, where they could recombine nonradiatively and thus deplete laser gain. Optical wave of the laser mode back-reflecting from the on-chip laser cavity mirror sets up an intracavity standing wave inside the chip. Quantum wells have to be placed near the antinodes of this standing wave in order to provide efficient gain to the laser. This is the so-called resonant periodic gain (RPG) arrangement [42]; one or more closely spaced wells can be placed near a given standing wave antinode. Typically, gain region thickness covers several periods of this laser mode standing wave.

Incident pump photons have higher energy than the emitted laser photons, the difference of the two photon energies is the quantum defect. This quantum defect is one of the major contributors to the overall laser operating efficiency; this pump–laser photon energy difference, together with contributions from other lasing inefficiencies, has to be dissipated as heat from the device active region. Heat dissipation from the VECSEL active semiconductor chip is provided by heat spreaders connected to heat sinks: either a soldered heat spreader below the mirror structure or a transparent heat spreader above the surface window of the chip, or possibly both (Chapter 2).

Good heat dissipation and heat sinking are critical for high-power operation of all semiconductor lasers. Without these, temperature of the active region would rise and excited carriers would escape thermally from the quantum wells into the barrier region, thus depleting laser gain and turning the laser off in a thermal rollover process. Such thermal rollover is typically the dominant mechanism that limits output power in VECSEL lasers [43]. Smaller quantum defect produces less excess heat, but typically also implies smaller energy difference, or confinement energy, between electron and hole states in the wells and the barriers, making it easier for electrons to escape thermally from the wells into the barriers, and thus making lasers more sensitive to the temperature rise. Optimization of the quantum defect and electron confinement energy is required for high-power room temperature device operation.

Optical absorption in semiconductors is very strong for pump photon energies above the bandgap, of the order of $10^4\,\mathrm{cm}^{-1} = 1\,\mu\mathrm{m}^{-1}$. This means that ~63% of pump light is absorbed on a single pass through 1 μm thick semiconductor absorbing layer, 86% is absorbed in 2 μm. In most cases, single-pass pump absorption is sufficient; a pump-reflecting mirror can be included on the chip if double-pass absorption is desired. A very simple pump-focusing optics can be used, since multimode pump light does not have a chance to diverge in a few microns before it is absorbed; no depth of focus is required for pump optics and high brightness is not required of the multimode pump sources. Compare this with $\sim 7\,\mathrm{cm}^{-1}$ absorption in Yb:YAG, a typical active medium in solid-state disk lasers. Such a thousand times weaker absorption requires a much thicker absorbing region, 100–300 μm, and, in addition, multiple pump beam passes for efficient pump absorption, with correspondingly complex pump optics to handle divergent multimode pump beams on multiple absorption passes [40, 41]. In an attempt to reduce quantum defect and improve efficiency in VECSEL lasers, in-well, rather than barrier, optical pumping has also been used for these devices [44–48]. Another important advantage of optically pumped semiconductor gain medium is its spectrally broad absorption and hence tolerance of broad pump wavelength variation. Essentially, any pump wavelength is useful that is shorter than the absorber region bandgap wavelength. Therefore, tight wavelength selection and temperature control of pump diode lasers are not required, unlike the case for solid-state and fiber lasers. Diode laser pumping of VECSELs also offers fast direct VECSEL modulation capability via pump laser current modulation, since VECSEL semiconductor gain medium has short, sub-nanosecond, carrier lifetimes, as compared with microseconds to milliseconds lifetimes of typical solid-state gain media.

Since laser optical axis is perpendicular to the surface of the gain chip and quantum well gain layers are very thin, the single-pass optical gain is at most only a few percent. This means that external output coupling mirror transmission should also be of the order of a few percent and the on-chip mirror reflectivity should be as high as possible, say greater than 99.9%. Intracavity losses should also be kept very low, less than a percent, in order to maintain efficient laser operation.

1.2.3
Basic Properties of VECSEL Lasers: Power Scaling, Beam Quality, and Intracavity Optical Elements

Basic configuration of VECSEL lasers enables their many key advantageous properties, such as power scaling, beam quality, and laser functional versatility; in this section, we describe these connections between VECSEL laser structure and device functionality.

1.2.3.1 **Power Scaling**

One of the key important properties of VECSEL lasers is their output power scalability: efficient research and commercial optically pumped devices have been demonstrated with power levels between 10 mW and 60 W, a range of almost four orders of magnitude, while maintaining good beam quality. Such efficient power scalability is enabled by the laser mode and pump spot-size scalability on the VECSEL semiconductor laser chip. Since output power of semiconductor lasers is typically limited by heat dissipation and optical intensity-induced damage, increasing beam diameter in a VECSEL helps on both accounts, distributing heat and optical power over larger beam area. For well-designed heat sinking with thin semiconductor chips, heat flow from the laser active region into heat sink is essentially one-dimensional. Therefore, increasing beam area is essentially equivalent to operating multiple lasing elements in parallel, without changing thermal or optical intensity regime of the individual lasing elements. In this scenario, both output laser power and pump power scale linearly with the active area. VECSELs have been operated with on-chip beam diameters between 30 and 900 μm, which scale the beam area and potentially output power by a factor of 900. For such power scaling, the same semiconductor wafer and chip structure can be used, adjusting only the laser cavity optics and pump laser arrangement. Optical pumping allows simple uniform excitation of such widely scalable mode areas. In contrast, with electrical pumping, uniform carrier injection over hundreds of microns wide area is extremely difficult, typically leaving a weakly pumped region in the center of the active area and making power scaling of electrically pumped devices very challenging. Direct optical coupling of pump diode chips into the VECSEL chip is possible with relatively simple pump lens arrangements; alternatively, multimode fiber-coupled pump diode sources can also be used. If pump power available from a single pump diode is limited, multiple pump diodes can be used with multiple pump beams incident on a single VECSEL chip from different angles. When heat dissipation from a single semiconductor chip becomes the limiting factor, further scaling of optical power is possible by arranging multiple semiconductor gain chips within a single VECSEL laser cavity and reflecting the laser beam sequentially from these reflecting vertical amplifier chips [22, 49–52]. All of these factors combined make it possible to scale optically pumped VECSEL power by the demonstrated four orders of magnitude, and potentially more in the future.

1.2.3.2 Beam Quality

Another critically important property of VECSEL lasers is their beam quality: VECSELs operate with a circular beam, fundamental transverse TEM_{00} mode, and essentially diffraction-limited low beam divergence with $M^2 \sim 1.0$–1.3. Here, beam spatial quality parameter M^2 [9] indicates how much faster a laser beam diverges angularly in the two transverse directions as compared with a single-transverse mode diffraction-limited beam, which has $M^2 = 1$. Several factors contribute to this beam quality in VECSELs. Most important, VECSEL laser external-cavity optics defines and stabilizes the circular fundamental laser transverse mode; such optical elements and their stabilization effect are not available with the more conventional edge- and surface-emitting semiconductor lasers. Using pump and laser cavity optics, VECSELs have independent control allowing matching of the pump spot size and the laser fundamental transverse mode size. If the pump spot is too small, compared to the fundamental mode size, laser threshold will be high because of the lossy unpumped regions encountered by the laser mode. If the pump spot is too large, higher order transverse laser modes with a larger transverse extent will be excited, causing multimode laser operation and thus degraded beam quality. Optimally adjusted pump spot size gives preferentially higher gain to the fundamental laser mode, while giving excess loss from the unpumped regions to the spatially wider higher order transverse modes; this stabilizes the fundamental transverse mode operation. Large VECSEL laser beam and pump spot sizes on the chip, tens to hundreds of microns, as compared with just a few microns for edge-emitting semiconductor lasers, contribute to the ease of alignment and thus to the mechanical stability of the VECSEL laser cavity, and thus also to the stability of its fundamental transverse mode operation. Such a large VECSEL beam diameter also conveniently has very low divergence angles, as compared with extremely fast divergence of micron-sized beams of the edge-emitting, and even surface-emitting, lasers.

The second important factor contributing to spatial beam quality and stability of VECSEL lasers is the negligible thermal lensing in the thin, 2–8 μm, VECSEL semiconductor chip [22] when proper heat spreading/heat sinking is used. Thermal lensing and other beam phase profile distortions are caused by thermally induced refractive index gradients in the laser gain material. In VECSELs, thin semiconductor active region with good heat sinking implies that optical path length thermal distortions and hence beam profile changes and distortions are negligible. In contrast, such thermal lensing is much stronger in solid-state lasers that require much longer, hundreds of microns, gain path length. As a result, thermal lensing typically forces optimal solid-state laser operation only within a narrow range of pump and output powers where the thermal gradients and the resulting thermal intracavity lens produce laser mode size consistent with the pumping profile. VECSEL semiconductor lasers operate efficiently and with excellent beam quality across a wide range of operating power regimes from near to high above threshold. There is some trade-off between output power and beam quality in VECSELs: a multimode laser beam can better overlap the pump spot and thus produce somewhat higher output power. Thus, when a few transverse modes can be tolerated with a somewhat degraded $M^2 \sim 3$–4 beam parameter, VECSELs have been operated in

such regime with higher efficiency and higher output power than for single-transverse mode regime [22].

1.2.3.3 Laser Functional Versatility Through Intracavity Optical Elements

The external optical cavity of semiconductor VECSELs, which controls the laser transverse modes, can be viewed as mechanically cumbersome, making these lasers more complex and requiring assembly and alignment as compared with the simple integrated edge-emitting and surface-emitting semiconductor lasers. On the other hand, such an external cavity gives tremendous versatility to VECSEL device configurations and functions. Flexible VECSEL laser cavities, such as linear two-mirror cavity, three-mirror V-shaped cavity, and four-mirror Z-shaped cavity [18, 20, 49–54], allow flexible insertion of intracavity optical elements. Such intracavity functional elements are very difficult or impossible to use with integrated semiconductor devices. We have already discussed one example of such extended cavity versatility – inserting multiple gain elements in the cavity in series for power scaling of VECSELs.

One important option allowed by the external cavity is the insertion of intracavity spectral filters, such as etalons [55, 56], Brewster's angle birefringent filters [54, 57, 58], volume gratings (Chapter 7) [59], or high-reflectivity gratings [60], to control longitudinal spectral modes of the laser and possibly to select a single longitudinal lasing mode. Tuning a birefringent filter by rotation then achieves tunable VECSEL operation; greater than 20 nm tuning range with multiwatt output was demonstrated with this approach [61].

VECSEL external cavity also allows the insertion of intracavity saturable absorber elements to achieve laser passive mode locking with picosecond and subpicosecond pulse generation (Chapter 6) [20]. In this case, the length of the external cavity also allows control of the pulse repetition rates, with rates as high as 50 GHz demonstrated with short cavities [62]. External cavity optics also allows different beam spot sizes on the gain and absorber elements, which controls optical intensity of the beam spots and is typically required to achieve mode locking [20, 63, 64].

The open cavity of VECSELs allows placement of transparent intracavity heat spreaders in direct contact with the laser gain element without thermally resistive laser mirrors in the path of heat dissipation (Chapter 2) [53, 65–68]. Since thermal management is critical for high-power VECSEL operation, the possibility of using such heat spreaders tremendously broadens laser design options with chip gain, mirror, and substrate materials that do not allow effective heat removal through the on-chip mirror. Another option for VECSELs allowed by the external cavity is the microchip laser regime [69–72]. Here, an imperfectly heat-sunk semiconductor VECSEL chip produces an intracavity thermal lens that stabilizes laser transverse modes in a short external plane–plane laser cavity.

Low intracavity loss of VECSELs, combined with their wide gain bandwidth, allows insertion of intracavity absorption cells, such as gas cells, for intracavity laser absorption spectroscopy (ICLAS) [73, 74]. Laser output spectrum then reflects the absorption spectrum of the intracavity absorption cell. With intracavity real absorption length of the order of 1 m, equivalent laser intracavity absorption path length

as long as 130 km has been produced [75], allowing sensitive measurements of extremely weak absorption lines.

VECSEL output power coupling with only a few percent of transmission implies that its intracavity laser power is 20–100 times higher than the output power. Availability of such high intracavity power, together with high beam quality, allows very efficient nonlinear optical operation, such as second harmonic generation, by inserting nonlinear optical crystals inside the external laser cavity (Chapter 3) [14, 22, 24, 53, 54, 58, 76]. Using intracavity second harmonic generation, VECSELs have provided efficient laser output at wavelengths not accessible by other laser materials and techniques (Chapter 3).

Several examples discussed here show the tremendous versatility of VECSELs allowed by its external cavity and the various intracavity functional elements; these allow VECSELs to operate in a wide variety of operating regimes with a correspondingly large variety of laser applications.

To summarize this section, some of the key properties of VECSELs that make them so useful, namely, output power scaling, beam quality, and functional device versatility, follow from the unique structure of these devices, including semiconductor chip, external laser cavity, and optical pumping configuration.

1.2.4 VECSEL Wavelength Versatility Through Materials and Nonlinear Optics

One of the most important properties of VECSEL lasers is their wavelength versatility: VECSELs have been made with output wavelengths ranging from 244 nm [77] and 338 nm [24, 78] in the UV; through the 460–675 nm range of blue, green, yellow, orange, and red in the visible (Chapter 3) [22, 24, 52–54, 58, 79]; through the 0.9–2.4 μm in the near-infrared (NIR) (Chapter 4) [18, 23, 67, 68, 80, 81]; to the 5 μm in the mid-IR [82–85]. In principle, any wavelength in this range is accessible by design. This is simply not possible with any other laser type, not with the power, beam quality, and efficiency available from VECSELs. In this section, we discuss how such wavelength versatility of VECSELs is made possible by using different semiconductor materials and structures, in combination with the use of efficient nonlinear optical conversion.

1.2.4.1 Wavelength Versatility Through Semiconductor Materials and Structures

Compound semiconductor materials have different bandgap energies, and thus different photon emission wavelengths, for different material compositions. Controlling bandgaps of multiple layers of semiconductor structures, including the quantum well photon-emitting layers, allows control of laser emission wavelength by design. Such bandgap control of semiconductor heterostructures is required for VECSEL structures as in Figure 1.3, which also includes mirror layers, pump absorbing layers, and so on. Over more than 40 years of compound semiconductor technology, several semiconductor material systems have been developed that allow reliable growth of such bandgap-engineered multilayer structures. Starting substrates for VECSEL structures are binary semiconductor wafers; lattice constants of

the multiple layers of an epitaxially grown structure have to be closely matched to the substrate to avoid large strain and the resulting growth of crystalline defects that destroy laser operation. Epitaxial growth of ternary, quaternary, and even quinary semiconductor alloys has been developed, which allows independent control of semiconductor layer bandgap energy while maintaining lattice match to the substrate. Using group III–V semiconductor GaAs substrate material system with its ternary (e.g., InGaP, AlGaAs, InGaAs, GaAsP, GaAsSb), quaternary (e.g., InGaNAs, InAlGaAs), and quinary (e.g., InAlGaAsP) alloys, VECSEL lasers have been demonstrated with emission wavelengths in the 660–1300 nm wavelength range [18, 23, 68, 79, 86–88]. InP-based material system using quaternary alloys (e.g., InGaAsP, InGaAlAs) allows VECSEL lasers to access the 1500–1600 nm optical fiber communication wavelength regions [23, 80, 89–93]. Starting with GaSb substrate with ternary (e.g., GaInSb, AlAsSb) and quaternary (e.g., GaInAsSb, GaAlAsSb) alloys, VECSELs with emission wavelengths in the 2.0–2.3 μm range have been demonstrated (Chapter 4) [23, 48, 81, 94]. Recently, group IV–VI semiconductor PbTe/PbEuTe and PbSe/PbEuTe-based material systems have been used to demonstrate VECSELs in the 4.5–5 μm wavelength range [82–85]. VECSELs have also been fabricated in the GaN/InGaN material system [95, 96], which opens the 400 nm wavelength region for direct VECSEL operation.

It is important to note that a lattice-matched semiconductor material system for VECSELs must allow not only the desired emission wavelength but also the creation of very high reflectivity on-chip Bragg mirror. To achieve such high reflectivity, high refractive index contrast is required between the high- and low-index mirror materials. High index contrast is available in the GaAs material system. However, such contrast is poor in the InP material system, requiring thicker mirrors with more layers and correspondingly larger thermal impedance, which is detrimental to laser operation. InP material system is important because of its access to the 1500–1600 nm telecom wavelength emission range. Improved VECSEL laser performance at these wavelengths has been achieved by bonding or fusing InP-based gain region wafers with high-reflectivity GaAs-based Bragg mirror wafers [97, 98]. No lattice matching is required for this wafer fusion approach, thus broadening the choices available for laser emission wavelength materials and mirror materials.

The use of dimensionally, or quantum, confined semiconductor active regions [4, 8] allows further control of the VECSEL emission wavelengths. By adjusting the thickness of quantum wells (2D) or diameter of quantum wires (1D) and dots (0D), as well as the composition of confining barrier layers, the quantum-confined electron and hole energy levels are shifted and VECSEL designer acquires the additional fine control of laser emission wavelength (Chapter 5) [4, 8, 18, 87, 99–102]. Using a controlled amount of strain [4, 8, 18, 87] in the quantum-confined light-emitting regions further expands the range of available material compositions and thus emission wavelengths for a semiconductor material system. Thus, for example, the strained InGaAs on GaAs material system is used very successfully for light emission in the 950–1150 nm wavelength region [43, 68, 87].

Such diversity and flexibility of alloyed compound semiconductor material systems allows designing VECSELs with direct laser emission in the wide 0.6–5 μm

wavelength range [18, 23, 79]; many of these emission wavelengths have already been demonstrated, both in research and in commercial devices.

Semiconductor gain media, especially with engineered quantum-confined quantum well and quantum dot structures, can have very large gain bandwidths, from tens to more than a hundred nanometers in wavelength [4–9]. Using intracavity tunable filters, tunable VECSELs have been demonstrated, for example, with 80 nm near 2.0 μm [103], 30 nm near 1175 nm [58], 33 nm near 975 nm [51], 30 nm near 850 [66], and 10 nm near 674 nm [79]. Such tunability is useful for such laser applications as spectroscopy. At the same time, the use of intracavity tunable filters allows to set VECSEL output wavelength to a specific precise stable value required for a given application. This ability to set VECSEL output wavelengths has proven very valuable in certain applications, such as exciting marker fluorescent proteins in biological imaging applications, where specific excitation wavelengths, for example, 488 nm, are most efficient for a given marker protein [16]. Using intracavity filters, VECSELs have also been operated in the single longitudinal mode, or single-frequency regime [104], important for some applications, such as spectroscopy. In this way, VECSELs, by design, access not only a wide output wavelength range but also very specific desired wavelengths at arbitrary locations within that range.

An optically pumped laser is not very useful if a suitable pump laser is not easily available; this is frequently the case with solid-state lasers, which require pump lasers with a very narrow, only several nanometers wide, range of pumping wavelengths. An important factor that makes the wide VECSEL emission wavelength range possible is the wide pump wavelength range, tens to hundreds of nanometers wide, allowed by optically pumped VECSELs. In practice, this means that a desired emission wavelength can be achieved in VECSELs while using widely available efficient pump diode lasers at commonly available pump wavelengths. For example, the 808 nm wavelength pump lasers, the standard pumping wavelength for Nd:YAG solid-state lasers and thus wavelength where pump diodes are easily available, have been used for VECSEL lasers emitting in the 920–1300 nm wavelength range [18, 67, 68, 87]. The common 980 nm pump lasers, the standard wavelength for pumping Er-doped fiber amplifiers, have been used to pump 1550 nm VECSELs [97]. Pump lasers at 790, 808, 830, and 980 nm have been used to pump 2.0–2.3 μm lasers [81, 94, 105, 106]. Pump wavelength of 1.55 μm has been used for pumping 5 μm lasers [82–85]. Thus, pump wavelength versatility is an important contributor to the emission wavelength versatility in VECSELs.

1.2.4.2 Wavelength Versatility Through Nonlinear Optical Conversion

Perhaps the biggest contributor to the wavelength versatility of VECSEL lasers, as well as to their commercial success so far, has been efficient nonlinear optical conversion possible with VECSELs. Nonlinear optical conversion uses a nonlinear optical crystal to generate light at harmonics, as well as sum or difference frequencies of the incoming light beams (Chapter 3) [14, 24, 25]. The most common is the second harmonic generation SHG process, where light is generated at twice the frequency or half the wavelength of the fundamental laser emission. For example, a very useful 488 nm wavelength visible blue output can be produced as a second harmonic of the

fundamental 976 nm near-infrared laser emission. The nonlinear optical processes can be further cascaded to generate third, fourth, and so on harmonics of the fundamental input light frequency. Using this approach, fundamental wavelengths in the near-infrared between 0.8 and 1.3 μm, which are more readily accessible directly by semiconductor VCSELS, have been converted efficiently to the 0.24–0.65 μm ultraviolet and visible, including blue, green, yellow, orange, and red, wavelength range (Chapter 3) [22, 24, 53, 54, 57, 58, 78]. Nonlinear optical conversion has tremendously broadened the wavelength range accessible by VECSELs and made efficient light sources available at wavelengths that previously had been accessible only by inefficient gas lasers, such as Ar laser at 488 nm for fluorescent marker applications, or where no effective light sources had been available at all, such as 577 nm yellow wavelength for photocoagulation treatment in ophthalmology [57, 58].

Efficient nonlinear optical conversion requires high optical intensity; this is provided by high optical power and good beam quality, which allows focusing laser beam to small diameters. High optical power and good beam quality are precisely the fundamental properties of VECSEL lasers, which make them very efficient sources for nonlinear optical conversion. The efficiency of nonlinear optical conversion increases with the increase in optical intensity. Even though the fundamental output power of VECSELs is high, their intracavity power is still much higher. With typical output coupling mirror in VECSELs having a transmission of between 1 and 5%, intracavity laser power is remarkably 20–100 times higher than the output power. Thus, a 20 W output power VECSEL with output coupling transmission of 0.7% has an intracavity power of 2.8 kW [107], while beam quality $M^2 \sim 1.1$ is also very high. Such high VECSEL intracavity powers allow the use of very efficient intracavity nonlinear optical conversion (Chapter 3) [14, 24, 25], which because of the higher intracavity power can be much more efficient than similar conversion done outside the laser cavity. For intracavity SHG, for example, a nonlinear optical crystal is inserted inside the laser cavity and a dichroic laser output mirror has 100% reflectivity at the fundamental laser wavelength and 100% transmission at the second harmonic frequency; laser cavity output is then emitted at the second harmonic frequency (Chapter 3). Such nonlinear optical processes can be further cascaded inside the laser cavity to produce third and fourth harmonic laser output [108], producing, for example, 355 nm third harmonic UV radiation from the fundamental 1065 nm near-infrared laser emission. Alternatively, intracavity-doubled laser output can then be further doubled in frequency outside the laser cavity; in this way, 244 nm UV output has been produced from the 976 nm fundamental laser wavelength [77].

Another approach to extend wavelengths accessible by VECSEL lasers is to operate these lasers in a dual wavelength mode with intracavity nonlinear optical sum or difference frequency generation [109–113]. Also possible is intracavity sum frequency generation in a VECSEL laser with externally injected solid-state laser beam [114]. Using such intracavity difference frequency generation, VECSEL laser becomes a room temperature source of 4–20 μm wavelength mid- to far-infrared radiation. Still longer wavelength terahertz radiation, 0.1–2.0 THz or 150–3000 μm wavelength, can be generated using short-pulse mode-locked VECSELs [115]. In this approach,

very short 260–480 fs optical pulses incident on a photoconductive antenna produce terahertz radiation with bandwidth inversely proportional to the pulse width. A similar short pulse-driven photoconductive antenna is used for time domain detection of the terahertz radiation [115].

In summary, VECSEL lasers can access an extraordinarily wide range of wavelengths from the UV, through the visible and near-infrared, to mid- and far-infrared, and even to the terahertz frequency range. Two key factors are the source of such a wide wavelength range: flexibility of semiconductor material systems and structures in combination with nonlinear optical conversion techniques. More important, in contrast with other laser systems, such as gas- and solid-state laser systems, which emit only at discrete wavelengths of existing electronic transitions of active ions, semiconductor VECSELs can generate light by design within this wide range at essentially arbitrary specific target wavelengths required for different applications.

1.3
How Do You Make a VECSEL Laser

Now that we have described what VECSEL lasers are, their basic operating principles and fundamental properties that make them so uniquely useful, in this section we outline the key elements in designing and making VECSELs. First, we describe the design of basic building blocks of VECSELs, see Figures 1.2 and 1.3: gain medium, on-chip Bragg mirror, laser optical cavity, and optical pumping arrangement. Finally, we describe VECSEL laser characterization. Note that here we describe the design principles of the more common optically pumped version of VECSELs; the electrically pumped VECSEL is described in detail in Chapter 7 of this book; the two differently pumped versions share most of the design principles that are not related to pumping.

1.3.1
Semiconductor Gain Medium and On-Chip Bragg Mirror

The main component of VECSEL lasers is the semiconductor laser chip, which includes the semiconductor gain medium and the laser-cavity multilayer Bragg mirror. First, we address the design of the semiconductor gain medium; this will tell us the key design and operational parameters of VECSEL lasers: the required gain level and number of quantum wells, laser mirror reflectivities required, laser threshold and operational pump powers, and laser output power and efficiency. We then describe the semiconductor mirror design and show an example of a full VECSEL semiconductor wafer structure.

1.3.1.1 Semiconductor Gain Design for VECSELs

To model VECSEL lasers, we use a simple analytical phenomenological model of semiconductor quantum well gain, which then gives us a very useful analytical description of VECSEL laser design and operation [18]. The model here does not

include thermal considerations, which are very important in the laser design and are considered in detail in Chapter 2 of this book .

Semiconductor quantum well gain g, cm^{-1}, has an approximately logarithmic dependence on well carrier density N, cm^{-3},

$$g = g_0 \ln(N/N_0), \tag{1.1}$$

where g_0 is the semiconductor material gain parameter and N_0 is the transparency carrier density. VECSEL laser threshold condition states that intracavity optical field is reproduced upon a round-trip inside the cavity:

$$R_1 R_2 T_{\mathrm{loss}} \exp(2\Gamma g_{\mathrm{th}} N_{\mathrm{w}} L_{\mathrm{w}}) = 1, \tag{1.2}$$

where R_1 and R_2 are the cavity mirror reflectivities, T_{loss} is the transmission factor due to round-trip cavity loss, g_{th} is the threshold material gain, N_{w} is the number of quantum wells in the gain medium, and L_{w} is the thickness of a quantum well. Longitudinal confinement factor Γ [116] of this resonant periodic gain structure characterizes overlap between the intracavity optical standing wave and the quantum wells spaced inside the active region. Carrier density N below threshold can be calculated from the incident pump power P_{p}:

$$N = \frac{\eta_{\mathrm{abs}} P_{\mathrm{p}}}{h\nu_{\mathrm{p}}(N_{\mathrm{w}} L_{\mathrm{w}} A_{\mathrm{p}})} \tau(N). \tag{1.3}$$

Here η_{abs} is the pump absorption efficiency, $h\nu_{\mathrm{p}}$ is the pump photon energy, A_{p} is the pump spot area, and τ is the carrier lifetime. Carrier lifetime is given by

$$\frac{1}{\tau(N)} = A + BN + CN^2, \tag{1.4}$$

where A, B, and C are the monomolecular, bimolecular, and Auger recombination coefficients. From Eqs (1.1)–(1.4), we derive simple expressions for the threshold carrier density N_{th} and the threshold pump power P_{th}:

$$N_{\mathrm{th}} = N_0 (R_1 R_2 T_{\mathrm{loss}})^{-(2\Gamma g_0 N_{\mathrm{w}} L_{\mathrm{w}})^{-1}}, \tag{1.5}$$

$$P_{\mathrm{th}} = N_{\mathrm{th}} \frac{h\nu(N_{\mathrm{w}} L_{\mathrm{w}} A_{\mathrm{p}})}{\eta_{\mathrm{abs}} \tau(N_{\mathrm{th}})}. \tag{1.6}$$

VECSEL output power is then given by

$$P_{\mathrm{las}} = (P_{\mathrm{p}} - P_{\mathrm{th}})\eta_{\mathrm{diff}}, \tag{1.7}$$

where laser differential efficiency η_{diff} is

$$\eta_{\mathrm{diff}} = \eta_{\mathrm{out}} \eta_{\mathrm{quant}} \eta_{\mathrm{rad}} \eta_{\mathrm{abs}}. \tag{1.8}$$

The components of the differential efficiency are the output efficiency η_{out}:

$$\eta_{\mathrm{out}} = \frac{\ln(R_2)}{\ln(R_1 R_2 T_{\mathrm{loss}})}, \tag{1.9}$$

Table 1.1 Laser and material parameters used in the OPS-VECSEL laser threshold and output power calculations.

Parameter	Description	Value	Units
g_0	Material gain coefficient	2000	cm^{-1}
N_0	Transparency carrier density	$1.7 \times 10^{+18}$	cm^{-3}
Γ	RPG longitudinal confinement factor	2.0	—
L_w	Quantum well thickness	8.0	nm
R_1	On-wafer mirror reflectivity	0.999	—
T_{loss}	Round-trip loss transmission factor	0.990	—
λ_{laser}	Laser wavelength	980	nm
λ_{pump}	Pump wavelength	808	nm
d_{pump}	Pump spot diameter	100	μm
η_{abs}	Pump absorption efficiency	0.85	—
A	Monomolecular recombination coefficient	$1.0 \times 10^{+7}$	s^{-1}
B	Bimolecular recombination coefficient	1.0×10^{-10}	$cm^3\,s^{-1}$
C	Auger recombination coefficient	6.0×10^{-30}	$cm^6\,s^{-1}$

where R_2 is the laser output mirror reflectivity; the quantum-defect efficiency η_{quant}:

$$\eta_{quant} = \frac{\lambda_{pump}}{\lambda_{laser}}, \tag{1.10}$$

given by the ratio of pump λ_{pump} and laser λ_{laser} wavelengths; and the radiative efficiency η_{rad}:

$$\eta_{rad} = \frac{BN_{th}}{A + BN_{th} + CN_{th}^2}. \tag{1.11}$$

To illustrate laser design and operation, we choose typical material and laser parameter values for a ~1 μm emission wavelength InGaAs/GaAs optically pumped VECSEL laser, as summarized in Table 1.1. Figure 1.4 shows the interplay between the laser design and operational parameters, as calculated using the above model. Figures 1.4a and b show the threshold pump power and laser output power, respectively, as a function of the number of quantum wells in the structure for several external mirror reflectivities $R_{ext} = R_2$. Because quantum wells are so thin, only ~8 nm, they provide only a small amount of gain to an optical wave propagating normal to the plane of the well. With on-chip mirror reflectivity of 99.9%, typical output coupling mirror reflectivities need also be high and range between 96 and 99%; intracavity laser loss is assumed here to be 1%. Multiple wells are required for lasing, with approximately 5–15 wells minimizing laser threshold depending on the output mirror reflectivity. Lower output mirror reflectivity provides higher output coupling but has higher threshold and requires larger number of quantum wells for operation. With 100 μm pump spot size here, threshold pump powers range between 100 and 300 mW. For smaller number of wells, threshold power rises very rapidly, whereas for larger number of wells, the threshold increases only slowly.

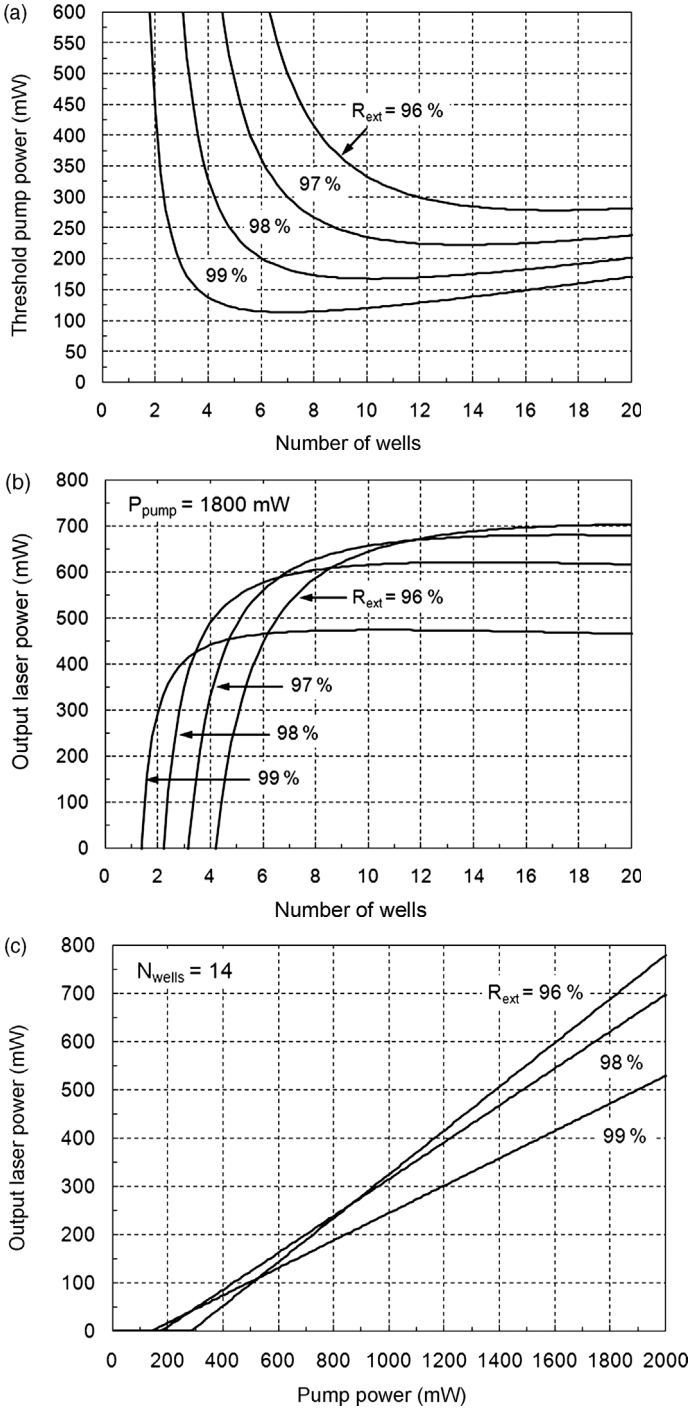

Figure 1.4 Calculated characteristics of the OPS-VECSEL lasers. (a) Threshold pump power versus the number of quantum wells. (b) Maximum output power versus the number of quantum wells. (c) Output power versus input power.

Figure 1.4b shows the calculated output laser power as a function of the number of quantum wells in the structure for several different external mirror reflectivities; the calculation assumes pump power of 1800 mW. Output power is maximized above 650 mW for the number of wells greater than 8–10 and external mirror reflectivities of 96–97%. Figure 1.4c shows the calculated output power of the laser as a function of the input pump power. Lower external mirror reflectivity increases output slope efficiency at the expense of the higher laser threshold.

Note that threshold power, Eq. (1.6), scales linearly with the pump, and laser, spot area; thus smaller pump spot areas are desired for lower thresholds. However, thermal impedance between VECSEL active region and heat sink increases with the decrease in pump area (Chapter 2), which leads to increasing active region temperatures, with the corresponding decrease in semiconductor gain and increase in laser threshold for such smaller pump areas. VECSEL lasers should be designed with the target output power in mind, and thus with approximate pump and thermal load levels. Given these power levels, pump spot size should be minimized such that thermal impedance and temperature rise are not too high; the number of quantum wells is then optimized for lower thresholds, and the output coupling mirror is optimized for highest output power at the available pump levels.

Here we have described a simple phenomenological analytical model of the semiconductor VECSEL; this model is useful to describe very simply and quickly the basic design and scaling principles of VECSELs, such as the number of quantum wells required, threshold pump levels and output power levels, output coupling optimization, and so on. This laser gain and power model should then be coupled with thermal models of VECSELs (Chapter 2) to define device thermal impedance and the desired pump/mode spot sizes, temperature rise of the active region, and the design wavelength offsets of the material photoluminescence PL peak and various cavity resonances [18]. Alternatively, detailed numerical microscopic models of semiconductor lasers can be used [117, 118]. Such models predict gain and emission properties of semiconductor materials without resorting to phenomenological description with adjustable model parameters; however such models are much more complex.

Multiple quantum wells required for laser gain are placed at the antinodes of the laser optical field standing wave, with none, one, or more closely spaced wells at each antinode, see Figure 1.3. Pump absorbing regions form the space between the antinodes. The number of quantum wells at the different antinodes is chosen such as to produce uniform quantum well excitation from the pump power that decays exponentially from the wafer surface as it is absorbed in the semiconductor. Placing quantum wells at the laser field antinodes resonantly enhances gain in this resonant periodic gain structure, as described by the confinement factor Γ. Such resonant periodic gain arrangement effectively eliminates spatial hole burning of the laser gain medium and enables simple single-frequency operation of these lasers, both with [55, 104] and sometimes without [119, 120] intracavity spectral filtering. Resonant gain enhancement, however, narrows the otherwise broad spectral bandwidth available from the laser gain medium. Such broad spectral bandwidth is desired, for example, for tunable laser operation or for ultrashort pulse generation. In

this case, quantum wells can be displaced from their antinode positions in the structure to provide larger gain bandwidth at the expense of lower gain enhancement that comes with the lower confinement factor Γ [18]. Another structural factor that affects VECSEL gain bandwidth is the etalon formed between the on-chip laser mirror and the residual reflectivity at the chip surface. When this etalon is resonant, gain bandwidth is narrowed, laser gain is enhanced, and laser threshold is lowered. Designing this etalon to be antiresonant enhances gain bandwidth at the expense of the lower gain [20, 74].

In semiconductor lasers, strained quantum wells are frequently used, both because this allows access to a larger range of laser wavelengths and because of the improved operating characteristics of strained quantum well lasers [4, 8], such as lower threshold and improved temperature dependence. Because a large number of strained quantum wells are typically used in a VECSEL wafer structure, their total thickness can easily exceed the Matthews and Blakeslee strain critical thickness limit [4, 8], leading to strain relaxation via crystalline defect formation, which destroys laser operation because of strong nonradiative recombination at such "dark line" defects. Strain compensation [8, 18] must be used in this case, where layers of semiconductor material with the opposite sign of strain are introduced near the strained quantum wells such as to balance out net strain in the wafer structure. For example, compressively strained InGaAs quantum wells on GaAs are commonly used for $\sim$1 μm laser emission. Here, using more than three strained quantum wells in the laser structure exceeds the critical thickness limit and requires strain compensation; tensile-strained GaAsP layers are typically used for strain compensation in this material system. Reliable semiconductor VECSEL operation has been obtained with such strain-compensated wafer structures [18] with over 35 000 h of lifetime data [54]. Using quantum dots in the laser active layers (Chapter 5) [99–102], instead of quantum wells, can provide further laser advantages, such as increased material gain bandwidth and improved temperature dependence [101]. VECSEL lasers utilizing quantum dot active regions are described in detail in Chapter 5.

1.3.1.2 On-Chip Multilayer Laser Bragg Mirror

The second critical component of the VECSEL semiconductor chip is the multilayer Bragg mirror that serves as one of the mirrors of the laser cavity, see Figures 1.2 and 1.3. As we have seen from the laser designs in Figure 1.4, on-chip laser mirror reflectivity should be very high, of the order of 99.9%, to keep laser thresholds low and output differential efficiency high. Since this mirror also forms a thermal barrier between the active region and the heat sink, another requirement is that mirror thermal impedance be low so that the active region has its heat dissipated efficiently and its temperature rise is limited. To produce efficient on-chip mirrors, multiple quarter-wave layer pairs of semiconductor materials with a high refractive index contrast are required. This yields high reflectivity with fewest layer pairs and thus lowest thickness and thermal impedance; good thermal conductivity of the mirror materials is also important. In addition, mirror materials should be nonabsorbing at the laser and, possibly, pump wavelengths. For optically pumped VECSELs, the mirror layers can be undoped, which significantly simplifies their epitaxial growth;

electrically pumped VECSELs require complex doping profiles in the mirror layers (Chapter 7). To achieve more efficient pump absorption in the pump absorbing regions, a pump light reflecting mirror can be included with the on-chip laser mirror; this, however, detrimentally increases the overall mirror thermal impedance. Higher thermal impedance of the on-chip laser mirrors can be counteracted somewhat by using front-side transparent heat spreaders (Chapter 2).

In the GaAs material system near 1 μm wavelength, high index contrast lattice-matched mirror materials, GaAs and AlAs, are available; a 30-pair mirror of such materials has the desired reflectivity with the mirror thickness of about 4.5 μm [18]. In contrast to GaAs, InP material system near 1.55 μm does not have such high contrast materials available; the InGaAsP/InP mirrors here require 48 quarter-wave pairs to achieve the desired reflectivity [121], with the resulting higher thermal impedance and significantly lower demonstrated output powers. Several alternatives have been explored for improved mirrors in this case. Metamorphic, or non-lattice-matched, semiconductor mirror materials have been used, for example, GaAs/AlAs mirrors on InP substrate, as well as hybrid metal-enhanced metamorphic mirrors [122, 123]. Dielectric mirrors [124] have also been used in VECSELs with optical pumping since no current injection is required in this case. But metamorphic and dielectric materials have poor thermal conductivity and such mirrors still have higher than desired thermal impedance. A novel way to overcome this material limitation is to use wafer fusion [97, 98]. In this approach, lattice-matched laser mirrors are grown on one substrate in a semiconductor material system with available high index contrast materials, while the gain medium is grown on a different substrate in another material system with the desired output wavelength range. The laser mirror and laser gain wafers with different lattice constants are then fused together; this is again much simpler for optically pumped structures where no current injection is required across the fusion interface. A dramatically improved output power performance, from 0.8 to 2.6 W CW, of 1.3 and 1.57 μm VECSELs was demonstrated using such an approach with InP-based gain wafer fused with GaAs/AlAs-based mirror wafer [97, 98].

1.3.1.3 **Semiconductor Wafer Structure**

Figure 1.5 shows an example of the full semiconductor window-on-substrate wafer structure of a 980 nm VECSEL. It follows the design principles outlined above and has been used in the first demonstration of high-power VECSEL lasers [18]. Starting from GaAs substrate, first the output window and then the gain region are grown, followed on top by the on-chip Bragg mirror structure. The active region contains 14 $In_{0.16}Ga_{0.84}As$ quantum wells of 8.0 nm thickness with 1.15% compressive strain. Each quantum well is paired with a 25.7 nm thick $GaAs_{0.90}P_{0.10}$ strain compensating layer with 0.36% tensile strain such that the net averaged strain of the structure is zero. These strain-compensated quantum wells are placed at the consecutive antinodes of the laser standing wave using $Al_{0.08}Ga_{0.92}As$ spacers that serve as pump absorbing layers and are designed for optical pumping at 808 nm. High-reflectivity Bragg mirror at the top of the structure consists of 30 pairs of $Al_{0.8}Ga_{0.2}As$/GaAs quarter-wave thick mirror layers. The total mirror thickness is 4.5 μm and it has a

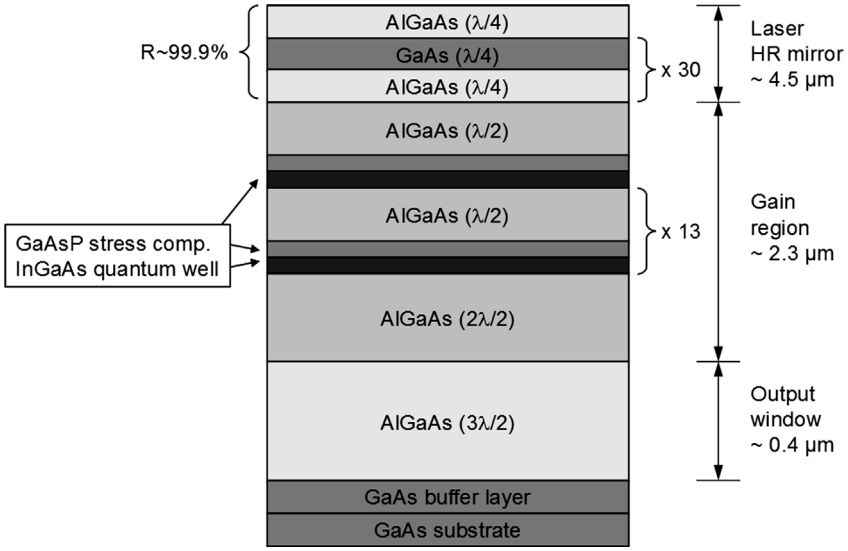

Figure 1.5 Semiconductor wafer structure of a 980 nm InGaAs/GaAs VECSEL laser.

thermal impedance of $21^{\circ}\,\mathrm{K\,W^{-1}}$ for a $100 \times 100\,\mu\mathrm{m}^2$ laser spot size [18]. VECSEL semiconductor wafer structures require very good epitaxial growth control of the layer compositions, thicknesses and strains; such control is available with the modern metal-organic vapor-phase epitaxy (MOVPE) [18, 57, 125, 126] and molecular beam epitaxy (MBE) [127–129] semiconductor growth techniques.

Optically pumped VECSELs require very little processing after wafer growth; no lithographic processing is required. To use such semiconductor chip in a laser, it is first metallized, thinned, and soldered mirror side down onto a diamond heat spreader; subsequently, the thinned GaAs substrate is removed by selective wet chemical etching [18, 130] and the exposed window surface is antireflection (AR) coated. This AR coating serves to eliminate pump reflection loss at the OPS chip surface. It also strongly reduces chip surface intracavity reflection at the laser wavelengths, thus weakening the subcavity etalon formed by the on-chip mirror and the surface reflection, which otherwise can limit tuning bandwidth of the laser. This AR coating can also be made with semiconductor layers grown epitaxially on the semiconductor wafer together with the other structure layers [107]. Diamond heat spreader with the soldered OPS chip is in turn soldered onto a thermoelectrically temperature-controlled heat sink. Copper heat sink is typically used; however, using diamond in place of copper heat sink [107] can further decrease the chip thermal impedance, limit its temperature rise, and produce higher output powers.

The VECSEL window-on-substrate wafer layer arrangement leaves no extraneous substrate material, with its excess thermal impedance, between the mirror and heat spreader and gives excellent high-power laser operation. An alternative is the mirror-on-substrate wafer structure, where mirror layers are grown first on the substrate,

followed by the active region and the output window [18]. Such mirror-on-substrate structures require back side substrate thinning, metallization, and soldering to heat sink. Handling thin semiconductor chips is very difficult; as a result, the residual substrate thickness is 15–30 μm with the corresponding thermal impedance and severe limitation to high-power laser operation [18]. Using front side transparent heat sinks with such structures, using materials such as sapphire [65], silicon carbide SiC [66], or single-crystal diamond [67], is very effective in addressing the thermal impedance problem and has demonstrated high-power laser operation (Chapter 2) [131].

1.3.2
Optical Cavity: Geometry, Mode Control, and Intracavity Elements

We next outline external optical cavity configurations used for VECSEL lasers; other than on-chip laser mirror, optical elements forming these cavities are external to the laser chip. VECSEL optical cavities allow control of the laser fundamental transverse mode operation as well as the insertion of various intracavity elements: saturable absorbers for laser passive mode locking, optical filters for laser wavelength selection and tuning, nonlinear optical crystals for intracavity second harmonic generation, and so on. Such optical cavities also allow combining of multiple gain elements in series for higher-power laser operation.

VECSEL lasers were first demonstrated with simple two mirror cavities [18, 65], as illustrated in Figures 1.2 and 1.6a. Later, as additional optical functional elements were added to the lasers, more complex three-mirror V-shaped cavities emerged. In one version of the V-shaped cavity, as illustrated in Figure 1.6b, the OPS gain chip serves as one end mirror of the cavity [57, 66, 97, 132], with the laser output taken variously either through the other end mirror [66, 97] or through the folding mirror [57, 132] of the cavity. In another version of the V-shaped cavity, as illustrated in Figure 1.6c, the OPS gain chip serves as the folding mirror in the middle of the cavity [20, 62, 133]. Four-mirror Z-shaped cavities, as shown in Figure 1.6d, give even more flexibility in placing intracavity functional elements and manipulating laser beam size at these elements [53, 131, 134]. Even more complex multimirror cavities have been used with two (Figure 1.6e) [49, 50] and three (Figure 1.6f) [135] active OPS gain chips in the cavity. Going beyond the above linear cavity configurations, a planar ring cavity has been used for a passively mode-locked VECSEL [136], and a nonplanar ring laser cavity has been used for a VECSEL-based ring laser gyro [137]. A diffractive unstable optical resonator has also been used with VECSELs where Gaussian beam output was extracted from a hard-edged outcoupling aperture [138].

A two-mirror, stable, plane–curved optical cavity (Figure 1.6a) [139] of length L_c and with curved mirror radius R_c has fundamental TEM_{00} laser mode beam $1/e^2$ diameters w_1 on the planar semiconductor chip and w_2 on the output spherical mirror given by

$$w_1^2 = \frac{4\lambda_{laser} L_c}{\pi} \sqrt{(R_c - L_c)/L_c}, \tag{1.12}$$

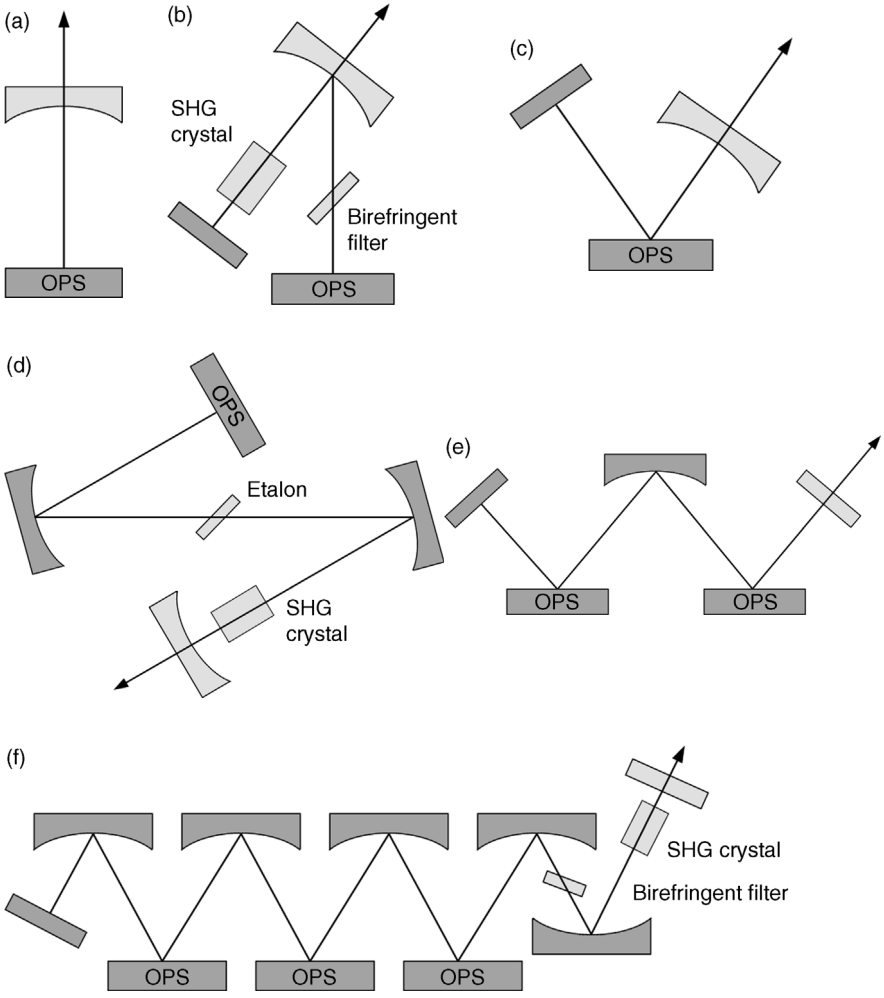

Figure 1.6 VECSEL laser cavities. (a) Two-mirror linear cavity. (b) Three-mirror V-shaped cavity for second harmonic generation (SHG). (c) Three-mirror V-shaped cavity for passive mode locking. (d) Four-mirror Z-shaped cavity. (e) VECSEL cavity with two gain chips. (f) VECSEL cavity with three gain chips.

$$w_2^2 = \frac{4\lambda_{\text{laser}} R_c}{\pi} \sqrt{L_c/(R_c - L_c)}. \tag{1.13}$$

Figures 1.7a and b illustrate variation of the laser mode diameters on the two cavity end mirrors as a function of the cavity length. Mode diameters on the chip between 100 and 200 μm can be easily achieved in this simple cavity for cavity lengths less than

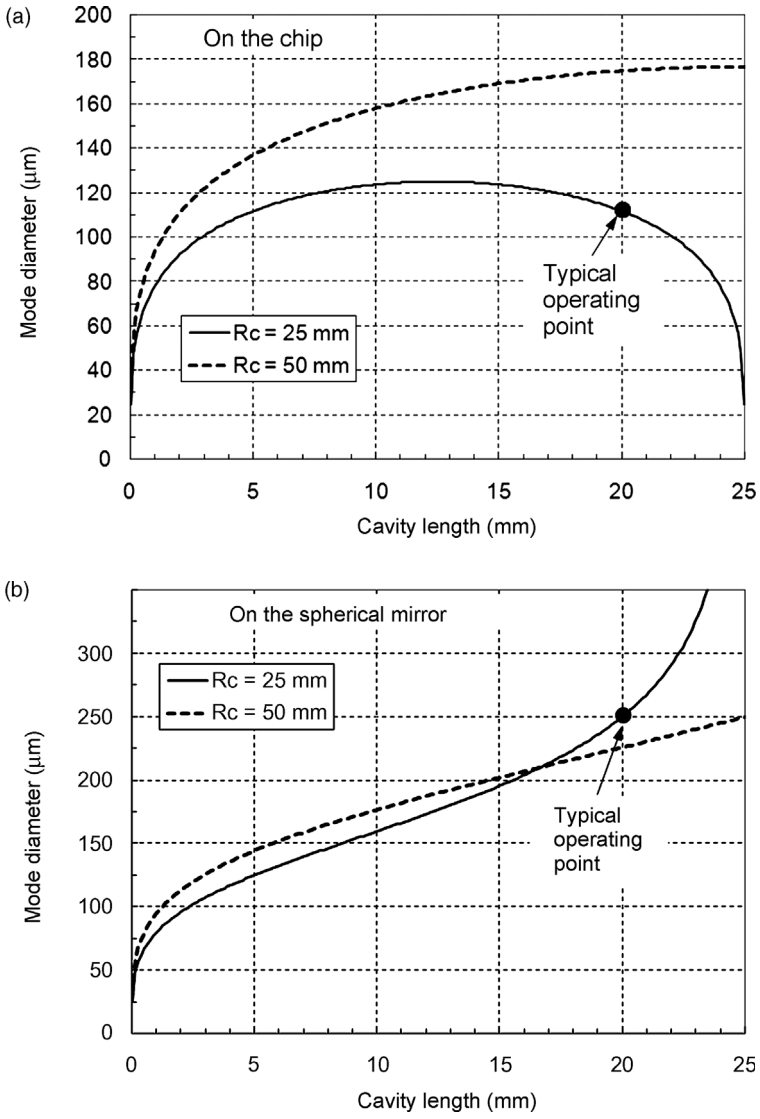

Figure 1.7 Mode spot $1/e^2$ diameters of the planar–spherical cavity (a) on the semiconductor chip w_1 and (b) on the output spherical mirror w_2 for spherical mirror radii of curvature of $R_c = 25$ and 50 mm and $\lambda_{laser} = 980$ nm.

25 mm. Pump spot size should be of the order of the laser mode size on the chip to provide efficient gain aperturing for fundamental transverse mode selection. Such two-mirror cavity VECSEL lasers have also been operated in unstable resonator regime with cavity lengths longer than mirror radius of curvature [18]. In this case, laser transverse mode is stabilized by gain aperturing with strong optical loss outside the pumped spot on the chip.

Another compact version of the two-mirror VECSEL cavity is the microchip laser configuration [69–71, 140], where a short plane–plane laser cavity is transverse mode stabilized by a thermal lens formed in the gain medium due to temperature gradients within the pump spot. Here, intracavity diamond heat spreader was used, with its planar outer surface coated with high-reflectivity output coupling mirror [70]; on-chip mirror is the second mirror of the cavity. Such arrangement allows very compact cavities; array laser operation was demonstrated for such microchip VECSELs [70]. Since thermally optimized VECSEL chip mounting, with on-chip mirror soldered on heat sink without intervening substrate, produces negligible thermal lensing [22], for microchip laser operation sufficient thermal impedance by design is required between the VECSEL chip and the heat sink. Microchip VECSELs operate optimally only within a well-defined window of pump powers and pump spot sizes. Intracavity thermal lens and a microchip mode of laser operation are also used in electrically pumped VECSELs (Chapter 7). Another version of a compact microchip VECSEL laser cavity does not rely on thermal lensing in the semiconductor, but instead uses spherical microlenses, or micromirrors, etched directly into outer surface of diamond heat spreaders in contact with the OPS chip surface [141–144]; arrays of such microchip lasers have also been demonstrated [143]. A potential compact laser cavity for VECSELs is the single-transverse mode optical resonator cavity [145], where shaping of the nonplanar resonator mirror can make all higher order transverse modes fundamentally unstable. Unlike other optically pumped VECSEL laser implementations, this resonator would require some lithographic processing of the semiconductor chip.

Inserting additional intracavity functional optical elements in the VECSEL typically requires additional mirrors for the laser cavity. Thus, a three-mirror V-shaped laser cavity was used for VECSEL passive mode locking [62], as in Figure 1.6c, with a flat SESAM semiconductor saturable absorber mirror at one end of the cavity, OPS gain chip as the folding mirror in the middle of the cavity, and a spherical output coupling mirror at the other end of the cavity. This cavity was only 3 mm long and demonstrated mode locking at 50 GHz high pulse repetition rate. The V-shaped laser cavity arrangement also allows controlling relative mode spot sizes on the gain and saturable absorber elements, with saturation intensity conditions of passive mode locking typically requiring smaller beam area on the absorber than the gain element (Chapter 6) [20].

An important enabling spatial flexibility of VECSEL laser cavities is the ability to inject pump light at various angles to the OPS chip without concern for pump beam divergence or specific beam angle. Thus, for passive mode locking in Ref. [62], pump beam was injected at 45° to the chip with incident beam direction in the plane perpendicular to the plane of the picture in Figure 1.6c. This pump flexibility is enabled by the thin disk nature of the laser gain medium with pump absorption length of the order of only 1 μm. A similar three-mirror V-shaped laser cavity (Figure 1.6b) is used extensively for VECSELs with intracavity second harmonic generation [57, 97, 132]. A four-mirror double-folded Z-shaped laser cavity with intracavity optical elements, such as the one shown in Figure 1.6d, has been used, for example, for VECSELs with intracavity second harmonic generation [88] and for passively mode-locked VECSELs [20].

Open multimirror cavities allow convenient insertion of intracavity optical elements. As shown in Figure 1.6c, for second harmonic generation [57], an intracavity birefringent filter is used for longitudinal mode, or wavelength, control and an intracavity nonlinear optical crystal is used for second harmonic generation. Several types of intracavity frequency-selective filters have been used for VECSEL laser frequency control, such as etalons [146], birefringent filters [104], volume Bragg gratings (Chapter 6) [59], and high-reflectivity gratings [60]. Such frequency-controlled VECSELs have demonstrated single-frequency laser operation with linewidth below 5 kHz [104].

Scaling VECSELs to very high output power levels can be accomplished by overcoming some of their thermal limitations with the use of multiple gain elements in series inside a more complex laser cavity, as first proposed in Ref. [18]. Two optically pumped semiconductor gain elements have been connected in series in the five-mirror VECSEL cavity illustrated in Figure 1.6e [50], producing 19 W CW at 970 nm. Two gain chips have been used in a four-mirror cavity for high-power generation in Refs [49, 147]. Scalable optically pumped two-, three-, and four-chip cavities of the type shown in Figure 1.6f have been used to generate as much as 66 W CW at the fundamental wavelength of 1064 nm and as much as 30 W CW at the second harmonic 532 nm green wavelength [135]. In order for such multielement VECSEL optical cavities to be practical, they must be stable to component and alignment perturbations as well as to long-term aging and drift; design of such dynamically stable cavities has been described in Ref. [52].

Power scaling of VECSELs typically requires large mode diameters on the gain chip to reduce device thermal impedance. A simple two-mirror cavity would need to be very long to achieve such large mode diameters, while a compact laser cavity is desirable. The design of such compact miniaturized cavities using Keplerian or Galilean telescopes to expand laser mode size has been described in Ref. [52]. A large 480 μm diameter mode size has been demonstrated in a small 8 cm footprint Keplerian telescope folded cavity, with 531 nm green laser TEM_{00} output power in the 10–20 W CW range [52]. A Galilean telescope folded cavity also demonstrated a large 480 μm diameter spot size in a miniature footprint of only ~1.5 cm, with 486 nm blue laser TEM_{00} output power of 7.3 W CW [52]. Such compact cavities are possible because of the thin disk nature of the optically pumped semiconductor medium with very short pump absorption depths and gain lengths. As a result, high power VECSEL lasers can be made with a footprint an order of magnitude smaller than conventional diode-pumped solid-state lasers [52].

Electrically pumped VECSELs use a modified version of the two-mirror cavity of Figure 1.6a; here a third "intracavity" partially transmitting mirror is added on the semiconductor chip such that the quantum well gain region is sandwiched between two planar on-chip mirrors (Chapter 7). This additional mirror helps reduce laser intensity and optical absorption in the lossy intracavity doped semiconductor substrate that serves as the current spreading layer and lies outside the "sandwiched" gain layer (Chapter 7). In this scenario, the low-loss laser cavity is predominantly defined by the high-reflectivity planar on-chip mirrors; relatively weak external spherical reflector serves only to stabilize the fundamental spatial transverse mode.

Another version of electrically pumped VECSELs with intracavity second harmonic generation uses a similar cavity configuration but with all planar mirrors and a volume Bragg grating serving as the output coupling mirror at the second harmonic (Chapter 7). Here, a thermal lens is used to stabilize the fundamental transverse mode of the laser.

VECSEL optical cavities acquire different dimensions when they are used for intracavity laser absorption spectroscopy [73, 75, 148, 149]. For ICLAS applications, one arm of the three-mirror resonator in Figure 1.6b, the one without the OPS gain chip, is made about 1 m long and an ~50 cm gas absorption cell is inserted inside the laser cavity. Equivalent intracavity absorption path lengths of greater than 100 km have been obtained with this technique, making ICLAS-VECSELs an extremely sensitive tool for absorption spectroscopy.

Note that OPS chip is sometimes used at normal reflection as an end mirror of the laser cavity, such as in cavity configurations shown in Figure 1.6a, b, and d. In these cases, laser optical wave on a single round-trip in the cavity passes the OPS gain medium twice. On the other hand, at other times, OPS chip is used as a cavity folding mirror reflecting laser optical beam at an angle, such as in cavity configurations shown in Figure 1.6c, e, and f, the last two being multichip cavity configurations. In these cases, laser optical wave on a single round-trip in the cavity passes the reflection folding OPS gain medium four times. Thus, the folding-mirror OPS chip provides twice the gain per round-trip in the laser, as compared with the end-mirror OPS chip configurations; this has to be taken properly into account when designing the laser.

As we have illustrated here, VECSELs use a rich variety of optical cavities [139] that have been originally developed for other types of lasers, such as diode-pumped solid-state DPSS lasers [13, 14]. Many of these cavities have been specialized for VECSEL lasers to allow compact size, when needed, and, using intracavity elements, a wide range of optical functions, such as single-frequency operation, short pulse generation, second harmonic generation, and ultrasensitive intracavity absorption spectroscopy. Such functional richness simply would not be possible in an integrated semiconductor device without external optical cavity.

1.3.3
Optical and Electrical Pumping

VECSEL lasers have been made with two types of excitation: optical [18, 22] and electrical (Chapter 7) [92, 93, 141, 150–153]. Electrical excitation of the laser by a diode current injection across a p–n junction is very appealing, as it requires only a simple low-voltage current source to drive the laser, rather than separate pump lasers with their pump optics and power supplies. For VECSEL lasers, however, electrical pumping has significant limitations. First, intracavity laser absorption in doped semiconductor regions required for current injection degrades laser threshold and efficiency. The second major problem is the difficulty of uniform current injection across the several hundred microns wide emission areas required for high-power operation. Pump current is injected from the perimeter of the light-emitting laser

aperture; thick current spreading doped semiconductor layers attempt to provide a more uniform current distribution across this aperture; however, intracavity free-carrier absorption in these doped layers is detrimental to the laser. This problem is somewhat mitigated by the three-mirror laser cavity that places current spreading absorbing regions in the lower light intensity section of the cavity (Chapter 7). Carrier transport across the multiple quantum wells and nonuniform electron and hole distributions across the wells also have to be considered. Significantly, as compared with optically pumped OPS wafers, electrically pumped VECSELs require a much more complex semiconductor wafer growth process with complex layer doping profiles, as well as post-growth lithographic processing (Chapter 7).

Optical pumping approach divides the functions of laser pumping and laser light emission between separate devices. While the final device requires multiple components and is more complex than the integrated electrically pumped approach, the individual components of an optically pumped VECSEL can be independently optimized, avoiding painful, or impossible, compromises inherent in an integrated device. Thus, a pump laser can be optimized separately for efficient high-power light generation without regard to beam spatial quality. OPS VECSEL structure is optimized for efficient pump power conversion to a high spatial quality beam, with wide output wavelength access and rich functionality, such as short pulse generation. As a result of such separate optimizations, optically pumped VECSELs have demonstrated more than an order of magnitude higher output power levels than their electrically pumped counterparts. In a hybrid approach, separate edge-emitting pump lasers have been integrated on the same substrate for optical pumping of a VECSEL structure [154].

What are the main advantages of the optical pumping of VECSELs? Optical pumping allows simple uniform transverse carrier excitation across very wide range of VECSEL emission apertures from 50 to 1000 μm in diameter. Also, no carrier transport from the surfaces through the multiple quantum wells across the device thickness is required, as pump light propagates throughout the device thickness to deliver the excitation. OPS wafer structures are undoped, which is easier to grow and produces no free-carrier absorption; also, no lithographic wafer processing is required. Multiple pump beams incident on a single pump spot from different directions can be used to excite a VECSEL. In an analogy with diode-pumped solid-state lasers [13, 14], an optical end-pumping scheme has also been used with VECSELs [155–158]. In this configuration, pump light enters through a transparent heat sink on one side of the OPS chip, and laser output is taken from the other side of the chip. In addition to single-stripe multimode semiconductor pump diode lasers, high-power multiple stripe diode arrays can also be used for direct VECSEL pumping [52]. The use of such poor beam quality pumps is made possible by the short absorption depth of semiconductors and is not possible with diode-pumped solid-state lasers that typically have absorption lengths on the scale of millimeters.

Pump diodes can be directly coupled to the OPS chip by means of relatively simple pump optics; alternatively, fiber-coupled pumps can be used. Pump optics should deliver a pump spot on the OPS chip that is approximately matched in diameter and serves as the gain aperture to the laser fundamental TEM_{00} transverse spatial

mode. Note that when pump beam is incident at an angle to the OPS chip surface, say between 30° and 60°, one incident pump beam dimension is elongated upon projection onto the OPS chip. Fiber-coupled pumps require simple spherical lenses for coupling to the OPS chip. Directly coupled pump diodes can use a combination of spherical or cylindrical lenses [18] and shape the highly elongated high aspect ratio pump beam to a square-shaped pump spot on the chip with aspect ratio close to unity. Figure 1.8 shows examples of pump optics arrangement [18] for VECSEL directly pumped by a pump diode chip. It is important to note that VECSEL pump optics is not an imaging arrangement; pump spot dimensions have to be right in a very thin plane of the OPS chip where pump light is absorbed. Pump beam does not have to be in focus in this plane; it does not matter how pump beam diverges before or beyond this plane. Pump beams are typically highly spatially multimoded, only an approximately uniform pump light distribution is required across the VECSEL laser mode aperture. If the pump spot becomes too large in diameter, in-plane amplified spontaneous emission (ASE) can potentially deplete laser gain [159]. Such in-plane ASE, if not controlled, will limit the lateral size of the laser pump spot and thus limit scaling of the output power of the laser. Photonic crystal structures can help in this regard. Connecting multiple OPS gain elements in series inside VECSEL laser cavity avoids such limitation to VECSEL power scaling.

As we have already mentioned, pump wavelength flexibility is a key feature of optically pumped VECSELs as compared to diode-pumped solid-state DPSS lasers. Semiconductors absorb light for all wavelengths shorter than the material bandgap

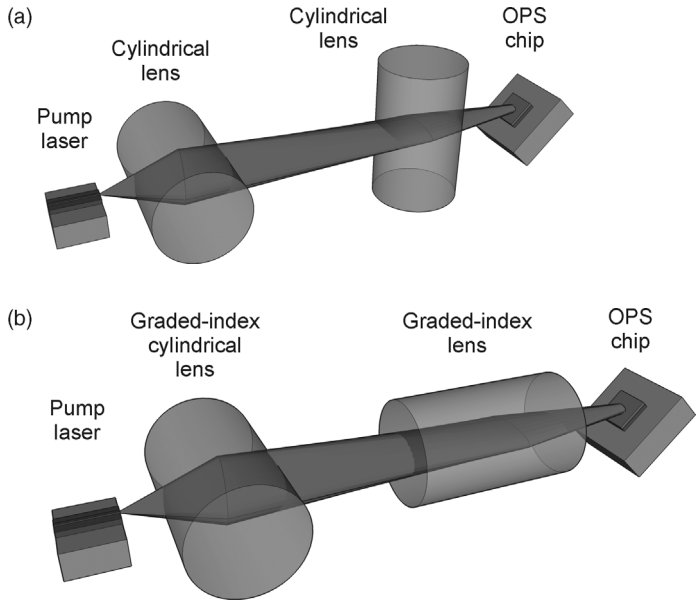

Figure 1.8 Examples of pump optics arrangement for direct pump diode pumping of VECSEL lasers. (a) Crossed cylindrical pump optics. (b) Cylindrical graded index (GRIN) lens followed by a graded index (GRIN) lens.

wavelength. Thus, pump diode lasers, which have a strong temperature dependence of their output wavelength, do not need to be temperature stabilized for VECSEL pumping applications. This significantly simplifies overall VECSEL laser system and avoids large power consumption of the temperature stabilization devices. Pump wavelength selection is also not critical, leading to a much higher yield, and hence lower cost, of the pump laser chips. As such, standard available wavelength pump lasers can be used for VECSELs, unlike solid-state lasers, where each laser type requires its own custom pump wavelength, for example, 808 nm for pumping ubiquitous Nd:YAG lasers or 941 nm for pumping Yb:YAG disk lasers. Pump wavelength can be very far from the laser emission wavelength; for example, 790 nm wavelength pump lasers have been used to pump 2.0 μm emission wavelength Sb-based VECSELs [94].

To prevent gain carriers from thermally escaping quantum wells, and thus depleting gain, energy difference between the confined well states of electrons and holes and the corresponding conduction and valence band edges of barriers between wells has to be at least 4–5 k_BT. Here, k_B is the Boltzmann constant and T is the absolute temperature; at room temperature, k_BT is ∼25 meV. If VECSEL pump light is to be absorbed in the barrier layers, this implies wavelength difference between pump and laser wavelengths has to be greater than ∼130 nm for laser emission near 1000 nm. This energy difference between pump and laser photons, the quantum defect, reduces laser-operating efficiency and also leads to excess heat generation. To improve VECSEL efficiency, it has been proposed that instead of barrier pumping, direct in-well pumping can be used with VECSELs, without changing barrier bandgap, thus reducing pump–laser quantum defect [44, 46]. One difficulty with this approach is that quantum wells are very thin and single-pass absorption in just a few wells is weak. Placing quantum wells at the antinodes of the pump wavelength resonant sub-cavity resonantly enhances such weak in-well pump absorption [47, 48]. One disadvantage of such resonant in-well pumping scheme is that tight, ∼4 nm, pump wavelength control is required [47], negating the broad acceptable pump wavelengths with barrier-pumped VECSELs. Another approach to alleviate weak in-well absorption problem is to use multiple pump passes [47], much as it is done with solid-state disk lasers [40, 41], using an on-chip pump mirror and pump-recycling optics outside the OPS chip.

An on-chip pump light mirror has been used to produce a more efficient double-pass pump absorption with barrier [64, 107] or in-well [47] pumping. Also, pump light mirror has been used to block pump light from bleaching saturable absorber in mode-locked VECSELs with integrated saturable absorber, MIXSEL [160, 161]. Such pump mirrors, however, can introduce additional undesired thermal impedance between the gain layer and the heat sink. Pump intensity decays exponentially with depth into semiconductor as pump photons are absorbed, while relatively uniform excitation of quantum wells is desired. Such a more uniform quantum well excitation can be achieved by varying the number of quantum wells at different antinodes, possibly skipping some antinodes, and also by adjusting with depth bandgap of the pump absorbing layers. Quantum well structures with graded gap barriers have been

used to improve pump absorption by reducing absorption saturation in the barriers through more efficient carrier collection in the wells [162].

Because of quantum defect between pump and laser light, as well as nonunity laser emission efficiency, excess heat is generated that has to be dissipated efficiently to the heat sink. This is done with back or front, transparent, surface heat spreaders, as discussed in detail in Chapter 2. Thermal impedance between the chip active region and the heat spreaders needs to be minimized. Proper heat sinking limits temperature rise of the gain region, which is critically important for laser operation since semiconductor gain can degrade significantly with temperature as carriers spread in the band due to thermal broadening of their energy distribution. Such temperature rise is typically the limiting mechanism for laser output power at higher pump powers. Another effect of temperature rise is wavelength red shift of the semiconductor bandgap and gain peak. In parallel, temperature rise also causes increase in semiconductor refractive indices with the resulting red shifts of the Bragg resonance wavelengths of the on-chip mirror and of the resonant periodic gain spectral peak, as well as of resonance wavelengths of the on-chip subcavities. Gain peak shifts with temperature much faster than the refractive-index-related wavelengths. Optimal VECSEL operation requires design of the gain and resonance spectral positions such that they overlap at the elevated laser active region operating temperature, which depends on the heat sink temperature and the chip active region dissipated power (Chapter 2) [18].

1.3.4
VECSEL Laser Characterization

A number of measurements can be performed on VECSEL laser components, for example, chip mirror and quantum well gain region, to characterize their operation and compare them to the design parameters. Some of these measurements can be performed on the wafer level; others are done on the thinned and AR-coated OPS chip already mounted on a heat sink. Another set of measurements characterizes the complete VECSEL laser operation.

VECSEL semiconductor wafer structure with its Bragg mirror and gain region layers can be characterized very effectively by using a spectrophotometer, which measures reflectivity spectra of these structures [18]. Both front and back side spectra can be measured, giving complementary information. Figure 1.9 shows such reflectivity spectra for the window-on-substrate and mirror-on-substrate wafer structures. The window-on-substrate reflectivity in Figure 1.9a, corresponding to the wafer structure in Figure 1.5, shows the broad, ~90 nm wide, mirror reflectivity band in the front side measurement; back side measurement shows the onset of quantum well absorption for wavelengths below 976 nm in the middle of the mirror band. The absorption dip is weak due to thinness of the wells. Subcavity etalon effects are not visible here since the weakly reflecting window–substrate interface in the wafer replaces the strongly reflecting window–air interface. Upon chip mounting and substrate removal, the window–air interface is exposed and wafer reflectivities look

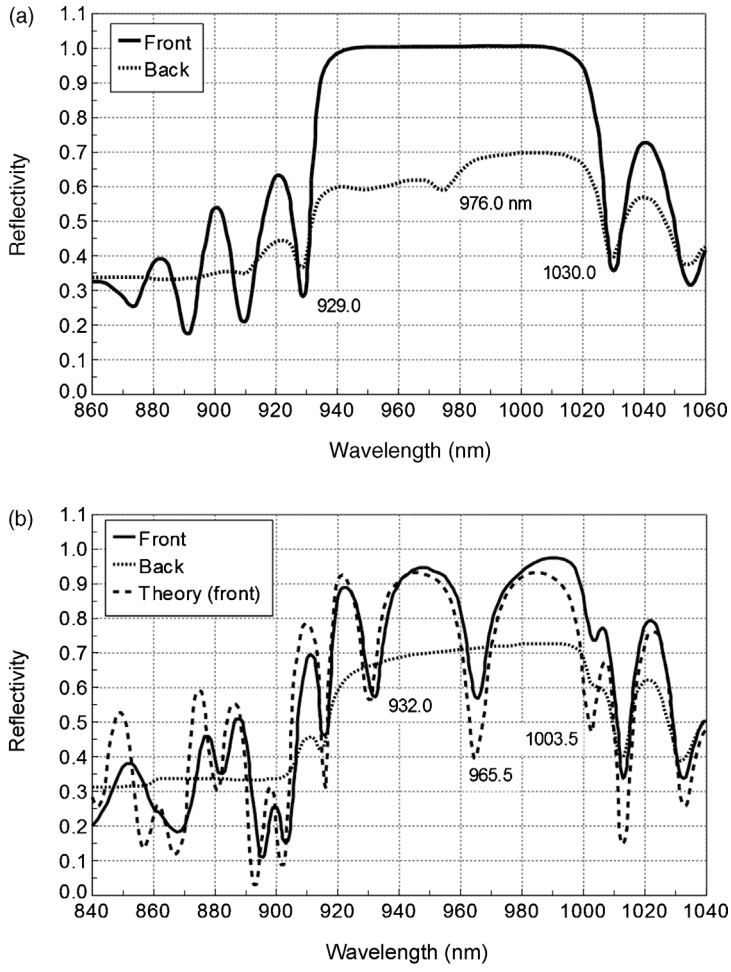

Figure 1.9 Reflectivity spectra of the OPS semiconductor wafers. (a) Window-on-substrate structure: front (epi) and back surface reflectivities; subcavity etalon effects are not visible. (b) Mirror-on-substrate wafer structure: front (epi) surface, back surface, and front surface theoretical reflectivities. Reflectivity dips at $\lambda = 932$, 966, and 1004 nm resonances of the mirror to chip surface subcavity etalon.

like those in Figure 1.9b. Figure 1.9b shows reflectivity spectra for mirror-on-substrate VECSEL structure similar to the one shown in Figure 1.5, except that the substrate appears on the mirror, rather than window, side of the structure. The back side reflectivity here is indicative of the intrinsic reflectivity spectrum of the multilayer mirror. The front side reflectivity spectrum shows strong effects of the subcavity etalon formed between the mirror and the semiconductor–air interface. In addition, weak intrinsic absorption of quantum wells located inside the subcavity etalon is strongly enhanced here by the etalon resonances. Thus, the front reflectivity

of the wafer shows strong dips near $\lambda = 932.0$, 965.5, and 1003.5 nm, corresponding to enhanced quantum well absorption at the longitudinal modes of this etalon. Such strong resonant enhancement of quantum well absorption is used effectively for in-well optical pumping of VECSELs [47, 48]. Reflectivity spectrum of the structure can be calculated from the layer thicknesses, refractive indices, and absorptions, and shows good agreement with the measured data. Semiconductor layer composition and thickness growth errors are immediately apparent from such measured wafer reflectivity spectra. Applying AR coating to the front surface of the OPS chip reduces and somewhat shifts the residual etalon dips, but does not eliminate them completely [18]. Upon optical pumping, VECSEL laser lases at the wavelength of one of these residual etalon resonances that corresponds to the highest available quantum well gain [18].

Quantum well gain medium is characterized at the wafer level by measuring its photoluminescence PL spectrum [18, 23, 163, 164]. Quantum wells emit light from inside the residual subcavity etalon; their photoluminescence spectrum is strongly modified by this etalon when emitting normal to the wafer surface and largely unaffected when light is emitted from the edge of the wafer [18]. Figure 1.10 shows measured photoluminescence spectra of a VECSEL wafer: broad edge-emitted spectrum and strongly narrowed surface-emitted spectrum with PL peaks corresponding to the etalon resonances [18]. Also shown is the surface-emitted spectrum from an AR-coated wafer that shows that etalon resonances are weakened and broadened but not completely eliminated. It is important to use edge-emitted PL spectrum for determining true spectral peak location of the quantum well material gain. Combination of the wafer reflectivity spectra and photoluminescence spectra shows spectral locations of the laser material gain and resonances peaks that localize laser emission. These spectral locations have to match at the operating temperature of the laser active region.

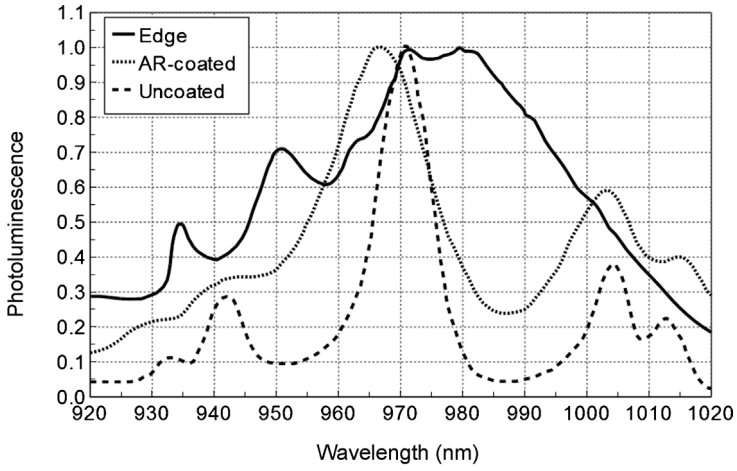

Figure 1.10 Normalized photoluminescence spectra of the OPS chips: surface-emission spectra of the AR-coated and uncoated OPS chips, and the edge-emission spectrum.

For strained quantum well OPS wafers, photoluminescence can be a strong indicator for the presence of dark line defects when total strained well thickness exceeds critical thickness [4, 8]. For example, for InGaAs/GaAs VECSELs emitting near 1 μm, when illuminating broad area of the wafer or a full OPS chip with pump light and observing photoluminescence with a camera, one can see in the PL image a pattern of crossed dark lines oriented along crystallographic [001] axes forming over time, especially about points on the chip that had been exposed to focused pump light. Such dark line defects form quickly over time and severely degrade laser performance [64]; using strain-balanced VECSEL structures [18] completely eliminates such dark line defects and produces fully reliable VECSEL lasers.

Once laser cavity and pump optics are aligned, there are a number of measurements that characterize the full VECSEL laser performance. The most revealing measurement is the output power versus pump power dependence, similar to theoretical calculation in Figure 1.4c; this measurement also produces the important values of laser threshold, output slope efficiency, total output efficiency, and maximum output power, whether limited by pump power or thermal rollover. Temperature dependence of these laser characteristics is another important measurement; here two temperatures are significant: the heat sink temperature, typically set by a thermoelectric cooler and measured by a thermistor, and the active region temperature, which can sometimes be estimated from the laser emission wavelength and its temperature dependence or from pump-dissipated power and OPS chip thermal impedance. The above laser output characteristics also depend strongly on the output coupling mirror reflectivity/transmission, as illustrated in Figure 1.4c; measuring this dependence gives an estimate of intracavity losses and enables the selection of the optimal output coupler. It is important to note that several pump powers are of relevance here: power emitted by the pump laser, pump power coupled to the OPS region by the pump optics, and finally the pump power absorbed in the OPS pump absorbing region. Spatial overlap, in size and shape, of the pump spot and laser mode should also be taken into account.

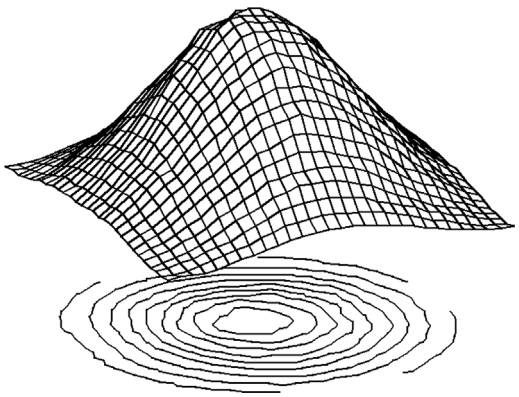

Figure 1.11 Measured output beam profile of the OPS-VECSEL laser.

For most applications, VECSEL output spatial beam quality is of utmost importance. Figure 1.11 shows an example of a measured OPS-VECSEL output beam profile with the desired circular fundamental transverse TEM_{00} mode operation. Beam quality can be characterized quantitatively by measuring its M^2 parameter [9, 50, 107, 142], which describes how much faster laser beam diverges in two transverse dimensions as compared with a diffraction limited $M^2 = 1$ Gaussian beam. The measured beam quality of $M^2 \sim 1.0$–1.5 for many VECSELs is considered to be very good. Such high-quality beam is required, for example, for confocal laser fluorescence imaging with free-space delivered [165] and single-mode fiber delivered beam [69]. $M^2 \sim 3$–4 beams have stronger divergence due to several transverse modes but are adequate for many other VECSEL applications [167], such as Coherent Inc. TracER™ laser illuminator for fingerprint detection [22]. Typically, somewhat higher powers can be extracted from VECSEL lasers in a multimode regime.

Determining spectral characteristics of VECSELs involves measurement of laser emission wavelength and spectral lineshape, as well as the dependence of these on the operating temperature and pump power [18]. For example, keeping pump power constant and adjusting chip temperature via the heat sink thermoelectric cooler, we can measure laser wavelength, typically defined by subcavity resonance, shift with temperature. This gives us a very useful "thermometer" of the active region. Later measurement of the laser wavelength shift with pump power above threshold, and using the above "thermometer" information, gives us the temperature rise of the active region with pump power and thus also an estimate of the active region thermal impedance and active region temperature at the laser-operating point. Additional measurements of the temperature and pump power dependences of the semiconductor photoluminescence spectra, both edge and surface emission, together with the above laser wavelength measurements, are important for ensuring proper spectral alignment of the laser emission and the gain and PL peaks at the laser-operating conditions (Chapter 2) [18, 163].

With intracavity tunable filter, tunable power dependence on emission wavelength becomes important [51]. For single-frequency VECSEL operation, laser linewidth and noise measurements define the relevant laser characteristics [120, 168]. Characterization of optical harmonic generation (Chapter 3) and mode-locked picosecond pulse generation (Chapter 6) in VECSELs is covered in detail in the other chapters in this book.

This section has outlined basic elements in designing, making, and characterizing VECSEL lasers. As is typical of semiconductor lasers, the many functional degrees of freedom offered by VECSELs require good understanding and precise control of the corresponding design and fabrication degrees of freedom. Extensive device characterization is critical as well, both for determining VECSEL operating parameters and for closing the design-fabrication-characterization loop and ensuring the above-mentioned laser design understanding and fabrication control. In the next section, we will describe the demonstrated performance ranges of VECSEL lasers as well as their applications and future scientific directions.

1.4
Demonstrated Performance of VECSELs and Future Directions

1.4.1
Demonstrated Power Scaling and Wavelength Coverage

Since the first demonstration of high-power optically pumped VECSELs in 1997 [17, 18], which emitted at wavelengths near 1000 nm and had output powers of about 0.5 W, many different VECSELs have been demonstrated with power levels from milliwatts to tens of watts and wavelengths from 244 nm in the UV to 5 μm in the mid-IR. Here we shall overview the power and wavelength scaling demonstrated with VECSEL lasers and the semiconductor material systems that have been used. Other chapters in this book describe in detail a variety of other aspects of VECSEL lasers and their demonstrated performance, such as mode locking and high repetition rate short pulse generation, thermal management of high-power VECSELs, visible light generation via second harmonic generation, quantum dot gain media VECSELs, long-wavelength NIR VECSELs, and electrically pumped VECSELs.

VECSEL lasers with a wide range of powers and wavelengths have been demonstrated both in university and government research laboratories across the world – United States, United Kingdom, France, Switzerland, Germany, Sweden, Finland, Korea, and Ireland – and in several commercial companies – Coherent, Novalux/Arasor, OSRAM, Samsung, Solus Technologies. VECSEL-related work has been published by scientists in Russia, Poland, Spain, Denmark, and China. There are also a number of commercial products based on the VECSEL technology. In a measure of the scientific, technological and commercial activities in VECSEL/OPSL/SDL lasers, more than 250 papers have been published in this field and more than 100 U.S. and international WIPO patents have been issued on the subject of these lasers. Utilizing flexibility of the VECSEL approach and with appropriate designs, efficient VECSEL operation has been demonstrated across a wide range of laser-operating parameters: from low to high output powers; for fixed and tunable wavelength operation; for fundamental and multiple transverse mode operation; for single-frequency and multiple longitudinal mode operation; for fundamental, second, third, and fourth harmonic wavelength operation; and for single and multiple gain chip laser operation.

Figure 1.12 summarizes in graphical form the demonstrated power and wavelength performance of VECSEL lasers, also shown are the major semiconductor material systems used in these demonstrations. Tables 1.2 and 1.3 list these results in tabular form and also include some other relevant VECSEL-operating parameters. Table 1.2 lists VECSELs with the fundamental wavelength output, while Table 1.3 has the frequency-doubled second harmonic output VECSELs.

The strain-compensated InGaAs/GaAsP/GaAs material system with fundamental output wavelengths in ~920–1180 nm NIR range is most widely used for VECSELs. In this material system, output power greater than 20W has been demonstrated in a single-transverse mode with excellent beam quality $M^2 \sim 1.1$ [107]. Still higher 30–40 W power levels were demonstrated in a slightly multimode regime with $M^2 \sim 3$ [22, 167]. This remarkable material system from its fundamental wavelength

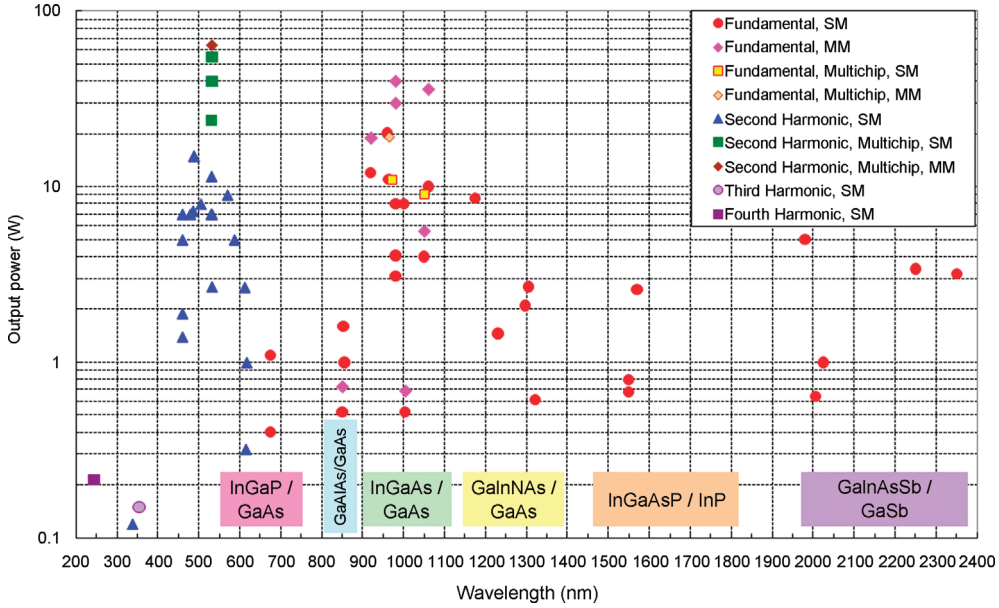

Figure 1.12 Demonstrated power and wavelength performance of VECSEL lasers.

range allows convenient and efficient intracavity frequency doubling to the visible blue–green–yellow range with the blue 460–490 nm, green 505–535 nm, and yellow 570–590 nm wavelength regimes. Power levels of 15 W in the blue [22] and 12 W in the green [52] have been demonstrated in a single-transverse mode with a single OPS gain chip. Using multiple gain chips, doubled green output powers of 40 and 55 W have been demonstrated with two and three gain chips, respectively [22], still in the fundamental transverse mode. Powers as high as 64 W in the doubled green have been demonstrated with three gain chips by going to a slightly multimode operation with $M^2 \sim 4$ [22]. Electrically pumped VECSELs in the NIR and doubled into the blue have also been made in the InGaAs/GaAs material system [177]. Using highly strained quantum wells in this material system, direct emission wavelengths can be pushed to the 1140–1180 nm range [87]. Here, intracavity-doubled output is in the yellow wavelength range, demonstrating with optical pumping output powers of 9 W at 570 nm [22] and 5 W at 587 nm [58]. Furthermore, in the same material system, using intracavity frequency tripling of the fundamental 1065 nm emission produces 355 nm ultraviolet output [108]. A commercial Genesis™ laser, from the OPSL laser family, from Coherent Inc., produces up to 150 mW at the tripled 355 nm UV wavelength [178]. In a different approach for short-wavelength UV generation, fundamental VECSEL emission at 976 nm in the NIR has been laser intracavity doubled to 488 nm blue, with this doubled VECSEL output further frequency doubled in an external cavity to the 244 nm deep UV wavelength, the fourth harmonic of the fundamental VECSEL NIR emission; 215 mW of deep UV radiation has been produced by this technique [77]. Thus, VECSELs with the InGaAs/GaAsP/GaAs material system, using fundamental, doubled, tripled, and quadrupled frequency

Table 1.2 Demonstrated wavelengths and powers of VECSEL lasers for the fundamental wavelength operation.

Operating wavelength (nm)	Pump wavelength (nm)	Output power, single mode (W)	Output power, multimode (W)	Pump power (W)	Material system	Transverse mode, M^2	Mode diameter (μm)	Transparent heat spreader or inverted structure	Output Coupling, %	No. of QWs	Tuning range, nm	References
674	532	0.4		3.3	GaInP/AlGaInP/GaAs		72	Tr.HS	2	20	10	[79]
675	532	1.1		7	GaInP/AlInGaP/GaAs		75	Tr.HS	3	20		[78]
850	660	0.523		2.4	AlGaAs/GaAs		100	Tr.HS	2.4	15	30	[66]
850	670		0.73	2.4	InAlGaAs/GaAs	5	70	Tr.HS	4	17		[86]
853	822	1.6		3.2	AlGaAs/GaAs	1.x	100	Tr.HS	3.8	14		[47]
855	806	1		30	AlGaAs/GaAs		110	Tr.HS	2	17		[45]
920	808		19		InGaAs/GaAsP/GaAs	3	500–900	Inv.			—	[167]
920	808		19	70	InGaAs/GaAsP/GaAs			Inv.				[22]
920	808	12		24	InGaAs/GaAsP/GaAs	2	250	Tr.HS	6	15		[68]
960	808	20.2		55	InGaAs/GaAsP/GaAs	1.1	430	Inv.	0.7	7	—	[107]
964	808	11		60	InGaAs/GaAsP/GaAs	1.75	355	Inv.	9	14/10		[50]
966	808		19.2	60	InGaAs/GaAsP/GaAs	2.14	355	Inv.	9	14/10		[50]
972	808	11		46	InGaAs/GaAsP/GaAs	1.7	355/410 + 420/480	Inv.	8	14/10	33	[51]
980	808		30		InGaAs/GaAsP/GaAs	3	500–900	Inv.			—	[167]
980	808		40	80	InGaAs/GaAsP/GaAs			Inv.				[22]
980	808	3.1		11	InGaAs/GaAsP/GaAs	1.15	220	Inv.		14		[169]
980	808	4.05		14	InGaAs/GaAsP/GaAs	1.6	230	Inv.	6	18		[130]
980	808	8		30	InGaAs/GaAsP/GaAs	TEM_{00}	430/500	Inv.	8	18	20	[61]
1000	808	8		20	InGaAs/GaAsP/GaAs	1.8	367	Inv.	6	14	—	[43]
1004	808	0.52	0.69	1.5	InGaAs/GaAsP/GaAs	TEM_{00}	100	Inv.	2-4	14	—	[17, 18]

1050	808	4	5.6	20	InGaAs/GaAs	1.15	165	Tr.HS	2	13	11.6	[170]
1050	800	9		42	InGaAs/GaAs	1.45	180	Tr.HS		13		[49]
1060	808		36	80	InGaAs/GaAsP/GaAs			Inv.				[22]
1060	808	10		24	InGaAs/GaAsP/GaAs	1.7	200	Tr.HS	6	15		[125]
1175	808	8.6		35	InGaAs/GaAsP/GaAs	1.5	500	Inv.	4	10	30	[58]
1220		3.5			GaInNAs/GaAs							[171]
1220		5			GaInNAs/GaAs							[172]
1230	808	1.46		18.2	GaInNAs/GaAs		180	Tr.HS	1	12	4.5	[88]
1297	808	2.1		23	AlGaInAs/InP		180	Tr.HS	1	10		[98]
1305	980	2.7		26	AlGaInAs/InP		180	Tr.HS	2.5	10		[98]
1322	810	0.612		8.62	GaInNAs/GaAs	1.2	75	Tr.HS	2	10		[67]
1550	1250	0.68		4.6	InGaAsP/InP	1.5/1.2	250	Tr.HS	1	20		[121]
1550	1250	0.8			InGaAsP/InP			Tr.HS				[80]
1570	980	2.6		25	AlGaInAs/InP		180	Tr.HS	2			[97]
1980	980	5		24	GaInSb/GaSb	1.4	160/175	Tr.HS	9	10	80	[103]
2005	808	0.64		16	GaInSb/GaSb			Tr.HS		15	35	[172]
2025	790	1		18	GaInSb/GaSb	1.45	180	Tr.HS	2	15		[94]
2250	980	3.4		21	GaInAsSb/GaSb	1.5	375/425	Tr.HS	5	10		[81]
2350	1960	3.2		13	GaInAsSb/GaSb		300	Tr.HS		15		[48]
5000	1550	0.003			PbTe/PbEuTe/BaF_2		200					[83]

Table 1.3 Demonstrated wavelengths and powers of VECSEL lasers for the frequency-doubled second harmonic output operation.

Operating wavelength (nm)	Pump wavelength (nm)	Output power, single mode (W)	Pump power (W)	Material system	Transverse mode (M^2)	Mode diameter (μm)	Transparent heat spreader or inverted structure	No. of QW	Tuning range (nm)	References
338	532	0.12	5.8	GaInP/AlInGaP/GaAs		75	Tr.HS	20	4	[78]
460	808	1.4		InGaAs/GaAsP/GaAs						[157]
460	808	1.9	20	InGaAs/GaAsP/GaAs		140	Tr.HS	30		[173]
460	808	5		InGaAs/GaAsP/GaAs	1.1	500–900	Inv.		—	[167]
460	808	7	52	InGaAs/GaAsP/GaAs			Inv.			[22]
479	808	7		InGaAs/GaAsP/GaAs			Inv.			[22]
486	808	7.3	38	InGaAs/GaAsP/GaAs	1.2	700	Inv.		—	[52]
488	808	15		InGaAs/GaAsP/GaAs	1.x	500–900	Inv.		—	[167]
488	808	15	55	InGaAs/GaAsP/GaAs			Inv.			[22]
505	808	8		InGaAs/GaAsP/GaAs			Inv.			[22]
530	808	7	33	InGaAs/GaAsP/GaAs			Inv.			[22]
531	808	11.5	40	InGaAs/GaAsP/GaAs	1.04	700	Inv.		—	[52]
531	808	24	110	InGaAs/GaAsP/GaAs	—	700	Inv.		—	[52]
532	808	2.7		InGaAs/GaAsP/GaAs						[157]
532	808	7	26	InGaAs/GaAsP/GaAs						[156]
532	808	40	140	InGaAs/GaAsP/GaAs	1.3	900	Inv.	Two chips		[22]
532	808	55	200	InGaAs/GaAsP/GaAs	1.3	900	Inv.	Three chips		[22]
532	808	64	250	InGaAs/GaAsP/GaAs	~4	900	Inv.	Three chips		[22]
570	808	9		InGaAs/GaAsP/GaAs			Inv.			[22]
587	808	5		InGaAs/GaAsP/GaAs		500		10	15	[58]
610	805	0.03	2.2	GaAsSb/GaAs		80	Inv.	6		[174]
612	788	2.68	36	GaInNAs/GaAs		290	Tr.HS	10	8	[53]
615	808	0.32	18.2	GaInNAs/GaAs		180	Tr.HS	12	4.5	[88]
617	790	1	45	GaInNAs/GaAs		290	Tr.HS	12		[175]
639		1			1.5		Inv.			[176]

output, have produced emission from 244 nm in the deep UV to the 1180 nm in the NIR, a span of more than two octaves, with output powers from a few milliwatts to 64 W.

As a side note, conventional intracavity frequency-doubled solid-state lasers are susceptible to the so-called "green problem" [179], where lasers exhibit strong intensity noise due to nonlinear interactions between multiple modes of the laser. Intracavity frequency-doubled OPSL lasers do not suffer from the green problem [54] because of the short carrier lifetime in semiconductors and the resonant periodic gain structure of OPSLs that does not allow spatial hole burning. Thus, intracavity frequency-doubled OPSLs have stable, low-noise output, so important for the majority of applications.

Still using GaAs substrates, the unstrained GaAlAs/GaAs material system accesses directly the 850 nm wavelength region [55, 66, 120, 146], with powers as high as 1.6 W [45, 47] demonstrated with in-well pumping. The same wavelength window is accessed with barrier pumping by the strained InAlGaAs/InAlGaAsP/GaAs material system using quaternary quantum wells and quinary strain compensating layers [86]. Still shorter wavelengths near 675 nm in the red are accessed directly using the InGaP/AlGaInP/GaAs material system [78, 79], demonstrating 1.1 W output power. Such direct red-emitting VECSELs have also been pumped by GaN diode lasers [180]. Red-emitting VECSELs allow intracavity frequency doubling into the UV wavelength regime, demonstrating 120 mW output at 338 nm wavelength [78].

The shortest wavelength direct emission VECSEL demonstrated so far is the InGaN/AlGaN/GaN device that operated near 390 nm violet wavelength [95, 96]. One difficulty with such short-wavelength devices is finding a suitable simple pump source; in this case, the device was pumped by a frequency-tripled Q-switched pulsed output of a Nd:YAG laser [95].

Extending VECSEL wavelengths to the 1200–1350 nm NIR range has been accomplished using the GaInNAs/GaAs dilute nitride material system on GaAs substrates [127]. Output powers as high as 1.4 W at 1230 nm [88] and 0.6 W at 1322 nm [67] have been demonstrated; microchip mode of operation has also been reported in this material system [181]. Watt-level emission has been demonstrated in this material system at wavelengths as short as 1160–1210 nm [182]. Recently, using AlGaInAs/InP material system and wafer fusion with GaAs-based mirror, output power of 2.7 W has been demonstrated at 1300 nm wavelengths [98]. This wavelength region is also important since it allows frequency doubling to the visible orange, 590–620 nm, and red, 625–700 nm, wavelengths. Powers as high as 2.7 W have been demonstrated by this approach in the 612–617 nm orange–red wavelength region [53, 88, 175]. Such doubled orange–red emission VECSEL has also been demonstrated using the GaAsSb/GaAs material system [174]. In fact, the NIR range of such GaAs substrate VECSELs should be extendable all the way to the 1550 nm wavelength region using the GaInNAsSb/GaAs quinary material system [183].

The important 1500–1600 nm wavelength window for optical fiber communication applications is covered by the InGaAsP/InP or InGaAlAs/InP material systems on InP substrates. Low refractive index contrast in this material system leads to thick,

high thermal impedance laser mirrors; nevertheless, VECSEL output powers as high as 0.8 W have been demonstrated [80, 121]. Using wafer fusion with GaAs-substrate-based mirrors, the InGaAlAs/InP active region has demonstrated still higher VECSEL powers of 2.6 W [97, 98]. Electrically pumped VECSELs have also been fabricated with 1550 nm emission wavelengths using InP-based material system [92, 93, 152].

The 2000–2400 nm emission wavelength mid-IR region is covered by the GaInAsSb/GaSb material system. Output power as high as 5 W has been demonstrated at 1980 nm using standard 980 nm diode pump [103]. More than 3 W output has been achieved at 2250 nm using 980 nm diode pump with a single-chip [81] and dual-chip [184] configurations, and at 2350 nm using 1960 nm thulium-doped fiber laser for in-well pumping [48, 185]. Even longer wavelength VECSELs with emission wavelength near 4.5 and 5 μm have been demonstrated using IV–VI lead–chalcogenide semiconductor material systems of PbTe (PbSe)/PbEuTe on both BaF_2 and Si substrates [82–85]. The long-wavelength VECSELs are discussed in more detail in Chapter 4.

Another approach to extend VECSEL emission to the mid-IR and THz wavelength region is to use difference frequency generation [186], for example, with a dual-wavelength VECSEL [109–111]. Such nonlinear optical difference frequency generation has been analyzed in Ref. [187], where dual emission VECSEL wavelengths at 984 and 1042 nm are considered for 17.7 μm wavelength generation.

VECSEL lasers have also been used for generation of even longer wavelength broadband terahertz radiation in the 0.1–0.8 THz frequency range [115], which corresponds to 0.4–3.0 mm wavelength range. In this terahertz spectrometer arrangement, 480 fs pulses from a passively mode-locked VECSEL laser at 1044 nm were used to illuminate both the emitter and the receiver photoconductive terahertz antennas [115]. The accessible terahertz spectral range in this technique is given by the broad spectral bandwidth of the short pulses from a passively mode-locked VECSEL.

Broad gain bandwidth of semiconductor materials allows appreciable amount of wavelength tuning from VECSELs, which has indeed been demonstrated in many of the above material systems, as indicated in Tables 1.2 and 1.3. For example, 80 nm tuning range has been demonstrated near 1980 nm emission wavelength in the GaSb material system [103]. Even higher tuning range of 156 nm from 1924 to 2080 nm is reported in Ref. [188]. A tuning range of 33 nm has been demonstrated near 972 nm emission wavelength in a two-gain-chip VECSEL laser in the InGaAs/GaAs material system [51]. Intracavity frequency-doubled VECSELs typically exhibit half the tuning range at the second harmonic wavelength as the laser is capable of at the fundamental wavelength. Thus, for example, frequency-doubled yellow laser at 587 nm wavelength exhibits 15 nm of tuning, as compared to the 30 nm tuning range at the fundamental 1174 nm wavelength [58].

To summarize, in the short time since VECSELs were first developed, their demonstrated wavelengths span from 244, 338, and 355 nm in the UV; to the violet, blue, green, yellow, orange, and red wavelengths in the visible 390–675 nm range; to the 850–1570 nm NIR wavelength range; to the 2.0–2.35 μm mid-IR range; to the

5 μm further out in the mid-IR, and even out to terahertz radiation with 0.4–3.0 mm wavelength range. What is important is that these wavelengths were targeted by design, often as required by specific application wavelength requirements. At some of these wavelengths, the materials for which had been subject of extensive development, power levels from watts to tens of watts had been demonstrated with excellent beam quality. At other wavelengths with less-developed materials, power levels of tens and hundreds of milliwatts are more typical. This wavelength and power flexibility of VECSELs, together with their beam quality and other advantageous properties, are key to the growing list of VECSEL applications, which we will discuss next.

1.4.2 Commercial Applications

In their initial application, VECSEL lasers were developed as high-power single-mode fiber-coupled sources at 980 nm for pumping Er-doped fiber and glass-waveguide amplifiers for optical fiber telecommunications systems [169, 189, 190]. Commercial optically pumped OPSL lasers from Coherent Inc. and electrically pumped NECSEL lasers from Novalux Inc. were targeting these potentially large telecom markets. Eventually, however, edge-emitting pump diode lasers came to dominate these applications. VECSEL lasers have been used in research for pumping other solid-state lasers, such as 2 μm emitting Tm- and Ho-doped lasers pumped by a 1 W GaInNAs/GaAs semiconductor disk laser at 1213 nm [182, 191, 192].

With the development of the intracavity frequency-doubled VECSEL lasers with emission wavelengths in the visible, the wavelength versatility of VECSEL, in combination with power scalability and beam quality, became key to their many successful commercial applications. Coherent Inc. pioneered the development and application of commercial OPSL lasers. Doubled into blue OPSL lasers with output at 460 and 488 nm became very successful solid-state replacements for Ar-ion lasers in a wide range of fields. As compared to the big, power inefficient, and limited lifetime Ar-ion lasers, blue OPSL lasers offer compact size, efficiency, low power consumption, beam pointing stability, excellent solid-state reliability with greater than 50 000 hours lifetime, and so on, thus bringing semiconductor laser advantages to visible wavelengths and power levels not previously addressable by these lasers. The option of fiber-coupled delivery of the OPSL laser output is also important for many applications. Relatively fast, 50 kHz–30 MHz and higher, direct modulation capability of OPSLs via pump current modulation is key to many applications, as it eliminates the need for separate acousto-optic modulators, required for the conventional diode-pumped solid-state DPSS lasers. One of the early applications of the OPSL 460 nm blue laser from Coherent Inc. was in laser-based digital to film recorders for transferring digitally produced or edited movies onto conventional 35 mm celluloid master film for cinema projection. ARRILASER film recorder from the ARRI Group uses a blue OPSL laser, together with red and green laser sources,

and has been awarded a Scientific and Engineering Award, Oscar, in 2002 by the US Academy of Motion Pictures Arts and Sciences.

With doubled into blue OPSL output powers scalable in the 10–200 mW, these lasers found wide application in bioinstrumentation for confocal fluorescence microscopy [165, 166, 193–197], flow cytometry [198], optical trapping, and manipulation of cells [199], cell sorting, DNA sequencing, proteomics, drug discovery, and so on [16]. In most of these bioapplications, fluorescent marker dyes are used to label functional molecules in the cells, and laser-excited fluorescence from these marker dyes is then detected or imaged. Alternatively, green fluorescent protein gene, and its other fruit color variants [200], can be directly expressed in the cells of many different organisms, and the GFP fluorescence is then used to monitor gene expression in the cells [16]. Specific wavelengths are required for optimal excitation of this imaging fluorescence [198, 200]; OPSL lasers have been designed with emission targeting these wavelengths. The initial blue wavelengths of commercial OPSL lasers have later been expanded to the green: 532 nm, yellow: 561 and 577 nm, red: 639 nm, and ultraviolet: 355 nm emission. The availability of true CW UV emission from OPSL lasers is important for biological applications, where pulsed UV light from the more conventional solid-state lasers can damage biological samples because of the high peak powers of the pulsed lasers.

Coherent Inc. has also developed commercial high-power versions of OPSL lasers with CW output powers in the 0.5–8 W range, with single- and multitransverse mode emission, and, remarkably, with a laser head size as small as $12 \times 5 \times 7\,\mathrm{cm}^3$. This combination of UV through visible wavelengths and a range output powers addresses a variety of new applications. Multiwatt green output OPSLs have been used to pump femtosecond mode-locked Ti:sapphire lasers [201]. Multiwatt green, blue, and yellow wavelength OPSL lasers have been used in a portable, battery-powered laser source for crime-scene fingerprint and trace evidence detection [22, 202]. For these applications, efficient battery-powered operation became possible because of the efficiency of the OPSL optical conversion of pump light and that the OPSL pump diodes do not require power-consuming tight wavelength/temperature stabilization of the kind required by the conventional diode-pumped solid-state lasers. Another application area for OPSL lasers is in entertainment, where multiwatt bright color blue, green, and yellow lasers with good beam quality are very effective for laser light shows.

Multiwatt 532 nm green and 577 nm yellow OPSL lasers have been used in ophthalmology for photocoagulation treatment of eye diseases, such as wet-form macular degeneration and diabetic retinopathy [203]. The yellow 577 nm wavelength is especially effective since it matches the absorption peak of the oxygenated hemoglobin in blood. As a result of this wavelength matching, the OPSL laser delivers effective treatment while less light is absorbed in the surrounding tissue.

Red, green, and blue lasers can be combined for RGB color projection displays [204], ranging in size from full cinema projection [205] to laser television [206], to mobile micro projectors [207]. Laser projection displays can be made in three different types [207]. The first type is a laser scanning or "flying spot" projector [208], where three primary color lasers are combined into a single beam and a mirror

system is used to scan this single-pixel beam in 2D over the imaging screen surface. The second type is a line scanning projector, where primary color lasers illuminate a linear array of pixels in a 1D spatial light modulator, such as grating light valve (GLV) [209], the resulting line image is then projected onto a screen and scanned by a mirror in 1D to produce a full image. The third type is an imaging projector, where primary color lasers illuminate a 2D spatial light modulator pixel array, such as Texas Instruments' digital micromirror digital light processor (DLP) chip, the resulting full image is then projected onto a screen. For example, Microvision's mobile pico projector uses the first "flying spot" approach [207]. Sony has been developing the second line scan approach for laser TV applications using GLV technology [207]. The same GLV line scan approach is used by Evans & Sutherland in its ESLP®-8K laser projector [205]. Mitsubishi's LaserVue® TV uses the third 2D imaging approach. Such laser projection displays with saturated primary RGB colors can access a much wider color gamut [204] than is available from other display technologies, such as liquid crystal and plasma displays. Different levels of laser power, from milliwatts to many watts, are required for different size displays. Visible OPSL lasers can be used with all three types of laser displays and will play an important role here because of their power scaling, efficiency, beam quality, fast direct modulation capability, and access to the desired emission wavelengths.

A number of companies have been working to develop OPSL/SDL/VECSEL lasers for these display applications, such as Coherent, OSRAM, Samsung, and Novalux/Arasor. For mobile micro/pico projectors, such as the one developed by Microvision Inc. using the "flying spot" laser scanning approach, direct emission blue and red diode lasers are available; however, the green lasers are not available because of the semiconductor material limitations. Doubled from NIR into green, several semiconductor laser approaches are being developed, including an externally doubled diode laser from Corning and an intracavity frequency-doubled OPSL laser from OSRAM Opto Semiconductors [207, 208]. OSRAM's green OPSL laser for mobile projectors emits 70 mW at 530 nm, measures only $13 \times 6.5 \times 4.8\,\text{mm}^3$, and is capable of direct modulation at rates greater than 30 MHz. Novalux/Arasor has been developing NECSEL™ electrically pumped VECSELs for display applications [210], such as DLP-based LaserVue TV from Mitsubishi [206]; these lasers are among the lasers used in the Evans & Sutherland ESLP-8K high-resolution $8\,\text{K} \times 4\,\text{K}$ digital theater laser video projector [205].

Accessing a mid-IR 1.9–2.5 μm wavelength range, Solus Technologies has developed a 100 mW narrow linewidth laser source for a range of applications from gas sensing and molecular spectroscopy [106] to medical. Such lasers are potentially capable of watt-level operating powers, 100 nm wide tuning range, and single-frequency operation.

It is remarkable for this young technology that such a diversity of commercial OPSL lasers is available, with wavelengths from UV to mid-IR and output powers from milliwatts to watts, and that such a wide variety of applications is addressed, from bio-medical to forensics and to displays. This testifies to the flexibility and versatility of OPSL lasers that can successfully address all these varied application

requirements and where there is simply no other laser that can do the job as effectively.

1.4.3 Current and Future Research Directions

Future research directions and applications of VECSELs will surely reflect the already demonstrated versatility of the VECSEL laser platform. Output power scaling of VECSELs will continue to be a topic of interest. Power scaling can utilize a number of approaches, such as increasing mode area and pump spot size while controlling and limiting the in-plane amplified spontaneous emission that can deplete the gain [159]. Further improvements in efficient heat removal (Chapter 2) will help, such as using the highest thermal conductivity diamond heat spreaders and heat sinks [107], front and back side heat removal from the OPS chip, design and fabrication of low thermal impedance semiconductor structures, and so on. Further power scaling will be achieved by using multiple gain chips [22, 49, 50, 52, 184], with larger mode area per chip, from the current maximum $\sim$0.9 mm diameter, and a larger number of OPS gain chips, from the presently demonstrated maximum of three chips. Still further power scaling is possible by spectrally combining multiple laser beams at different wavelengths, as demonstrated by combining two VECSEL lasers preserving excellent beam quality using a volume Bragg grating [211]. VECSEL output powers of several hundred watts, at the fundamental or the second harmonic, should be achievable with excellent beam quality using some combination of the above techniques. At the same time, demonstrating compact and efficient, low-cost, manufacturable VECSELs with modest milliwatt- to watt-level output powers will also be important for many applications, such as mobile projection displays [207].

Wavelength scaling of VECSELs will likely proceed along two paths: one will be application-driven demonstrations of new wavelengths using the existing semiconductor material systems and techniques; the other will explore new wavelengths by using novel material systems or novel nonlinear optical techniques to expand the versatility of the VECSEL approach. In addition to novel semiconductor material systems, finding suitable pump lasers and efficient pumping schemes for new VECSEL wavelength regions will also be important. For example, direct blue emission in the GaN material system [95, 96] with high powers and good beams would be very useful; however, suitable pump diode lasers are not readily available at the required wavelengths. Perhaps a multistage cascade of intracavity frequency-doubled VECSELs can be demonstrated, where output of one stage of such cascade is used to pump the next stage of the cascade. A variety of nonlinear optical frequency conversion schemes should expand the range of accessible wavelengths: intracavity frequency doubling, tripling, and quadrupling; sum frequency generation; difference frequency generation from dual wavelength lasers for accessing new mid-IR wavelengths [109, 111], such as 17.7 μm [187]; a combination of laser intracavity and extracavity nonlinear conversions [77]; and using single and

multiple lasers for nonlinear optical conversions. VECSELs can become an important compact source of broadband terahertz radiation by using ultrashort pulse mode-locked VECSELs in combination with photoconductive antennas [115]. To summarize, VECSELs wavelength coverage range will extend deeper into the UV and further into mid-IR, as well as start filling in the gaps in the existing wavelength coverage.

Tunable wavelength operation will prove important for many VECSEL applications. The target here will be to extend the relative wavelength tuning ranges from the currently demonstrated 3–8%, 33 nm tuning near 972 nm [51], 80 nm tuning near 1980 nm [103], and 156 nm tuning near 2000 nm [188], to the 10–15% level. The ways to achieve this will include using broadband gain semiconductor materials, such as quantum dots (Chapter 5); broadband OPS chip gain structures with quantum well, or dot, layers displaced somewhat from their periodic RPG positions [18, 130]; multiple, nonidentical gain chips in the cavity [51]; and, also important, low-loss tunable filters. Single-frequency tuning of VECSELs [55, 140, 164] is also important and will see further development for some applications, such as laser sources for atomic clocks [120, 146] and spectroscopy [106].

Development of new semiconductor materials both for gain and on-chip mirror structures will enable better performance of VECSELs and expand their operating range in terms of power, wavelength, tuning range, and so on. New semiconductor material systems with binary, ternary, quaternary, and quinary alloys can enable easier materials growth with fewer defects for the gain region and better index contrast and lower thermal impedance for the VECSEL mirrors. Unstrained or strain-compensated quantum well structures will be required in these material systems. Further development of the quantum dot active region (Chapter 5) [99–102] will enable VECSELs with reduced thresholds, wider gain bandwidth, and reduced temperature dependence [101]. Bonding wafers of different semiconductor materials using wafer fussion [97, 98], such as for bonding separate VECSEL mirror and gain wafers, eliminates some of the material limitations in VECSELs. Expanding the use of this technique will enable a range of novel better performing devices, for example, with higher powers and at new wavelengths. Wafer fusion of other VECSEL functional blocks might also prove useful, such as bonding of gain regions at different wavelengths, bonding of diode pump lasers to the gain region, and bonding gain and saturable absorbers for mode locking. New materials and epitaxial growth techniques have been driving the development of semiconductor lasers for more than 40 years, and they will also be critical for the future VECSEL development. Complex multilayer semiconductor VECSEL structures require state-of-the-art semiconductor materials and growth techniques. In addition, finding optimal nonlinear optical materials, including periodically poled crystals, will boost performance of the frequency-doubled visible emitting VECSELs.

Further development of electrically pumped VECSELs is an important topic of future research. While optically pumped VECSELs will reach comparatively higher output powers, electrical pumping capability will enable more compact, efficient, and simple devices for many applications of VECSELs in a variety of operating regimes:

cw and pulsed, tunable, intracavity doubled, and so on. Electrically pumped VECSELs are discussed in detail in Chapter 7.

Another important future direction for VECSEL research is the integration of multiple functional blocks on a common semiconductor substrate. For example, integration of pump lasers with the gain-mirror VECSEL structure has already been demonstrated [154]. Further development of such pump-integrated VECSELs can produce highly manufacturable high-power lasers that require significantly reduced component assembly, thus reducing the device cost and expanding the potential markets for these lasers. Another example of functional component integration is the MIXSEL laser (Chapter 6) [160, 161], where gain and saturable absorber regions of short-pulse mode-locked VECSELs are integrated on a common substrate. An important direction of functional integration is the development of various forms of VECSEL-integrated optical cavities; such integrated cavities are more compact and better manufacturable and might prove very valuable for some applications. This includes plane–plane microchip cavities with thermally stabilized transverse modes [69–71, 181]; compact plane–curved cavities where the curved surface is produced as a microlens on an optical substrate [141–144, 212, 213]; and single-transverse mode optical resonators, for example, in the pillbox configuration [145]. Such functional integration, including combinations of the above schemes, can produce simpler, more compact, easier manufacturable, and cheaper devices, as well as enable better device performance and novel functions. Future development of functional integration can help make VECSELs even more widely used commercially, especially in low-cost and high-volume applications, such as mobile projection displays.

A variety of optical cavity configurations have been used with VECSELs; development of optical cavities optimized for different applications will play an important role in expanding VECSEL function and application. While integrated optical cavities mentioned above are important, compact bulk optical cavities with large mode area for high-power operation [52] will also be valuable. Optical cavity design is an important factor in VECSELs incorporating multiple OPS chips [22, 49–52, 135, 184]. VECSELs using intracavity nonlinear optical crystals for harmonic generation or saturable absorbers for mode locking require optical cavities that control the absolute and relative laser mode diameters in the gain and the nonlinear element. In contrast with most VECSELs that use a linear laser cavity, even if with multiple cavity elements, ring laser cavity has been used in a VECSEL-based laser gyro [137] and a passively mode-locked VECSEL [136]. A diffractive unstable optical resonator has been used with VECSELs where Gaussian beam output was extracted from a hard-edged outcoupling aperture [138]. VECSELs have also been operated in unstable resonator regime with plane–spherical resonator cavities [18]. Optimized and novel optical cavities will enable VECSELs with enhanced performance, while making them more compact, stable, and manufacturable.

Array operation of VECSELs has been demonstrated both with electrical (Chapter 7) and optical [70, 143] pumping. This is a promising research direction for producing higher output powers from multiple beam incoherent arrays (Chapter 7) or phase-locked arrays [214]. Individually addressable VECSEL arrays

can be used for optical micromanipulation applications, such as optical trapping and transport of biological cells [215]. Incoherent arrays of VECSELs also produce reduced laser speckle for illumination applications, such as in imaging projection displays [210], where laser speckle reduces as the square root of the number of array elements.

VECSEL laser power modulation is important for many applications, such as for laser projection displays. Laser power can be modulated directly by current for electrically pumped VECSELs [49] or via pump diode current modulation for optically pumped VECSELs [207, 208]. Exploring modulation properties of VECSELs of both types and optimizing their high-speed modulation performance is an important future research direction. For example, pumping a VECSEL with multiple pump diodes connected in series can yield a high slope differential modulation capability useful in microwave photonics applications. Fast laser wavelength tuning might also prove important; such fast tuning is possible with MEMS-tunable optically pumped VECSELs that were developed for optical fiber communication applications [216–218].

A range of VECSEL applications require single-frequency laser operation, both tunable and nontunable, for example, molecular spectroscopy [106, 219], pumping of atomic clocks [120, 146], ring laser gyro [137], and microwave photonics applications [56, 220]. A number of studies have explored properties of VECSELs in their single-mode operating regime, such as laser linewidth, which can be very narrow in the kilohertz range [55, 104, 106, 119], and relative intensity noise (RIN) and its spectrum [56, 140]. Such single-mode operation has been achieved both with intracavity filters [55, 56, 59, 221], such as etalons, birefringent filters, and volume Bragg gratings, or alternatively free running without intracavity filters [106, 140]. Single-mode operation has been demonstrated both for the fundamental and intracavity frequency-doubled VECSELs [222]. Further investigation of the single-mode VECSEL regime and understanding of its properties can yield devices with unique characteristics for the above-mentioned applications, such as hertz-level quantum-limited linewidth [119] and shot-noise limited RIN [56], while at the same time with watt-level output powers and potentially tunable over several tens of nanometers wavelength range.

Short pulses at gigahertz repetition rates have been generated by saturable absorber passive mode locking of VECSELs [20]; this topic is discussed in detail in Chapter 6. Such passive mode locking has been demonstrated with both optically [62, 134, 223–226] and electrically [227–230] pumped VECSELs. Some of the remarkable characteristics demonstrated with passively mode-locked VECSELs are transform-limited pulses as short as 220 fs [231], repetition rates as high as 50 GHz [62], timing jitter as low as 160 fs with actively stabilized laser [232], and average output powers as high as 2.1 W [133], all with excellent circular output beams. Saturable absorbers have also been integrated with the gain medium on the same semiconductor substrate for a very simple and compact implementation of a passively mode-locked VECSEL or MIXSEL [160, 161]. Alternatively to saturable absorber passive mode locking, VECSELs have also been actively mode-locked by synchronous pumping with picosecond and femtosecond pulses from a Ti:sapphire

laser [233]. The resulting chirped picosecond pulses were compressed down to 185 fs by a grating pair compressor. Semiconductor gain medium, unlike traditional solid-state laser materials, for example, Yb:YAG, does not have long storage times; therefore, high pulse energy regime is outside the scope of VECSEL characteristics. VECSEL sources of high-power ultrashort pulses at gigahertz repetition rates will find applications in such areas as optical clock distribution in high-speed computing systems and metrology. Future research will expand the short pulse generation performance of VECSELs in the direction of shorter femtosecond pulses, higher repetition rates beyond 100 GHz, new operating wavelengths from UV to mid-IR with different material systems and nonlinearly converted optical frequencies, compact integrated implementations, and further development of electrically pumped devices. Such compact high-power ultrashort pulse sources will find many applications and will displace more conventional solid-state pulsed sources in many application areas.

Microwave photonics applications transmit analogue radio frequency (RF) or microwave signals modulated on top of an optical carrier. VECSELs are exceptionally suited as light sources for such microwave links because of their high power and shot-noise-limited RIN capability [56]. With a high-Q external cavity, VECSELs operate in the flat-noise oscillation-relaxation-free class-A laser regime, achieved because photon lifetime in the VECSEL laser cavity is much larger than the carrier lifetime in the gain chip [119, 220]. Application of VECSELs to microwave photonics links is a promising direction of future development.

With their high-power, tunable, single-mode, and narrow-linewidth operation capability, VECSELs are a good laser light source for pumping atomic clocks, such as Cs atomic clock near 852 nm [120, 146]. Here, VECSELs can be used for trapping, cooling, manipulation, and optical detection of atoms. The use of VECSELs for optical tweezers for trapping and manipulation of biological samples [199] is also an area of future research interest; output power, wavelength, and beam quality, all in compact size, are key VECSEL qualities for these applications.

Another interesting application of VECSELs is for rotation sensing using VECSEL-based ring laser gyro [137]; the initial demonstration of such laser gyros is certain to be followed by many others. High power, excellent beam quality, and wavelength selection of VECSELs have a natural application for a sodium laser guide star [58, 234]. Here a multiwatt 589 nm yellow laser beam is used to excite the D_2 sodium line in the mesospheric layer of sodium atoms, creating a glowing artificial "star" in the regions of the sky where no bright stars are available. This sodium guide star is then used for adaptive optics compensation of atmospheric distortion in ground-based astronomical telescopes [234, 235] and in space–ground optical links.

Important for the future development and broad application of VECSELs is detailed physical modeling, including analytical and numerical models, of various aspects of their behavior. One example that is already bearing fruit is the modeling of the thermal heat dissipation issues in VECSELs [20, 72, 236, 237]; this subject is discussed in detail in Chapter 2. Modeling and understanding of the short pulse

generation mechanisms in VECSELs, including cavity group delay dispersion (GDD), nonlinear self-phase modulation (SPM), and gain and loss saturation dynamics, has enabled decreasing mode-locked pulse widths from the picosecond to the femtosecond regime [20, 134, 238], with further pulse width decreases expected in the future. Modeling of the VECSEL single-mode regime nonlinear dynamics and noise [119, 239] will produce higher performing devices for microwave photonics and atomic clock applications. Further application of full numerical microscopic models of semiconductor lasers, including gain properties of semiconductor materials [117, 118], as well as modeling of gain and carrier behavior in VECSELs [240, 241], will lead to better understanding of the laser behavior and design of improved performance lasers. Detailed modeling is also required for improving the performance of electrically pumped VECSELs (Chapter 7).

An important application area of VECSELs of much research is in molecular spectroscopy. Tunable single-frequency VECSELs have been used directly to acquire spectra in the NIR by scanning the laser line across absorption features of interest, for example, methane absorption near 2.3 μm [106, 219, 242]. Detection sensitivity of VECSEL spectroscopy can be magnified with cavity-enhanced absorption spectroscopy [243], where a mode-locked VECSEL frequency comb is matched to the comb of resonances of a high-finesse cavity containing gas under study. Using this technique, acetylene absorption near 1 μm was measured with a 25 m effective absorption path length for a 13 cm long cell [243].

Even greater enhancement of detection sensitivity in molecular spectroscopy is obtained with an ultrasensitive ICLAS technique, first demonstrated with VECSELs in Refs [73, 74]. In this technique, the absorption cell is placed inside optical cavity of a homogeneously broadened multimode laser, the laser is turned on, and the lasing spectrum is measured by a spectrometer a time t_g later within a narrow time slot Δt_g. This approach gives effective absorption path length $L_p = \varrho c t_g$, where ϱ is the length fraction of the laser occupied by the absorption cell and c is the speed of light. For the typical generation times of 200–400 μs and a 50 cm long absorption cell, the effective absorption path lengths are 30–60 km; effective path lengths as long as 130 km have been demonstrated for a 1 m long absorbing path [244]. Due to the long effective path lengths, ICLAS-VECSEL allows measurement of absorption coefficients as low as 10^{-9}–10^{-10} cm^{-1} (sensitivity $\sim 10^{-11}$ cm^{-1} $Hz^{-1/2}$). Acousto-optic modulator is used to switch the laser beam to the measuring spectrometer; both grating and Fourier transform spectrometers have been used for spectrum acquisition in ICLAS. Several properties of VECSELs enable their application to ICLAS: wide range of available wavelengths, broad homogeneous gain bandwidth, and very low loss laser cavity; because of their high loss, edge-emitting semiconductor lasers are not very suitable for ICLAS. ICLAS-VECSEL technique has been applied for molecular spectroscopy measurements at wavelengths near 1.0 μm (8900–10 100 cm^{-1}) [74, 244, 245], 1.55 μm (6500 cm^{-1}) [148], and 2.3 μm (4300 cm^{-1}) [246]. With its high sensitivity, ICLAS-VECSEL can be used for trace gas detection or for measurement of weak absorption lines of atmospheric gases. A variety of molecular

gases have been measured by ICLAS-VECSEL, detecting thousands of spectral lines, including new ones. Rovibrational analysis has been used to assign the detected lines [247]. Some of the measured molecular species are nitrous oxide (N_2O) [245], water (H_2O) [148, 244, 246–248], carbon dioxide (CO_2) [148, 246], hydrogen sulfide (H_2S) [249], acetylene (HCCH) [248], and carbonyl sulfide (OCS) [250], as well as a variety of isotopic variants such as D_2O [251]. Prior to the development of semiconductor VECSELs, ICLAS relied primarily on Ti:sapphire laser in the 700–900 nm range and dye lasers in the visible range. Semiconductor VECSELs opened new wavelengths for ICLAS in the NIR and mid-IR 0.9–2.5 μm wavelength, 4000–11 000 cm^{-1} wave number, including the spectrally rich molecular overtone region. VECSELs also offer a simple and compact laser source for spectroscopy. Using VECSELs for ICLAS revealed an unexpected spectral condensation effect, where spectral absorption dips are replaced by blue-shifted emission peaks at longer generation times [248]. ICLAS-VECSEL promises to be an active research area in the future with more molecular species observed, improved detection sensitivities, and expanded spectral detection regions in the NIR and mid-IR. Highly sensitive ICLAS-VECSEL gas detection can have applications in understanding of atmospheric gases and in medicine.

To summarize this section, current research work has explored an amazing variety of applications that exploit the unique properties of VECSELs. Further research into expanding, improving, and understanding of the VECSEL properties will lead to even greater growth in the future of the research and commercial applications of these remarkable lasers.

1.4.4
Future of VECSEL Lasers: Scalable Power with Beam Quality from UV to IR

This chapter has outlined a new semiconductor laser technology that comes with several alternative names: vertical-external-cavity surface-emitting laser, semiconductor disk laser, or optically pumped semiconductor laser. This is one technology that, uniquely among various other laser technologies, addresses *simultaneously* multiple laser application requirements: power scaling, wavelength versatility, beam quality, compact size, efficiency, reliability, and so on. This technology allows laser *design* with characteristics to match application requirements optimally, for example, output power from milliwatts to tens of watts, wavelength from UV to mid-IR, and an excellent beam quality. It should be emphasized that VECSEL technology achieves the desired laser characteristics by *design*, rather than by hoping for a *serendipitous coincidence*, as with solid-state and gas laser wavelength targeting.

What is the source of these remarkable properties of VECSEL technology? The answer is, as this chapter has described, that VECSELs combine some of the best qualities of semiconductor lasers and solid-state lasers, while avoiding many of the weaknesses of these two laser classes.

What are VECSEL strengths acquired from semiconductor lasers? VECSELs take from semiconductor lasers the use of semiconductor materials with their various

binary compounds and multicomponent alloys that can target a very wide range of emission wavelengths. VECSELs have also incorporated bandgap-engineered semiconductor heterostructures that are used to engineer by design the desired laser emission and pump absorption properties. Due to the semiconductor laser materials, optically pumped VECSELs have strong pump absorption in a very thin layer, just a few microns thick, and over extremely wide range of pump wavelengths, tens and hundreds of nanometers. VECSELs have also inherited the excellent circular output beam of a VCSEL surface-emitting semiconductor laser.

What are VECSEL strengths acquired from the solid-state lasers? The key contribution of solid-state lasers to VECSELs is the flexible optical laser cavity, which enables many of the key VECSEL properties. Optical cavity provides transverse mode control to VECSELs, which enables their excellent beam quality. VECSEL optical cavity also enables mode size scaling for laser output power scaling. More important, flexible open laser cavity makes possible for VECSELs the insertion of various intracavity functional optical elements, such as nonlinear optical crystals for harmonic generation, saturable absorbers for short pulse passive mode locking, multiple gain chips, optical filters for spectral control, and so on. This gives VECSELs many different regimes of operation and underlies their tremendous functional flexibility. Significantly, both solid-state laser and VECSEL optical cavity has low intracavity loss. This has important consequences by allowing efficient use of low transmission output coupling, which in turn results in high intracavity power compared to output laser power and thus enables very high nonlinear optical conversion efficiency. Another feature acquired by VECSELs from solid-state lasers is optical pumping. While electrical pumping of VECSELs is preferred in some cases, optical pumping produces much higher VECSEL output powers and allows much simpler VECSEL laser wafer structure.

Many VECSEL properties are enabled by avoiding some of the key weaknesses of semiconductor lasers. Edge-emitting semiconductor lasers have their light locked in a waveguide; good beam quality requires this to be a single-mode waveguide, which results in a nonscalable small laser mode size that limits laser output power with good beam quality. Surface-emitting VCSEL lasers have no adequate transverse mode control and good beam quality single-transverse mode output power is again limited. In contrast, VECSELs avoid these limitations; they have open cavities, allowing both transverse mode control for fundamental circular mode operation and mode size scaling for higher output powers. Another disadvantage of edge-emitting semiconductor lasers is their lossy optical cavity, both due to lossy waveguides, which give loss of several tens of percent per cavity pass, and due to lossy coupling to external optical cavity. Lossy cavities of edge-emitting lasers require for output power efficiency the use of high-transmission output couplers, hence intracavity power becomes comparable to output power, and thus no efficient intracavity-enhanced nonlinear optical frequency doubling is possible. Lossy cavity also produces strong spontaneous emission noise. In contrast, VECSELs with their low-loss laser cavities do not have these limitations.

What are the weaknesses of solid-state lasers avoided by VECSELs? The key weakness of solid-state lasers is very inflexible emission wavelengths, which are

constrained to the few available transitions of active ions. The second weakness, for similar reasons, is the very inflexible narrow range of pump wavelengths; pump diode lasers at such wavelengths might not be readily available, when available, they require costly wavelength stabilization, for example, by temperature stabilization. Another limitation of solid-state lasers is relatively weak, compared to semiconductors, pump absorption, thus requiring thicker crystals for efficient pump absorption. Thicker absorbing crystals require complex pump optics and relatively good quality pump beams; thicker crystals also produce thermal lensing, which distorts beam and limits output power. VECSELs avoid these limitations due to strong broadband pump absorption of semiconductors.

The solid-state lasers typically have fairly long excited-state lifetimes, which can be as long as a millisecond, allowing energy storage and high-energy pulse generation in these lasers. On the other hand, the long carrier lifetime of solid-state lasers severely limits their output modulation rate and typically requires external modulation. In contrast, semiconductor materials of VECSEL have very short carrier lifetimes of the order of a nanosecond. As a result, VECSELs lose the energy storage and the high pulse energy capabilities of solid-state lasers. However, due to the short carrier lifetime, VECSELs acquire fast modulation capability, either directly via current modulation for electrically pumped VECSELs or via pump diode power modulation for optically pumped VECSELs.

This combination of advantageous laser properties in VECSELs produces a very flexible and versatile laser technology, as illustrated by the multitude of research directions described above: power scaling from milliwatts to tens of watts with single or multiple gain chips, UV and visible output wavelengths via harmonic generation, wavelength tunable operation, femtosecond short pulse generation at gigahertz high rates, single-frequency operation, intracavity laser absorption spectroscopy, laser gyros, microwave photonics, terahertz spectroscopy, and so on. Versatile VECSEL laser technology leads to an impressive and surprising variety of commercial applications already demonstrated for this new technology: from biomedical fluorescence imaging to ophthalmic photocoagulation treatment, to projection displays, to forensic evidence analysis, to pumping Ti:sapphire lasers. VECSEL applications so far have been mostly in the UV and visible wavelengths, where compact and efficient sources with other laser technologies have been lacking. The accomplishments until now for the young VECSEL laser technology only illustrate its rich potentials; future research and development are going to expand even wider the scope of VECSEL performance, functional versatility, and the range of scientific and commercial applications.

What is the future of VECSEL lasers? VECSELs will expand the range of their capabilities both through technology push and a market pull. VECSEL technology will expand the range of VECSEL-operating parameters: output powers will increase to the hundreds of watts levels maintaining excellent beam quality; wavelength coverage will expand deeper into UV below 200 nm and further into mid-IR beyond 5 μm with more complete wavelength coverage inside this range; shorter pulses in the tens of femtoseconds will become possible, with increased average power levels of multiple watts; single-frequency operation with subkilohertz linewidth will be demonstrated;

and VECSELs will become efficient sources of terahertz radiation. At the same time, various VECSEL performance parameters will be optimized: expect higher power efficiencies; smaller laser packages; further integration of various functional components, such as pump lasers, saturable absorbers, and optical cavities; and electrical pumping will be used more widely when needed and possible. VECSELs will be used more widely in novel scientific applications, such as molecular spectroscopy with ICLAS, laser gyros, microwave photonics, and atomic clocks. Market pull from existing and developing applications will stimulate appearance of new commercial devices, for example, multiwatt red, green, and blue (RGB) VECSEL lasers for cinema projection applications. The availability of compact, efficient, and high-performance lasers with targeted custom-designed wavelength and other parameters will expand their use in existing commercial applications and will enable new applications that could not be addressed previously with other laser technologies. VECSELs will be displacing other laser technologies in some applications areas, for example, Ar-ion gas lasers with the blue and green wavelength outputs have been used in the past as the only suitable source for confocal fluorescence microscopy and for pumping Ti: sapphire lasers. These gas lasers have largely been displaced by diode-pumped solid-state lasers at these wavelengths; solid-state lasers in turn are in the process of being themselves displaced by VECSELs in these application areas. For these applications, VECSELs offer wavelength flexibility, power scalability, beam quality, compact size, good efficiency, and high reliability.

We are entering a new era of VECSEL/SDL/OPSL lasers that are poised to become ubiquitous laser sources in scientific and commercial applications. Perhaps some of the more interesting future VECSEL developments are the unexpected ones; future of VECSELs will be full of bright surprises.

Acknowledgments

I would like to acknowledge my former colleagues at Micracor Inc. who greatly contributed to the development of the first VECSEL lasers: Aram Mooradian, Farhad Hakimi, and Robert Sprague. I am also grateful to Oleg Okhotnikov for putting this book collection together.

References

1 Svelto, O. (1998) *Principles of Lasers*, 4th edn, Springer.
2 Agarwal, G.P. (2002) *Fiber-Optic Communication Systems*, 3rd edn, Wiley–Interscience.
3 Agrawal, G.P. and Dutta, N.K. (1986) *Long-Wavelength Semiconductor Lasers*, Van Nostrand Reinhold Co., New York.
4 Zory, P.S. (ed.) (1993) *Quantum Well Lasers*, Academic Press, San Diego.
5 Chuang, S.L. (1995) *Physics of Optoelectronic Devices*, John Wiley & Sons, Inc., New York.
6 Coldren, L.A. and Corzine, S.W. (1995) *Diode Lasers and Photonic Integrated Circuits*, John Wiley & Sons, Inc., New York.
7 Chow, W. and Koch, S.W. (1999) *Semiconductor Laser Fundamentals*, Springer, Berlin.

8 Kapon, E. (ed.) (1999) *Semiconductor Lasers I: Fundamentals*, Academic Press.

9 Kapon, E. (ed.) (1999) *Semiconductor Lasers II: Materials and Structures*, Academic Press.

10 Wilmsen, C.W., Temkin, H., and Coldren, L.A. (eds) (1999) *Vertical-Cavity Surface-Emitting Lasers: Design, Fabrication, Characterization, and Applications*, Cambridge University Press.

11 Li, H. and Iga, K. (eds) (2002) *Vertical-Cavity Surface-Emitting Laser Devices*, Springer.

12 Diehl, R. (ed.) (2000) *High Power Diode Lasers*, Springer.

13 Koechner, W. (2006) *Solid-State Laser Engineering*, 6th edn, Springer.

14 Koechner, W. and Bass, M. (2003) *Solid-State Lasers: A Graduate Text*, Springer.

15 Digonnet, M.J.F. (ed.) (2001) *Rare-Earth-Doped Fiber Lasers and Amplifiers*, 2nd edn, CRC Press.

16 Prasad, P.N. (2003) *Introduction to Biophotonics*, Wiley-Interscience.

17 Kuznetsov, M., Hakimi, F., Sprague, R., and Mooradian, A. (1997) High-power (>0.5-W CW) diode-pumped vertical-external-cavity surface-emitting semiconductor lasers with circular TEM_{00} beams. *IEEE Photon. Technol. Lett.*, **9**, 1063–1065.

18 Kuznetsov, M., Hakimi, F., Sprague, R., and Mooradian, A. (1999) Design and characteristics of high-power (>0.5-W CW) diode-pumped vertical-external-cavity surface-emitting semiconductor lasers with circular TEM_{00} beams. *IEEE J. Sel. Top. Quantum Electron.*, **5**, 561–573.

19 Tropper, A.C., Foreman, H.D., Garnache, A., Wilcox, K.G., and Hoogland, S.H. (2004) Vertical-external-cavity semiconductor lasers. *J. Phys. D: Appl. Phys.*, **37**, R75–R85.

20 Keller, U. and Tropper, A.C. (2006) Passively modelocked surface-emitting semiconductor lasers. *Phys. Rep.*, **429**, 67–120.

21 Tropper, A.C. and Hoogland, S. (2006) Extended cavity surface-emitting semiconductor lasers. *Prog. Quantum Electron.*, **30**, 1–43.

22 Chilla, J., Shu, Q.-Z., Zhou, H., Weiss, E., Reed, M., and Spinelli, L. (2007) Recent advances in optically pumped semiconductor lasers. *Proc. SPIE*, **6451**, 645109.

23 Schulz, N., Hopkins, J.M., Rattunde, M., Burns, D., and Wagner, J. (2008) High-brightness long-wavelength semiconductor disk lasers. *Laser Photon. Rev.*, **2**, 160–181.

24 Calvez, S., Hastie, J.E., Guina, M., Okhotnikov, O.G., and Dawson, M.D. (2009) Semiconductor disk lasers for the generation of visible and ultraviolet radiation. *Laser Photon. Rev.*, **3** (5), 407–434.

25 Boyd, R.W. (2008) *Nonlinear Optics*, 3rd edn, Academic Press.

26 Seurin, J.-F., Xu, G., Khalfin, V., Miglo, A., Wynn, J.D., Pradhan, P., Ghosh, C.L., and D'Asaro, L.A. (2009) Progress in high-power high-efficiency VCSEL arrays. *Proc. SPIE*, **7229**, 722903–722911.

27 Delfyett, P.J., Shi, H., Gee, S., Barty, C.P.J., Alphones, G., and Connolly, J. (1998) Intracavity spectral shaping in external cavity mode-locked semiconductor diode lasers. *IEEE J. Sel. Top. Quantum Electron.*, **4**, 216–223.

28 Hadley, M.A., Wilson, G.C., Lau, K.Y., and Smith, J.S. (1993) High single-transverse-mode output from external-cavity surface-emitting laser diodes. *Appl. Phys. Lett.*, **63**, 1607–1609.

29 Chinn, S.R., Rossi, J.A., Wolfe, C.M., and Mooradian, A. (1973) Optically pumped room-temperature GaAs lasers. *IEEE J. Quantum Electron.*, **QE-9**, 294–300.

30 Stone, J., Wiesenfeld, J.M., Dentai, A.G., Damen, T.C., Duguay, M.A., Chang, T.Y., and Caridi, E.A. (1981) Optically pumped ultrashort cavity $In_{1-x}Ga_xAs_yP_{1-y}$ lasers: picosecond operation between 0.83 and 1.59 μm. *Opt. Lett.*, **6**, 534–536.

31 Roxlo, C.B. and Salour, M.M. (1981) Synchronously pumped mode-locked CdS platelet laser. *Appl. Phys. Lett.*, **38**, 738–740.

32 Le, H.Q., Di Cecca, S., and Mooradian, A. (1991) Scalable high-power optically

pumped GaAs laser. *Appl. Phys. Lett.*, **58**, 1967–1969.

33 McDaniel, D.L., Jr., McInerney, J.G., Raja, M.Y.A., Schaus, C.F., and Brueck, S.R.J. (1990) Vertical cavity surface-emitting semiconductor laser with cw injection laser pumping. *IEEE Photon. Technol. Lett.*, **2**, 156–158.

34 Sandusky, J.V. and Brueck, S.R.J. (1996) A CW external-cavity surface-emitting laser. *IEEE Photon. Technol. Lett.*, **8**, 313–315.

35 Hanaizumi, O., Jeong, K.T., Kashiwada, S.-Y., Syuaib, I., Kawase, K., and Kawakami, S. (1996) Observation of gain in an optically pumped surface-normal mutiple-quantum-well optical amplifier. *Opt. Lett.*, **21**, 269–271.

36 Jiang, W.B., Friberg, S.R., Iwamura, H., and Yamamoto, Y. (1991) High powers and subpicosecond pulses from an external-cavity surface-emitting InGaAs/InP multiple quantum well laser. *Appl. Phys. Lett.*, **58**, 807–809.

37 Sun, D.C., Friberg, S.R., Watanabe, K., Machida, S., Horikoshi, Y., and Yamamoto, Y. (1992) High power and high efficiency vertical cavity surface emitting GaAs laser. *Appl. Phys. Lett.*, **61**, 1502–1503.

38 Le, H.Q., Goodhue, W.D., and Di Cecca, S. (1992) High-brightness diode-laser-pumped semiconductor heterostructure lasers. *Appl. Phys. Lett.*, **60**, 1280–1282.

39 Le, H.Q., Goodhue, W.D., Maki, P.A., and Di Cecca, S. (1993) Diode-laser-pumped InGaAs/GaAs/AlGaAs heterostructure lasers with low internal loss and 4-W average power. *Appl. Phys. Lett.*, **63**, 1465–1467.

40 Stewen, C., Contag, K., Larionov, M., Giesen, A., and Hugel, H. (2000) A 1-kW CW thin disc laser. *IEEE J. Sel. Top. Quantum Electron.*, **6**, 650–657.

41 Giesen, A. and Speiser, J. (2007) Fifteen years of work on thin-disk lasers: results and scaling laws. *IEEE J. Sel. Top. Quantum Electron.*, **13**, 598–609.

42 Corzine, S.W., Geels, R.S., Scott, J.W., Yan, R.-H., and Coldren, L.A. (1989) Design of Fabry–Perot surface-emitting lasers with a periodic gain structure. *IEEE J. Quantum Electron.*, **QE-25**, 1513–1524.

43 Lutgen, S., Albrecht, T., Brick, P., Reill, W., Luft, J., and Spath, W. (2003) 8-W high-efficiency continuous-wave semiconductor disk laser at 1000 nm. *Appl. Phys. Lett.*, **82**, 3620–3622.

44 Schmid, M., Benchabane, S., Torabi-Goudarzi, F., Abram, R., Ferguson, A.I., and Riis, E. (2004) Optical in-well pumping of a vertical-external-cavity surface-emitting laser. *Appl. Phys. Lett.*, **84**, 4860–4862.

45 Zhang, W., Ackemann, T., McGinily, S., Schmid, M., Riis, E., and Ferguson, A.I. (2006) Operation of an optical in-well-pumped vertical-external-cavity surface-emitting laser. *Appl. Opt.*, **45**, 7729–7735.

46 Beyertt, S.S., Zorn, M., Kubler, T., Wenzel, H., Weyers, M., Giesen, A., Trankle, G., and Brauch, U. (2005) Optical in-well pumping of a semiconductor disk laser with high optical efficiency. *IEEE J. Quantum Electron.*, **41**, 1439–1449.

47 Beyertt, S.S., Brauch, U., Demaria, F., Dhidah, N., Giesen, A., Kubler, T., Lorch, S., Rinaldi, F., and Unger, P. (2007) Efficient gallium–arsenide disk laser. *IEEE J. Quantum Electron.*, **43**, 869–875.

48 Schulz, N., Rattunde, M., Ritzenthaler, C., Rosener, B., Manz, C., Kohler, K., and Wagner, J. (2007) Resonant optical in-well pumping of an (AlGaIn)(AsSb)-based vertical-external-cavity surface-emitting laser emitting at 2.35 μm. *Appl. Phys. Lett.*, **91**, 091113.

49 Saarinen, E.J., Harkonen, A., Suomalainen, S., and Okhotnikov, O.G. (2006) Power scalable semiconductor disk laser using multiple gain cavity. *Opt. Express*, **14**, 12868–12871.

50 Fan, L., Fallahi, M., Hader, J., Zakharian, A.R., Moloney, J.V., Murray, J.T., Bedford, R., Stolz, W., and Koch, S.W. (2006) Multichip vertical-external-cavity surface-emitting lasers: a coherent power scaling scheme. *Opt. Lett.*, **31**, 3612–3614.

51 Fan, L., Fallahi, M., Zakharian, A., Hader, J., Moloney, J.V., Bedford, R., Murray, J.T., Stolz, W., and Koch, S.W. (2007) Extended tunability in a two-chip VECSEL. *IEEE Photon. Technol. Lett.*, **19**, 544–546.

52 Hunziker, L.E., Ihli, C., and Steingrube, D.S. (2007) Miniaturization and power

scaling of fundamental mode optically pumped semiconductor lasers. *IEEE J. Sel. Top. Quantum Electron.*, **13**, 610–618.

53 Rautiainen, J., Harkanen, A., Korpijarvi, V.M., Tuomisto, P., Guina, M., and Okhotnikov, O.G. (2007) 2.7 W tunable orange–red GaInNAs semiconductor disk laser. *Opt. Express*, **15**, 18345–18350.

54 Seelert, W., Butterworth, S., Rosperich, J., Walter, C., Elm, R.v., Ostroumov, V., Chilla, J., Zhou, H., Weiss, E., and Caprara, A. (2005) Optically pumped semiconductor lasers: a new reliable technique for realizing highly efficient visible lasers. *Proc. SPIE*, **5707**, 33–37.

55 Holm, M.A., Ferguson, D., and Dawson, M.D. (1999) Actively stabilized single-frequency vertical-external-cavity AlGaAs laser. *IEEE Photon. Technol. Lett.*, **11**, 1551–1553.

56 Baili, G., Alouini, M., Dolfi, D., Bretenaker, F., Sagnes, I., and Garnache, A. (2007) Shot-noise-limited operation of a monomode high-cavity-finesse semiconductor laser for microwave photonics applications. *Opt. Lett.*, **32**, 650–652.

57 Hilbich, S., Seelert, W., Ostroumov, V., Kannengiesser, C., Elm, R.v., Mueller, J., Weiss, E., Zhou, H., and Chilla, J. (2007) New wavelengths in the yellow orange range between 545 nm to 580 nm generated by an intracavity frequency-doubled optically pumped semiconductor laser. *Proc. SPIE*, **6451**, 64510C.

58 Fallahi, M., Fan, L., Kaneda, Y., Hessenius, C., Hader, J., Li, H., Moloney, J.V., Kunert, B., Stolz, W., Koch, S.W., Murray, J., and Bedford, R. (2008) 5-W yellow laser by intracavity frequency doubling of high-power vertical-external-cavity surface-emitting laser. *IEEE Photon. Technol. Lett.*, **20**, 1700–1702.

59 Giet, S., Sun, H.D., Calvez, S., Dawson, M.D., Suomalainen, S., Harkonen, A., Guina, M., Okhotnikov, O., and Pesa, M. (2006) Spectral narrowing and locking of a vertical-external-cavity surface-emitting laser using an intracavity volume Bragg grating. *IEEE Photon. Technol. Lett.*, **18**, 1786–1788.

60 Giet, S., Lee, C.-L., Calvez, S., Dawson, M.D., Destouches, N., Pommier, J.-C., and Parriaux, O. (2007) Stabilization of a semiconductor disk laser using an intra-cavity high reflectivity grating. *Opt. Express*, **15**, 16520–16526.

61 Fan, L., Fallahi, M., Murray, J.T., Bedford, R., Kaneda, Y., Zakharian, A.R., Hader, J., Moloney, J.V., Stolz, W., and Koch, S.W. (2006) Tunable high-power high-brightness linearly polarized vertical-external-cavity surface-emitting lasers. *Appl. Phys. Lett.*, **88**, 021105.

62 Lorenser, D., Maas, D., Unold, H.J., Bellancourt, A.R., Rudin, B., Gini, E., Ebling, D., and Keller, U. (2006) 50-GHz passively mode-locked surface-emitting semiconductor laser with 100-mW average output power. *IEEE J. Quantum Electron.*, **42**, 838–847.

63 Haring, R., Paschotta, R., Gini, E., Morier-Genoud, F., Martin, D., Melchior, H., and Keller, U. (2001) Picosecond surface-emitting semiconductor laser with >200 mW average power. *Electron. Lett.*, **37**, 766–767.

64 Haring, R., Paschotta, R., Aschwanden, A., Gini, E., Morier-Genoud, F., and Keller, U. (2002) High-power passively mode-locked semiconductor lasers. *IEEE J. Quantum Electron.*, **38**, 1268–1275.

65 Alford, W.J., Raymond, T.D., and Allerman, A.A. (2002) High power and good beam quality at 980 nm from a vertical external-cavity surface-emitting laser. *J. Opt. Soc. Am. B*, **19**, 663–666.

66 Hastie, J.E., Hopkins, J.M., Calvez, S., Jeon, C.W., Burns, D., Abram, R., Riis, E., Ferguson, A.I., and Dawson, M.D. (2003) 0.5-W single transverse-mode operation of an 850-nm diode-pumped surface-emitting semiconductor laser. *IEEE Photon. Technol. Lett.*, **15**, 894–896.

67 Hopkins, J.M., Smith, S.A., Jeon, C.W., Sun, H.D., Burns, D., Calvez, S., Dawson, M.D., Jouhti, T., and Pessa, M. (2004) 0.6 W CW GaInNAs vertical external-cavity surface emitting laser operating at 1.32 μm. *Electron. Lett.*, **40**, 30–31.

68 Kim, K.S., Yoo, J., Kim, G., Lee, S., Cho, S., Kim, J., Kim, T., and Park, Y. (2007) 920-nm vertical-external-cavity surface-emitting lasers with a slope efficiency of

58% at room temperature. *IEEE Photon. Technol. Lett.*, **19**, 1655–1657.

69 Hastie, J.E., Hopkins, J.M., Jeon, C.W., Calvez, S., Burns, D., Dawson, M.D., Abram, R., Riis, E., Ferguson, A.I., Alford, W.J., Raymond, T.D., and Allerman, A.A. (2003) Microchip vertical external cavity surface emitting lasers. *Electron. Lett.*, **39**, 1324–1326.

70 Hastie, J.E., Morton, L.G., Calvez, S., Dawson, M.D., Leinonen, T., Pessa, M., Gibson, G., and Padgett, M.J. (2005) Red microchip VECSEL array. *Opt. Express*, **13**, 7209–7214.

71 Kemp, A.J., Maclean, A.J., Hastie, J.E., Smith, S.A., Hopkins, J.M., Calvez, S., Valentine, G.J., Dawson, M.D., and Burns, D. (2006) Thermal lensing, thermal management and transverse mode control in microchip VECSELs. *Appl. Phys. B*, **83**, 189–194.

72 Kemp, A.J., Maclean, A.J., Hopkins, J.M., Hastie, J.E., Calvez, S., Dawson, M.D., and Burns, D. (2007) Thermal management in disc lasers: doped-dielectric and semiconductor laser gain media in thin-disc and microchip formats. *J. Mod. Opt.*, **54**, 1669–1676.

73 Garnache, A., Kachanov, A.A., Stoeckel, F., and Planel, R. (1999) High-sensitivity intracavity laser absorption spectroscopy with vertical-external-cavity surface-emitting semiconductor lasers. *Opt. Lett.*, **24**, 826–828.

74 Garnache, A., Kachanov, A.A., Stoeckel, F., and Houdré, R. (2000) Diode-pumped broadband vertical-external-cavity surface-emitting semiconductor laser applied to high-sensitivity intracavity absorption spectroscopy. *J. Opt. Soc. Am. B*, **17**, 1589–1598.

75 Picqué, N., Guelachvili, G., and Kachanov, A.A. (2003) High-sensitivity time-resolved intracavity laser Fourier transform spectroscopy with vertical-cavity surface-emitting multiple-quantum-well lasers. *Opt. Lett.*, **28**, 313–315.

76 Raymond, T.D., Alford, W.J., Crawford, M.H., and Allerman, A.A. (1999) Intracavity frequency doubling of a diode-pumped external-cavity surface-emitting semiconductor laser. *Opt. Lett.*, **24**, 1127–1129.

77 Kaneda, Y., Yarborough, J.M., Li, L., Peyghambarian, N., Fan, L., Hessenius, C., Fallahi, M., Hader, J., Moloney, J.V., Honda, Y., Nishioka, M., Shimizu, Y., Miyazono, K., Shimatani, H., Yoshimura, M., Mori, Y., Kitaoka, Y., and Sasaki, T. (2008) Continuous-wave all-solid-state 244 nm deep-ultraviolet laser source by fourth-harmonic generation of an optically pumped semiconductor laser using $CsLiB_6O_{10}$ in an external resonator. *Opt. Lett.*, **33**, 1705–1707.

78 Hastie, J.E., Morton, L.G., Kemp, A.J., Dawson, M.D., Krysa, A.B., and Roberts, J.S. (2006) Tunable ultraviolet output from an intracavity frequency-doubled red vertical-external-cavity surface-emitting laser. *Appl. Phys. Lett.*, **89**, 061114.

79 Hastie, J., Calvez, S., Dawson, M., Leinonen, T., Laakso, A., Lyytikäinen, J., and Pessa, M. (2005) High power CW red VECSEL with linearly polarized TEM_{00} output beam. *Opt. Express*, **13**, 77–81.

80 Lindberg, H., Strassner, A., Gerster, E., and Larsson, A. (2004) 0.8 W optically pumped vertical external cavity surface emitting laser operating CW at 1550 nm. *Electron. Lett.*, **40**, 601–602.

81 Rosener, B., Schulz, N., Rattunde, M., Manz, C., Kohler, K., and Wagner, J. (2008) High-power high-brightness operation of a 2.25-μm (AlGaIn)(AsSb)-based barrier-pumped vertical-external-cavity surface-emitting laser. *IEEE Photon. Technol. Lett.*, **20**, 502–504.

82 Rahim, M., Arnold, M., Felder, F., Behfar, K., and Zogg, H. (2007) Midinfrared lead–chalcogenide vertical external cavity surface emitting laser with 5 μm wavelength. *Appl. Phys. Lett.*, **91**, 151102.

83 Rahim, M., Felder, F., Fill, M., and Zogg, H. (2008) Optically pumped 5 μm IV–VI VECSEL with Al-heat spreader. *Opt. Lett.*, **33**, 3010–3012.

84 Rahim, M., Felder, F., Fill, M., Boye, D., and Zogg, H. (2008) Lead chalcogenide VECSEL on Si emitting at 5 μm. *Electron. Lett.*, **44** (25), 1467–1469.

85 Rahim, M., Khiar, A., Felder, F., Fill, M., and Zogg, H. (2009) 4.5 μm wavelength vertical external cavity surface emitting laser operating above room temperature. *Appl. Phys. Lett.*, **94**, 201112.

86 McGinily, S.J., Abram, R.H., Gardner, K.S., Riis, E., Ferguson, A.I., and Roberts, J.S. (2007) Novel gain medium design for short-wavelength vertical-external-cavity surface-emitting laser. *IEEE J. Quantum Electron.*, **43**, 445–450.

87 Fan, L., Hessenius, C., Fallahi, M., Hader, J., Li, H., Moloney, J.V., Stolz, W., Koch, S.W., Murray, J.T., and Bedford, R. (2007) Highly strained InGaAs/GaAs multiwatt vertical-external-cavity surface-emitting laser emitting around 1170 nm. *Appl. Phys. Lett.*, **91**, 131114.

88 Harkonen, A., Rautiainen, J., Guina, M., Konttinen, J., Tuomisto, P., Orsila, L., Pessa, M., and Okhotnikov, O.G. (2007) High power frequency doubled GaInNAs semiconductor disk laser emitting at 615 nm. *Opt. Express*, **15**, 3224–3229.

89 Lindberg, H., Larsson, A., and Strassner, M. (2005) Single-frequency operation of a high-power, long-wavelength semiconductor disk laser. *Opt. Lett.*, **30**, 2260–2262.

90 Lindberg, H., Sadeghi, M., Westlund, M., Wang, S.M., Larsson, A., Strassner, M., and Marcinkevicius, S. (2005) Mode locking a 1550 nm semiconductor disk laser by using a GaInNAs saturable absorber. *Opt. Lett.*, **30**, 2793–2795.

91 Lindberg, H., Strassner, M., Gerster, E., Bengtsson, J., and Larsson, A. (2005) Thermal management of optically pumped long-wavelength InP-based semiconductor disk lasers. *IEEE J. Sel. Top. Quantum Electron.*, **11**, 1126–1134.

92 Kurdi, M.E., Bouchoule, S., Bousseksou, A., Sagnes, I., Plais, A., Strassner, M., Symonds, C., Garnache, A., and Jacquet, J. (2004) Room-temperature continuous-wave laser operation of electrically-pumped 1.55 μm VECSEL. *Electron. Lett.*, **40**, 671–672.

93 Bousseksou, A., Kurdi, M.E., Salik, M.D., Sagnes, I., and Bouchoule, S. (2004) Wavelength tunable InP-based EP-VECSEL operating at room temperature and in CW at 1.55 μm. *Electron. Lett.*, **40**, 1490–1491.

94 Harkonen, A., Guina, M., Okhotnikov, O., Rossner, K., Hummer, M., Lehnhardt, T., Muller, M., Forchel, A., and Fischer, M. (2006) 1-W antimonide-based vertical external cavity surface emitting laser operating at 2-μm. *Opt. Express*, **14**, 6479–6484.

95 Park, S.-H., Kim, J., Jeon, H., Sakong, T., Lee, S.-N., Chae, S., Park, Y., Jeong, C.-H., Yeom, G.-Y., and Cho, Y.-H. (2003) Room-temperature GaN vertical-cavity surface-emitting laser operation in an extended cavity scheme. *Appl. Phys. Lett.*, **83**, 2121–2123.

96 Park, S.-H. and Jeon, H. (2006) Microchip-type InGaN vertical external-cavity surface-emitting laser. *Opt. Rev.*, **13**, 20–23.

97 Rautiainen, J., Lyytikäinen, J., Sirbu, A., Mereuta, A., Caliman, A., Kapon, E., and Okhotnikov, O.G. (2008) 2.6 W optically-pumped semiconductor disk laser operating at 1.57-μm using wafer fusion. *Opt. Express*, **16**, 21881–21886.

98 Lyytikäinen, J., Rautiainen, J., Toikkanen, L., Sirbu, A., Mereuta, A., Caliman, A., Kapon, E., and Okhotnikov, O.G. (2009) 1.3-μm optically-pumped semiconductor disk laser by wafer fusion. *Opt. Express*, **17**, 9047–9052.

99 Strittmatter, A., Germann, T.D., Pohl, J., Pohl, U.W., Bimberg, D., Rautiainen, J., Guina, M., and Okhotnikov, O.G. (2008) 1040 nm vertical external cavity surface emitting laser based on InGaAs quantum dots grown in Stranski–Krastanow regime. *Electron. Lett.*, **44**, 290–291.

100 Germann, T.D., Strittmatter, A., Pohl, J., Pohl, U.W., Bimberg, D., Rautiainen, J., Guina, M., and Okhotnikov, O.G. (2008) High-power semiconductor disk laser based on InAs/GaAs submonolayer quantum dots. *Appl. Phys. Lett.*, **92**, 101123.

101 Germann, T.D., Strittmatter, A., Pohl, J., Pohl, U.W., Bimberg, D., Rautiainen, J., Guina, M., and Okhotnikov, O.G. (2008) Temperature-stable operation of a quantum dot semiconductor disk laser. *Appl. Phys. Lett.*, **93**, 051104.

102 Butkus, M., Wilcox, K.G., Rautiainen, J., Okhotnikov, O.G., Mikhrin, S.S., Krestnikov, I.L., Kovsh, A.R., Hoffmann, M., Südmeyer, T., Keller, U., and Rafailov, E.U. (2009) High-power quantum-dot-based semiconductor disk laser. *Opt. Lett.*, **34**, 1672–1674.

103 Hopkins, J.M., Hempler, N., Rosener, B., Schulz, N., Rattunde, M., Manz, C., Kohler, K., Wagner, J., and Burns, D. (2008) High-power, (AlGaIn)(AsSb) semiconductor disk laser at 2.0 μm. *Opt. Lett.*, **33**, 201–203.

104 Abram, R.H., Gardner, K.S., Riis, E., and Ferguson, A.I. (2004) Narrow linewidth operation of a tunable optically pumped semiconductor laser. *Opt. Express*, **12**, 5434–5439.

105 Harkonen, A., Guina, M., Rossner, K., Hummer, M., Lehnhardt, T., Muller, M., Forchel, A., Fischer, M., Koeth, J., and Okhotnikov, O.G. (2007) Tunable self-seeded semiconductor disk laser operating at 2 μm. *Electron. Lett.*, **43**, 457–458.

106 Ouvrard, A., Garnache, A., Cerutti, L., Genty, F., and Romanini, D. (2005) Single-frequency tunable Sb-based VCSELs emitting at 2.3 μm. *IEEE Photon. Technol. Lett.*, **17**, 2020–2022.

107 Rudin, B., Rutz, A., Hoffmann, M., Maas, D.J.H.C., Bellancourt, A.-R., Gini, E., Südmeyer, T., and Keller, U. (2008) Highly efficient optically pumped vertical-emitting semiconductor laser with more than 20 W average output power in a fundamental transverse mode. *Opt. Lett.*, **33**, 2719–2721.

108 Spinelli, L.A. and Caprara, A. (2008) Intracavity frequency-tripled cw laser. US Patent 7,463,657, issued December 9.

109 Leinonen, T., Morozov, Y.A., Harkonen, A., and Pessa, M. (2005) Vertical external-cavity surface-emitting laser for dual-wavelength generation. *IEEE Photon. Technol. Lett.*, **17**, 2508–2510.

110 Morozov, Y.A., Leinonen, T., Harkonen, A., and Pessa, M. (2006) Simultaneous dual-wavelength emission from vertical external-cavity surface-emitting laser: a numerical modeling. *IEEE J. Quantum Electron.*, **42**, 1055–1061.

111 Leinonen, T., Ranta, S., Laakso, A., Morozov, Y., Saarinen, M., and Pessa, M. (2007) Dual-wavelength generation by vertical external cavity surface-emitting laser. *Opt. Express*, **15**, 13451–13456.

112 Harkonen, A., Rautiainen, J., Leinonen, T., Morozov, Y.A., Orsila, L., Guina, M., Pessa, M., and Okhotnikov, O.G. (2007) Intracavity sum-frequency generation in dual-wavelength semiconductor disk laser. *IEEE Photon. Technol. Lett.*, **19**, 1550–1552.

113 Fan, L., Fallahi, M., Hader, J., Zakharian, A.R., Moloney, J.V., Stolz, W., Koch, S.W., Bedford, R., and Murray, J.T. (2007) Linearly polarized dual-wavelength vertical-external-cavity surface-emitting laser. *Appl. Phys. Lett.*, **90**, 181124.

114 Andersen, M.T., Schlosser, P.J., Hastie, J.E., Tidemand-Lichtenberg, P., Dawson, M.D., and Pedersen, C. (2009) Singly-resonant sum frequency generation of visible light in a semiconductor disk laser. *Opt. Express*, **17**, 6010–6017.

115 Mihoubi, Z., Wilcox, K.G., Elsmere, S., Quarterman, A., Rungsawang, R., Farrer, I., Beere, H.E., Ritchie, D.A., Tropper, A., and Apostolopoulos, V. (2008) All-semiconductor room-temperature terahertz time domain spectrometer. *Opt. Lett.*, **33**, 2125–2127.

116 Raja, M.Y.A., Brueck, S.R.J., Osinsky, M., Schaus, C.F., McInerney, J.G., Brennan, T.M., and Hammons, B.E. (1989) Resonant periodic gain surface-emitting semiconductor lasers. *IEEE J. Quantum Electron.*, **25**, 1500–1512.

117 Hader, J., Moloney, J.V., Fallahi, M., Fan, L., and Koch, S.W. (2006) Closed-loop design of a semiconductor laser. *Opt. Lett.*, **31**, 3300–3302.

118 Moloney, J.V., Hader, J., and Koch, S.W. (2007) Quantum design of semiconductor active materials: laser and amplifier applications. *Laser Photon. Rev.*, **1**, 24–43.

119 Garnache, A., Ouvrard, A., and Romanini, D. (2007) Single-frequency operation of external-cavity VCSELs: nonlinear multimode temporal dynamics and quantum limit. *Opt. Express*, **15**, 9403–9417.

120 Cocquelin, B., Holleville, D., Lucas-Leclin, G., Sagnes, I., Garnache, A., Myara, M., and Georges, P. (2009) Tunable single-frequency operation of a diode-pumped vertical external-cavity laser at the cesium D_2 line. *Appl. Phys. B*, **95** (2), 315–321.

121 Lindberg, H., Strassner, M., and Larsson, A. (2005) Improved spectral properties of an optically pumped semiconductor disk laser using a thin diamond heat spreader as an intracavity filter. *IEEE Photon. Technol. Lett.*, **17**, 1363–1365.

122 Tourrenc, J.P., Bouchoule, S., Khadour, A., Decobert, J., Miard, A., Harmand, J.C., and Oudar, J.L. (2007) High power single-longitudinal-mode OP-VECSEL at 1.55 μm with hybrid metal-metamorphic Bragg mirror. *Electron. Lett.*, **43**, 754–755.

123 Tourrenc, J.P., Bouchoule, S., Khadour, A., Harmand, J.C., Miard, A., Decobert, J., Lagay, N., Lafosse, X., Sagnes, I., Leroy, L., and Oudar, J.L. (2008) Thermal optimization of 1.55 μm OP-VECSEL with hybrid metal-metamorphic mirror for single-mode high power operation. *Opt. Quantum Electron.*, **40**, 155–165.

124 Symonds, C., Dion, J., Sagnes, I., Dainese, M., Strassner, M., Leroy, L., and Oudar, J.L. (2004) High performance 1.55 μm vertical external cavity surface emitting laser with broadband integrated dielectric-metal mirror. *Electron. Lett.*, **40**, 734–735.

125 Kim, K.S., Yoo, J.R., Cho, S.H., Lee, S.M., Lim, S.J., Kim, J.Y., Lee, J.H., Kim, T., and Park, Y.J. (2006) 1060 nm vertical-external-cavity surface-emitting lasers with an optical-to-optical efficiency of 44% at room temperature. *Appl. Phys. Lett.*, **88**, 091107.

126 Zorn, M., Klopp, P., Saas, F., Ginolas, A., Krüger, O., Griebner, U., and Weyers, M. (2008) Semiconductor components for femtosecond semiconductor disk lasers grown by MOVPE. *J. Cryst. Growth*, **310**, 5187–5190.

127 Konttinen, J., Härkönen, A., Tuomisto, P., Guina, M., Rautiainen, J., Pessa, M., and Okhotnikov, O. (2007) High-power (>1 W) dilute nitride semiconductor disk laser emitting at 1240 nm. *New J. Phys.*, **9**, 140.

128 Manz, C., Yang, Q., Rattunde, M., Schulz, N., Rösener, B., Kirste, L., Wagner, J., and Köhler, K. (2009) Quaternary GaInAsSb/AlGaAsSb vertical-external-cavity surface-emitting lasers: a challenge for MBE growth. *J. Cryst. Growth*, **311**, 1920–1922.

129 Korpijärvi, V.-M., Guina, M., Puustinen, J., Tuomisto, P., Rautiainen, J., Härkönen, A., Tukiainen, A., Okhotnikov, O., and Pessa, M. (2009) MBE grown GaInNAs-based multi-Watt disk lasers. *J. Cryst. Growth*, **311**, 1868–1871.

130 Fan, L., Hader, J., Schillgalies, M., Fallahi, M., Zakharian, A.R., Moloney, J.V., Bedford, R., Murray, J.T., Koch, S.W., and Stolz, W. (2005) High-power optically pumped VECSEL using a double-well resonant periodic gain structure. *IEEE Photon. Technol. Lett.*, **17**, 1764–1766.

131 Maclean, A.J., Kemp, A.J., Calvez, S., Kim, J.Y., Kim, T., Dawson, M.D., and Burns, D. (2008) Continuous tuning and efficient intracavity second-harmonic generation in a semiconductor disk laser with an intracavity diamond heatspreader. *IEEE J. Quantum Electron.*, **44**, 216–225.

132 Seelert, W., Kubasiak, S., Negendank, J., von Elm, R., Chilla, J., Zhou, H., and Weiss, E. (2006) Optically-pumped semiconductor lasers at 505-nm in the power range above 100 mW. *Proc. SPIE*, **6100**, 610002.

133 Aschwanden, A., Lorenser, D., Unold, H.J., Paschotta, R., Gini, E., and Keller, U. (2005) 2.1-W picosecond passively mode-locked external-cavity semiconductor laser. *Opt. Lett.*, **30**, 272–274.

134 Garnache, A., Hoogland, S., Tropper, A.C., Sagnes, I., Saint-Girons, G., and Roberts, J.S. (2002) Sub-500-fs soliton-like pulse in a passively mode-locked broadband surface-emitting laser with 100 mW average power. *Appl. Phys. Lett.*, **80**, 3892–3894.

135 Hunziker, L.E., Shu, Q.-Z., Bauer, D., Ihli, C., Mahnke, G.J., Rebut, M., Chilla, J.R., Caprara, A.L., Zhou, H., Weiss, E.S., and Reed, M.K. (2007) Power-scaling of optically pumped semiconductor lasers. *Proc. SPIE*, **6451**, 64510.

136 Ochalski, T.J., de Burca, A., Huyet, G., Lyytikainen, J., Guina, M., Pessa, M., Jasik, A., Muszalski, J., and Bugajski, M. (2008) Passively modelocked bi-directional vertical external ring cavity surface emitting laser. Conference on Lasers and Electro-Optics, and Conference on Quantum Electronics and Laser Science (CLEO/QELS).

137 Mignot, A., Feugnet, G., Schwartz, S., Sagnes, I., Garnache, A., Fabre, C., and Pocholle, J.-P. (2009) Single-frequency external-cavity semiconductor ring-laser gyroscope. *Opt. Lett.*, **34**, 97–99.

138 Eckstein, H.-C. and Zeitner, U.D. (2008) Experimental realization of a diffractive unstable resonator with Gaussian outcoupled beam using a VECSEL amplifier. Conference on Lasers and Electro-Optics, and Conference on Quantum Electronics and Laser Science (CLEO/QELS).

139 Hodgson, N. and Weber, H. (2005) *Laser Resonators and Beam Propagation*, 2nd edn, Springer.

140 Laurain, A., Myara, M., Beaudoin, G., Sagnes, I., and Garnache, A. (2009) High power single-frequency continuously-tunable compact extended-cavity semiconductor laser. *Opt. Express*, **17**, 9503–9508.

141 Keeler, G.A., Serkland, D.K., Geib, K.M., Peake, G.M., and Mar, A. (2005) Single transverse mode operation of electrically pumped vertical-external-cavity surface-emitting lasers with micromirrors. *IEEE Photon. Technol. Lett.*, **17**, 522–524.

142 Laurand, N., Lee, C.L., Gu, E., Hastie, J.E., Calvez, S., and Dawson, M.D. (2007) Microlensed microchip VECSEL. *Opt. Express*, **15**, 9341–9346.

143 Laurand, N., Lee, C.-L., Gu, E., Hastie, J.E., Kemp, A.J., Calvez, S., and Dawson, M.D. (2008) Array-format microchip semiconductor disk lasers. *IEEE J. Quantum Electron.*, **44**, 1096–1103.

144 Laurand, N., Lee, C.-L., Gu, E., Calvez, S., and Dawson, M.D. (2009) Power-scaling of diamond microlensed microchip semiconductor disk lasers. *IEEE Photon. Technol. Lett.*, **21**, 152–154.

145 Kuznetsov, M., Stern, M., and Coppeta, J. (2005) Single transverse mode optical resonators. *Opt. Express*, **13**, 171–181.

146 Cocquelin, B., Lucas-Leclin, G., Georges, P., Sagnes, I., and Garnache, A. (2008) Design of a low-threshold VECSEL emitting at 852 nm for Cesium atomic clocks. *Opt. Quantum Electron.*, **40**, 167–173.

147 Okhotnikov, O.G. (2008) Power scalable semiconductor disk lasers for frequency conversion and mode-locking. *Quantum Electron.*, **38**, 1083–1096.

148 Jacquemet, M., Picqu,é, N., Guelachvili, G., Garnache, A., Sagnes, I., Strassner, M., and Symonds, C. (2007) Continuous-wave 1.55 μm diode-pumped surface emitting semiconductor laser for broadband multiplex spectroscopy. *Opt. Lett.*, **32**, 1387–1389.

149 Campargue, A., Wang, L., Cermak, P., and Hu, S.-M. (2005) ICLAS-VeCSEL and FTS spectroscopies of C_2H_2 between 9000 and 9500 cm^{-1}. *Chem. Phys. Lett.*, **403**, 287–292.

150 Mooradian, A. (2001) High brightness cavity-controlled surface emitting GaInAs lasers operating at 980 nm. Optical Fiber Communication Conference (OFC 2001), vol. 4, pp. PD17-1–PD17-3.

151 McInerney, J.G., Mooradian, A., Lewis, A., Shchegrov, A.V., Strzelecka, E.M., Lee, D., Watson, J.P., Liebman, M.K., Carey, G.P., Umbrasas, A., Amsden, C.A., Cantos, B.D., Hitchens, W.R., Heald, D.L., and Doan, V. (2003) Novel 980-nm and 490-nm light sources using vertical-cavity lasers with extended coupled cavities. *Proc. SPIE*, **4994**, 21.

152 Bousseksou, A., Bouchoule, S., El Kurdi, M., Strassner, M., Sagnes, I., Crozat, P., and Jacquet, J. (2006) Fabrication and characterization of 1.55 μm single transverse mode large diameter electrically pumped VECSEL. *Opt. Quantum Electron.*, **38**, 1269–1278.

153 Kardosh, I., Demaria, F., Rinaldi, F., Riedl, M.C., and Michalzik, R. (2008) Electrically pumped frequency-doubled surface emitting lasers operating at

485 nm emission wavelength. *Electron. Lett.*, **44**, 524–525.

154 Illek, S., Albrecht, T., Brick, P., Lutgen, S., Pietzonka, I., Furitsch, M., Diehl, W., Luft, J., and Streubel, K. (2007) Vertical-external-cavity surface-emitting laser with monolithically integrated pump lasers. *IEEE Photon. Technol. Lett.*, **19**, 1952–1954.

155 Lee, J.H., Kim, J.Y., Lee, S.M., Yoo, J.R., Kim, K.S., Cho, S.H., Lim, S.J., Kim, G.B., Hwang, S.M., Kim, T., and Park, Y.J. (2006) 9.1-W high-efficient continuous-wave end-pumped vertical-external-cavity surface-emitting semiconductor laser. *IEEE Photon. Technol. Lett.*, **18**, 2117–2119.

156 Lee, J.H., Lee, S.M., Kim, T., and Park, Y.J. (2006) 7 W high-efficiency continuous-wave green light generation by intracavity frequency doubling of an end-pumped vertical external-cavity surface emitting semiconductor laser. *Appl. Phys. Lett.*, **89**, 241107.

157 Kim, G.B., Kim, J.-Y., Lee, J., Yoo, J., Kim, K.-S., Lee, S.-M., Cho, S., Lim, S.-J., Kim, T., and Park, Y.J. (2006) End-pumped green and blue vertical external cavity surface emitting laser devices. *Appl. Phys. Lett.*, **89**, 181106.

158 Cho, S., Kim, G.B., Kim, J.-Y., Kim, K.-S., Lee, S.-M., Yoo, J., Kim, T., and Park, Y. (2007) Compact and efficient green VECSEL based on novel optical end-pumping scheme. *IEEE Photon. Technol. Lett.*, **19**, 1325–1327.

159 Bedford, R.G., Kolesik, M., Chilla, J.L.A., Reed, M.K., Nelson, T.R., and Moloney, J.V. (2005) Power-limiting mechanisms in VECSELs. *Proc. SPIE*, **5814**, 199–208.

160 Maas, D., Bellancourt, A.R., Rudin, B., Golling, M., Unold, H.J., Sudmeyer, T., and Keller, U. (2007) Vertical integration of ultrafast semiconductor lasers. *Appl. Phys. B*, **88**, 493–497.

161 Bellancourt, A.-R., Maas, D.J.H.C., Rudin, B., Golling, M., Südmeyer, T., and Keller, U. (2009) Modelocked integrated external-cavity surface emitting laser. *IET Optoelectron.*, **3**, 61–72.

162 Saas, F., Talalaev, V., Griebner, U., Tomm, J.W., Zorn, M., Knigge, A., and Weyers, M. (2006) Optically pumped semiconductor disk laser with graded and step indices. *Appl. Phys. Lett.*, **89**, 151120.

163 Schulz, N., Rattunde, A., Manz, C., Kohler, K., Wild, C., Wagner, J., Beyertt, S.S., Brauch, U., Kubler, T., and Giesen, A. (2006) Optically pumped GaSb-based VECSEL emitting 0.6 W at 2.3 μm. *IEEE Photon. Technol. Lett.*, **18**, 1070–1072.

164 Hopkins, J.M., Maclean, A.J., Burns, D., Riis, E., Schulz, N., Rattunde, M., Manz, C., Kohler, K., and Wagner, J. (2007) Tunable, single-frequency, diode-pumped 2.3 μm VECSEL. *Opt. Express*, **15**, 8212–8217.

165 Esposito, E., Keatings, S., Gardner, K., Harris, J., Riis, E., and McConnell, G. (2008) Confocal laser scanning microscopy using a frequency doubled vertical external cavity surface emitting laser. *Rev. Sci. Instrum.*, **79**, 083702.

166 Ra, H., Piyawattanametha, W., Mandella, M.J., Hsiung, P.-L., Hardy, J., Wang, T.D., Contag, C.H., Kino, G.S., and Solgaard, O. (2008) Three-dimensional *in vivo* imaging by a handheld dual-axes confocal microscope. *Opt. Express*, **16**, 7224–7232.

167 Chilla, J.L.A., Butterworth, S.D., Zeitschel, A., Charles, J.P., Caprara, A.L., Reed, M.K., and Spinelli, L. (2004) High-power optically pumped semiconductor lasers. *Proc. SPIE*, **5332**, 143.

168 Garnache, A., Myara, M., Bouchier, A., Perez, J.-P., Signoret, P., Sagnes, I., and Romanini, D. (2008) Single frequency free-running low noise compact external-cavity VCSELs at high power level (50 mW). 34th European Conference on Optical Communication (ECOC).

169 Fan, L., Fallahi, M., Hader, J., Zakharian, A.R., Kolesik, M., Moloney, J.V., Qiu, T., Schulzgen, A., Peyghambarian, N., Stolz, W., Koch, S.W., and Murray, J.T. (2005) Over 3 W high-efficiency vertical-external-cavity surface-emitting lasers and application as efficient fiber laser pump sources. *Appl. Phys. Lett.*, **86**, 211116.

170 Harkonen, A., Suomalainen, S., Saarinen, E., Orsila, L., Koskinen, R., Okhotnikov, O., Calvez, S., and Dawson, M. (2006) 4 W single-transverse

mode VECSEL utilising intra-cavity diamond heat spreader. *Electron. Lett.*, **42**, 693–694.

171 Guina, M., Korpijarvi, V.-M., Rautiainen, J., Tuomisto, P., Puustinen, J., Harkonen, A., and Okhotnikov, O. (2008) 3.5 W GaInNAs disk laser operating at 1220 nm. *Proc. SPIE*, **6997**, 69970.

172 Harkonen, A., Guina, M., Rossner, K., Hummer, M., Lehnhardt, T., Muller, M., Forchel, A., Fischer, M., Koeth, J., and Okhotnikov, O.G. (2007) Tunable self-seeded semiconductor disk laser operating at 2 μm. *Electron. Lett.*, **43**, 457–458.

173 Kim, J.-Y., Cho, S., Lim, S.-J., Yoo, J., Kim, G.B., Kim, K.-S., Lee, J., Lee, S.-M., Kim, T., and Park, Y. (2007) Efficient blue lasers based on gain structure optimizing of vertical-external-cavity surface-emitting laser with second harmonic generation. *J. Appl. Phys.*, **101**, 033103.

174 Gerster, E., Ecker, I., Lorch, S., Hahn, C., Menzel, S., and Unger, P. (2003) Orange-emitting frequency-doubled GaAsSb/GaAs semiconductor disk laser. *J. Appl. Phys.*, **94**, 7397–7401.

175 Rautiainen, J., Harkonen, A., Tuornisto, P., Konttinen, J., Orsila, L., Guina, M., and Okhotnikov, O.G. (2007) 1 W at 617 nm generation by intracavity frequency conversion in semiconductor disk laser. *Electron. Lett.*, **43**, 980–981.

176 Genesis™ Taipan™ 639M OPSL laser from Coherent Inc., www.coherent.com.

177 Rafailov, E.U., Sibbett, W., Mooradian, A., McInerney, J.G., Karlsson, H., Wang, S., and Laurell, F. (2003) Efficient frequency doubling of a vertical-extended-cavity surface-emitting laser diode by use of a periodically poled KTP crystal. *Opt. Lett.*, **28**, 2091–2093.

178 Genesis™ 355 OPSL laser from Coherent Inc., www.coherent.com.

179 Risk, W.P., Gosnell, T.R., and Nurmikko, A.V. (2003) *Compact Blue–Green Lasers*, Cambridge University Press.

180 Smith, A., Hastie, J.E., Foreman, H.D., Leinonen, T., Guina, M., and Dawson, M.D. (2008) GaN diode-pumping of a red semiconductor disk laser. *Electron. Lett.*, **44**, 1195–1196.

181 Smith, S.A., Hopkins, J.-M., Hastie, J.E., Burns, D., Calvez, S., Dawson, M.D., Jouhti, T., Kontinnen, J., and Pessa, M. (2004) Diamond-microchip GaInNAs vertical external-cavity surface-emitting laser operating CW at 1315 nm. *Electron. Lett.*, **40**, 935–936.

182 Vetter, S.L., Hastie, J.E., Korpijarvi, V.-M., Puustinen, J., Guina, M., Okhotnikov, O., Calvez, S., and Dawson, M.D. (2008) Short-wavelength GaInNAs/GaAs semiconductor disk lasers. *Electron. Lett.*, **44**, 1069–1070.

183 Laurand, N., Calvez, S., Sun, H.D., Dawson, M.D., Gupta, J.A., and Aers, G.C. (2006) C-band emission from GaInNAsSb VCSEL on GaAs. *Electron. Lett.*, **42**, 28–30.

184 Rosener, B., Schulz, N., Rattunde, M., Moser, R., Manz, C., Kohler, K., and Wagner, J. (2008) Optically pumped (AlGaIn)(AsSb) semiconductor disk laser employing a dual-chip cavity. IEEE Lasers and Electro-Optics Society Annual Meeting (LEOS), pp. 854–855.

185 Schulz, N., Rosener, B., Moser, R., Rattunde, M., Manz, C., Kohler, K., and Wagner, J. (2008) An improved active region concept for highly efficient GaSb-based optically in-well pumped vertical-external-cavity surface-emitting lasers. *Appl. Phys. Lett.*, **93**, 181113.

186 Hoffmann, S. and Hofmann, M.R. (2007) Generation of Terahertz radiation with two color semiconductor lasers. *Laser Photon. Rev.*, **1**, 44–56.

187 Morozov, Y.A., Nefedov, I.S., Leinonen, T., and Morozov, M.Y. (2008) Nonlinear-optical frequency conversion in a dual-wavelength vertical-external-cavity surface-emitting laser. *Semiconductors*, **42**, 463–469.

188 Harkonen, A. (2009) Antimonide disk lasers achieve multiwatt power and a wide tuning range. *SPIE Newsroom*. doi:

189 Giudice, G.E., Guy, S.C., Crigler, S.G., Zenteno, L.A., and Hallock, B.S. (2002) Effect of pump laser noise on an erbium-doped fiber-amplified signal. *IEEE Photon. Technol. Lett.*, **14**, 1403–1405.

190 Schlager, J.B., Callicoatt, B.E., Mirin, R.P., Sanford, N.A., Jones, D.J., and Ye, J.

(2003) Passively mode-locked glass waveguide laser with 14-fs timing jitter. *Opt. Lett.*, **28**, 2411–2413.

191 Vetter, S., Calvez, S., Dawson, M.D., Fusari, F., Lagatsky, A.A., Sibbett, W., Brown, C.T.A., Korpijarvi, V.-M., Guina, M., Richards, B., Jose, G., and Jha, A. (2008) 1213 nm semiconductor disk laser pumping of a Tm^{3+}-doped tellurite glass laser. IEEE Lasers and Electro-Optics Society Annual Meeting, pp. 840–841.

192 Vetter, S.L., McKnight, L.J., Calvez, S., Dawson, M.D., Fusari, F., Lagatsky, A.A., Sibbett, W., Brown, C.T.A., Korpijärvi, V.–M., Guina, M.D., Richards, B., Jose, G., and Jha, A. (2009) GaInNAs semiconductor disk lasers as pump sources for Tm^{3+} (,Ho^{3+})-doped glass, crystal and fibre lasers. *Proc. SPIE*, **7193**, 719317.

193 Wang, T.D., Mandella, M.J., Contag, C.H., and Kino, G.S. (2003) Dual-axis confocal microscope for high-resolution *in vivo* imaging. *Opt. Lett.*, **28**, 414–416.

194 Wang, T.D., Contag, C.H., Mandella, M.J., Chan, N.Y., and Kino, G.S. (2004) Confocal fluorescence microscope with dual-axis architecture and biaxial postobjective scanning. *J. Biomed. Opt.*, **9**, 735–742.

195 Simbuerger, E., Pflanz, T., and Masters, A. (2008) Confocal microscopy: new lasers enhance live cell imaging. *Physik Journal, (Physics' Best)*, 10.

196 Schulze, M. (2008) Laser microscopy continues to diversify, *Photonik International Online*, February, p. 36.

197 Pawley, J.B. (ed.) (2006) *Handbook of Biological Confocal Microscopy*, 3rd edn, Springer Science + Business Media, LLC.

198 Schiemann, M. and Busch, D.H. (2009) Selection and combination of fluorescent dyes, in *Cellular Diagnostics. Basics, Methods and Clinical Applications of Flow Cytometry* (eds U. Sack, A. Tárnok, and G. Rothe), Karger, Basel, pp. 107–140.

199 Lake, T., Carruthers, A., Taylor, M., Paterson, L., Gunn-Moore, F., Allen, J., Sibbett, W., and Dholakia, K. (2004) Optical trapping and fluorescence excitation with violet diode lasers and extended cavity surface emitting lasers. *Opt. Express*, **12**, 670–678.

200 Su, W.W. (2005) Fluorescent proteins as tools to aid protein production. *Microb. Cell Fact.*, **4**, 12.

201 Resan, B., Coadou, E., Petersen, S., Thomas, A., Walther, P., Viselga, R., Heritier, J.-M., Chilla, J., Tulloch, W., and Fry, A. (2008) Ultrashort pulse Ti: sapphire oscillators pumped by optically pumped semiconductor (OPS) pump lasers. *Proc. SPIE*, **6871**, 687116.

202 Harris, R. (2009) OPSL technology provides new wavelengths that benefit forensics, *Photonik International Online*, March, p. 2.

203 Masters, A. (2007) Yellow lasers target macular degeneration, *Biophotonics International*, June.

204 Masters, A. and Seaton, C. (2006) Laser-based displays will deliver superior images, *Laser Focus World*, November.

205 Evans & Sutherland ESLP® (2009) 8 K laser video projector, www.es.com.

206 Mitsubishi LaserVue® (2009) TV, www.laservuetv.com.

207 Freeman, M., Champion, M., and Madhavan, S. (2009) Scanned laser pico-projetors, *Optics and Photonics News*, May.

208 Schmitt, M. and Steegmüller, U. (2008) Green laser meets mobile projection requirements. *Opt. Laser Europe*, 17–19.

209 Trisnadi, J.I., Carlisle, C.B., and Monteverde, R., (2004) Overview and applications of grating-light-valve-based optical write engines for high-speed digital imaging. *Proc. SPIE*, **5348**, 52–64.

210 Niven, G. and Mooradian, A. (2006) Trends in laser light sources for projection display. 13th International Display Workshop (IDW 2006), Otsu, Japan, December 2006.

211 Kaneda, Y., Fan, L., Hsu, T.-C., Peyghambarian, N., Fallahi, M., Zakharian, A.R., Hader, J., Moloney, J.V., Stoltz, W., Koch, S., Bedford, R., Sevian, A., and Glebov, L. (2006) High brightness spectral beam combination of high-power vertical-external-cavity surface-emitting lasers. *IEEE Photon. Technol. Lett.*, **18**, 1795–1797.

212 Aldaz, R.I., Wiemer, M.W., Miller, D.A.B., and Harris, J.S. (2004) Monolithically-

integrated long vertical cavity surface emitting laser incorporating a concave micromirror on a glass substrate. *Opt. Express*, **12**, 3967–3971.

213 Wiemer, M.W., Aldaz, R.I., Miller, D.A.B., and Harris, J.S. (2005) A single transverse-mode monolithically integrated long vertical-cavity surface-emitting laser. *IEEE Photon. Technol. Lett.*, **17**, 1366–1368.

214 Khurgin, J.B., Vurgaftman, I., and Meyer, J.R. (2005) Analysis of phase locking in diffraction-coupled arrays of semiconductor lasers with gain/index coupling. *IEEE J. Quantum Electron.*, **41**, 1065–1074.

215 Flynn, R.A., Birkbeck, A.L., Gross, M., Ozkan, M., Shao, B., and Esener, S.C. (2003) Simultaneous transport of multiple biological cells by VCSEL array optical traps, in *Optics in Computing* (ed. A. Sawchuk), OSA Trends in Optics and Photonics, vol. 90, Paper OThB2, Optical Society of America.

216 Vakhshoori, D., Tayebati, P., Lu, C.C., Azimi, M., Wang, P., Zhou, J.H., and Canoglu, E. (1999) 2 mW CW single mode operation of a tunable 1550 nm vertical cavity surface emitting laser with 50 nm tuning range. *Electron. Lett.*, **35**, 900–901.

217 Matsui, Y., Vakhshoori, D., Wang, P., Chen, P., Lu, C.-C., Jiang, M., Knopp, K., Burroughs, S., and Tayebati, P. (2003) Complete polarization mode control of long-wavelength tunable vertical-cavity surface-emitting lasers over 65-nm tuning, up to 14-mW output power. *IEEE J. Quantum Electron.*, **39**, 1037–1048.

218 Knopp, K.J., Vakhshoori, D., Wang, P.D., Azimi, M., Jiang, M., Chen, P., Matsui, Y., McCallion, K., Baliga, A., Sakhitab, F., Letsch, M., Johnson, B., Huang, R., Jean, A., DeLargy, B., Pinzone, C., Fan, F., Liu, J., Lu, C., Zhou, J., Zhu, H., Gurjar, R., Tayebati, P., MacDaniel, D., Baorui, R., Waterson, R., and VanderRhodes, G. (2001) High power MEMs-tunable vertical-cavity surface-emitting lasers. Advanced Semiconductor Lasers and Applications/Ultraviolet and Blue Lasers and Their Applications/Ultralong Haul DWDM Transmission and Networking/WDM Components, IEEE LEOS Summer Topical Meetings.

219 Triki, M., Cermak, P., Cerutti, L., Garnache, A., and Romanini, D. (2008) Extended continuous tuning of a single-frequency diode-pumped vertical-external-cavity surface-emitting laser at 2.3 μm. *IEEE Photon. Technol. Lett.*, **20**, 1947–1949.

220 Baili, G., Alouini, M., Malherbe, T., Dolfi, D., Huignard, J.-P., Merlet, T., Chazelas, J., Sagnes, I., and Bretenaker, F. (2008) Evidence of ultra low microwave additive phase noise for an optical RF link based on a class-A semiconductor laser. *Opt. Express*, **16**, 10091–10097.

221 Gardner, K., Abram, R., and Riis, E. (2004) A birefringent etalon as single-mode selector in a laser cavity. *Opt. Express*, **12**, 2365–2370.

222 Jacquemet, M., Domenech, M., Lucas-Leclin, G., Georges, P., Dion, J., Strassner, M., Sagnes, I., and Garnache, A. (2007) Single-frequency cw vertical external cavity surface emitting semiconductor laser at 1003 nm and 501 nm by intracavity frequency doubling. *Appl. Phys. B*, **86**, 503–510.

223 Hoogland, S., Dhanjal, S., Tropper, A.C., Roberts, J.S., Haring, R., Paschotta, R., Morier-Genoud, F., and Keller, U. (2000) Passively mode-locked diode-pumped surface-emitting semiconductor laser. *IEEE Photon. Technol. Lett.*, **12**, 1135–1137.

224 Hoffmann, M., Barbarin, Y., Maas, D.J.H.C., Golling, M., Krestnikov, I.L., Mikhrin, S.S., Kovsh, A.R., Südmeyer, T., and Keller, U. (2008) Modelocked quantum dot vertical external cavity surface emitting laser. *Appl. Phys. B*, **93**, 733–736.

225 Klopp, P., Saas, F., Zorn, M., Weyers, M., and Griebner, U. (2008) 290-fs pulses from a semiconductor disk laser. *Opt. Express*, **16**, 5770–5775.

226 Wilcox, K.G., Mihoubi, Z., Daniell, G.J., Elsmere, S., Quarterman, A., Farrer, I., Ritchie, D.A., and Tropper, A. (2008) Ultrafast optical Stark mode-locked semiconductor laser. *Opt. Lett.*, **33**, 2797–2799.

227 Jasim, K., Zhang, Q., Nurmikko, A.V., Mooradian, A., Carey, G., Ha, W., and Ippen, E. (2003) Passively modelocked vertical extended cavity surface emitting diode laser. *Electron. Lett.*, **39**, 373–375.

228 Jasim, K., Zhang, Q., Nurmikko, A.V., Ippen, E., Mooradian, A., Carey, G., and Ha, W. (2004) Picosecond pulse generation from passively modelocked vertical cavity diode laser at up to 15 GHz pulse repetition rate. *Electron. Lett.*, **40**, 34–36.

229 Zhang, Q., Jasim, K., Nurmikko, A.V., Mooradian, A., Carey, G., Ha, W., and Ippen, E. (2004) Operation of a passively mode-locked extended-cavity surface-emitting diode laser in multi-GHz regime. *IEEE Photon. Technol. Lett.*, **16**, 885–887.

230 Zhang, Q., Jasim, K., Nurmikko, A.V., Ippen, E., Mooradian, A., Carey, G., and Ha, W. (2005) Characteristics of a high-speed passively mode-locked surface-emitting semiconductor InGaAs laser diode. *IEEE Photon. Technol. Lett.*, **17**, 525–527.

231 Klopp, P., Griebner, U., Zorn, M., Klehr, A., Liero, A., Erbert, G., and Weyers, M. (2009) InGaAs–AlGaAs disk laser generating sub-220-fs pulses and tapered diode amplifier with ultrafast pulse picking, in *Advanced Solid-State Photonics*, Optical Society of America.

232 Wilcox, K.G., Foreman, H.D., Roberts, J.S., and Tropper, A.C. (2006) Timing jitter of 897 MHz optical pulse train from actively stabilised passively modelocked surface-emitting semiconductor laser. *Electron. Lett.*, **42**, 159–160.

233 Zhang, W., Ackemann, T., Schmid, M., Langford, N., and Ferguson, A.I. (2006) Femtosecond synchronously mode-locked vertical-external cavity surface-emitting laser. *Opt. Express*, **14**, 1810–1821.

234 Max, C.E. *et al.* (1997) Image improvement from a sodium-layer laser guide star adaptive optics system. *Science*, **277**, 1649–1652.

235 Rutten, T.P., Veitch, P.J., and Munch, J. (2007) Development of a sodium laser guide star for astronomical adaptive optics systems. Conference on Lasers and Electro-Optics (CLEO).

236 Kemp, A.J., Valentine, G.J., Hopkins, J.M., Hastie, J.E., Smith, S.A., Calvez, S., Dawson, M.D., and Burns, D. (2005) Thermal management in vertical-external-cavity surface-emitting lasers: finite-element analysis of a heatspreader approach. *IEEE J. Quantum Electron.*, **41**, 148–155.

237 Kemp, A.J., Hopkins, J.M., Maclean, A.J., Schulz, N., Rattunde, M., Wagner, J., and Burns, D. (2008) Thermal management in 2.3-μm semiconductor disk lasers: a finite element analysis. *IEEE J. Quantum Electron.*, **44**, 125–135.

238 Love, D., Kolesik, M., and Moloney, J.V. (2009) Optimization of ultrashort pulse generation in passively mode-locked vertical external-cavity semiconductor lasers. *IEEE J. Quantum Electron.*, **45**, 439–445.

239 Baili, G., Bretenaker, F., Alouini, M., Morvan, L., Dolfi, D., and Sagnes, I. (2008) Experimental investigation and analytical modeling of excess intensity noise in semiconductor class-A lasers. *J. Lightwave Technol.*, **26**, 952–961.

240 Zakharian, A.R., Hader, J., Moloney, J.V., Koch, S.W., Brick, P., and Lutgen, S. (2003) Experimental and theoretical analysis of optically pumped semiconductor disk lasers. *Appl. Phys. Lett.*, **83**, 1313–1315.

241 Zakharian, A.R., Hader, J., Moloney, J.V., and Koch, S.W. (2005) VECSEL threshold and output power-shutoff dependence on the carrier recombination rates. *IEEE Photon. Technol. Lett.*, **17**, 2511–2513.

242 Ouvrard, A., Cerutti, L., and Garnache, A. (2009) Broad continuous tunable range with single frequency Sb-based external-cavity VCSEL emitting in MIR. *Electron. Lett.*, **45**, 629–631.

243 Gherman, T., Romanini, D., Sagnes, I., Garnache, A., and Zhang, Z. (2004) Cavity-enhanced absorption spectroscopy with a mode-locked diode-pumped vertical external-cavity surface-emitting laser. *Chem. Phys. Lett.*, **390**, 290–295.

244 Picqué, N., Guelachvili, G., and Kachanov, A.A. (2003) High-sensitivity time-resolved intracavity laser Fourier

transform spectroscopy with vertical-cavity surface-emitting multiple-quantum-well lasers. *Opt. Lett.*, **28**, 313–315.

245 Bertseva, E., Kachanov, A.A., and Campargue, A. (2002) Intracavity laser absorption spectroscopy of N_2O with a vertical external cavity surface emitting laser. *Chem. Phys. Lett.*, **351**, 18–26.

246 Garnache, A., Liu, A., Cerutti, L., and Campargue, A. (2005) Intracavity laser absorption spectroscopy with a vertical external cavity surface emitting laser at 2.3 μm: application to water and carbon dioxide. *Chem. Phys. Lett.*, **416**, 22–27.

247 Naumenko, O. and Campargue, A. (2003) Rovibrational analysis of the absorption spectrum of H_2O around 1.02 μm by ICLAS-VECSEL. *J. Mol. Spectrosc.*, **221**, 221–226.

248 Bertseva, E. and Campargue, A. (2004) Spectral condensation near molecular transitions in intracavity laser spectroscopy with vertical external cavity surface emitting lasers. *Opt. Commun.*, **232**, 251–261.

249 Ding, Y., Naumenko, O., Hu, S.-M., Zhu, Q., Bertseva, E., and Campargue, A. (2003) The absorption spectrum of H_2S between 9540 and 10 000 cm^{-1} by intracavity laser absorption spectroscopy with a vertical external cavity surface emitting laser. *J. Mol. Spectrosc.*, **217**, 222–238.

250 Bertseva, E., Campargue, A., Ding, Y., Fayt, A., Garnache, A., Roberts, J.S., and Romanini, D. (2003) The overtone spectrum of carbonyl sulfide in the region of the $\nu1 + 4\nu3$ and $5\nu3$ bands by ICLAS-VECSEL. *J. Mol. Spectrosc.*, **219**, 81–87.

251 Naumenko, O.V., Leshchishina, O., Shirin, S., Jenouvrier, A., Fally, S., Vandaele, A.C., Bertseva, E., and Campargue, A. (2006) Combined analysis of the high sensitivity Fourier transform and ICLAS-VeCSEL absorption spectra of D_2O between 8800 and 9520 cm^{-1}. *J. Mol. Spectrosc.*, **238**, 79–90.